

**Establishment of retinoic acid gradients
in the early development of *Xenopus laevis***

Dissertation zur Erlangung des Doktorgrades
der Mathematisch-Naturwissenschaftlichen Fakultäten
der Georg-August Universität zu Göttingen

vorgelegt von

Ina Strate
aus Detmold

Göttingen 2009

D7

Referent: Prof. Dr. Ernst Wimmer

Korreferent: Assoc. Prof. Dr. Edgar Pera

Tag der mündlichen Prüfung: 27. 04. 2009

gewidmet meinen Eltern

Table of Contents

	page
Table of Contents.....	I
List of Figures.....	IV
Table.....	V
Abbreviations.....	V
Abstract.....	VIII
Acknowledgments.....	IX
<i>Curriculum vitae</i>	XI

1. Introduction

1.1 <i>Xenopus laevis</i> as a model organism.....	1
1.2 Dorsal-ventral axis determination.....	2
1.3 The Spemann-Mangold organizer.....	4
1.4 Neural Induction.....	5
1.5 Anterior-posterior patterning of the nervous system.....	9
1.6 Retinoids.....	12
1.7 The morphogen retinoic acid.....	13
1.8 Vitamin A deficiency and excessive RA treatment.....	15
reveal essential functions of retinoids during embryonic development	
1.9 Retinoic acid signalling during organogenesis.....	16
1.10 Effects of retinoic acid on the central nervous system.....	18
1.11 Retinal dehydrogenases.....	22
1.12 CYP 26 hydroxylases.....	24
1.13 Retinol dehydrogenases.....	25
1.14 Retinol dehydrogenase 10.....	28
1.15 Aim of the study.....	29

2. Material and methods

2.1 Material

2.1.1 Chemicals.....	30
2.1.2 Solutions.....	30
2.1.3 Media and Antibiotics.....	33
2.1.4 Morpholino-Oligonucleotides.....	34
2.1.5 Constructs.....	35
2.1.6 Enzymes.....	38
2.1.7 Reaction-kits.....	39
2.1.8 Equipment.....	39
2.1.9 Experimental organism.....	41

2.2 Methods

2.2.1 Comparison of RDH10 protein sequences.....	42
2.2.2 Restriction digest of plasmid DNA.....	42
2.2.3 <i>In vitro</i> transcription of sense RNA for microinjections.....	43
2.2.4 <i>In vitro</i> transcription of antisense RNA for <i>in situ</i> hybridizations.....	43
2.2.5 Preparation of antisense morpholino oligonucleotides.....	44
2.2.6 TNT-assay.....	44
2.2.7 Digest and purification of the pCS2-vector using gel extraction to generate pCS2+ <i>XRDH10</i> *	45
2.2.8 Ligation.....	45
2.2.9 DNA transformation.....	45
2.2.10 Colony PCR.....	46
2.2.11 Plasmid DNA preparation.....	46
2.2.12 <i>In vitro</i> fertilization.....	46
2.2.13 Microinjection of <i>Xenopus laevis</i> embryos.....	47
2.2.14 Chemical treatments.....	47
2.2.15 Fixation of embryos.....	47

2.2.16 Red-gal staining.....	48
2.2.17 Whole mount <i>in situ</i> hybridization.....	48
2.2.18 Histological sections.....	49
2.2.19 Animal cap explants.....	50
2.2.20 RNA extraction.....	50
2.2.21 Reverse transcription PCR.....	51

3. Results

3.1 Protein structure of <i>Xenopus</i> RDH10.....	53
3.2 <i>XRDH10</i> is dynamically expressed during early embryogenesis.....	55
3.3 Retinoic acid suppresses <i>XRDH10</i> gene expression.....	59
3.4 XRDH10 has retinoic acid-like activity.....	61
3.5 XRDH10 modulates organizer-specific gene expression.....	63
3.6 XRDH10 co-operates with XRALDH2 during.....	66
axis development and central nervous system patterning	
3.7 Retinol is a limiting factor for XRDH10 activity.....	70
3.8 Loss of XRDH10 and XRALDH2 affects the.....	72
anterior-posterior and dorsal-ventral axis of the embryo	
3.9 Loss of XRDH10 and XRALDH2 affects the expression.....	74
of early organizer markers and early mesodermal markers	
3.10 Loss of XRDH10 and XRALDH2 affects.....	76
anterior-posterior patterning of the nervous system	
3.11 XRDH10 is required for the posteriorizing effect of retinol.....	79

4. Discussion	
4.1 Comparison of <i>RDH10</i> gene expression in <i>Xenopus</i> and mouse embryonic development	80
4.2 <i>XRDH10</i> gene expression demarcates sites of RA signaling in the developing embryo	82
4.3 <i>XRDH10</i> gene expression is regulated by retinoic acid	84
4.4 The role of <i>XRDH10</i> in dorsal-ventral patterning	86
4.5 The role of <i>XRDH10</i> in anterior-posterior patterning	89
4.6 Model for the establishment of the retinoic acid morphogen gradient	90
5. Conclusion	93
6. References	95

List of Figures

	Page
Fig. 1. <i>Xenopus</i> retinol dehydrogenase 10	54
Fig. 2. Gene expression of <i>XRDH10</i> in early <i>Xenopus</i>	57
Fig. 3. Retinoic acid downregulates <i>XRDH10</i> gene expression	60
Fig. 4. <i>XRDH10</i> induces RA signaling	62
Fig. 5. <i>XRDH10</i> upregulates <i>Chordin</i> and <i>Xlim-1</i> and downregulates <i>Gooseoid</i> and <i>ADMP</i> expression in the dorsal blastopore lip	64
Fig. 6. <i>XRDH10</i> does not affect the organizer genes <i>Noggin</i> , <i>Frzb</i> , <i>sFRP2</i> and <i>Crescent</i>	65
Fig. 7. Overexpression of <i>XRDH10</i> and <i>XRALDH2</i> results in an anteriorwards shift of neural markers, while <i>XCYP26A1</i> has the opposite effect	68

Fig. 8. XRDH10 co-operates with retinol during head development.....	71
Fig. 9. Knockdown of <i>XRDH10</i> and <i>XRALDH2</i> induces ventralization.....	73
Fig.10. Knockdown of <i>XRDH10</i> and <i>XRALDH2</i> influences.....	75
organizer markers and mesodermal gene expression	
Fig.11. XRDH10 is critical for CNS patterning.....	77
Fig.12. XRDH10 is critical for the posteriorizing effect of retinol.....	79
Fig.13. Model for the establishment of RA morphogen gradients.....	92
in the early embryo.	

Table

Tab. 1. Primers for RT-PCR.....	52
---------------------------------	----

Abbreviations

A	adenine
AP	alkaline phosphate buffer
ATP	adenosine triphosphate
BCIP	5-bromo-4-chloro-3-indolyl-phosphate
BMB	Bohringer Mannheim blocking reagent
BSA	bovine serum albumin
C	cytosine
°C	celsius degree
cDNA	complementary DNA
CHAPS	3-(3-cholamidopropyl)dimethylammonio-1-propansulphate
dd H ₂ O	double distilled water
DEPC	diethylpyrocarbonate

DMSO	dimethylsulfoxide
DNA	deoxyribonucleic acid
DNase	deoxyribonuclease
DTT	dithiothreitol
dNTP	deoxynucleoside-triphosphates
<i>E.coli</i>	<i>Escherichia coli</i>
EDTA	ethylendiaminetetraacetic acid
<i>et al.</i>	<i>et altera</i>
Fig.	figure
HEPES	4-(2- hydroxyethyl)-1-piperazin
HPLC	high liquid pressure chromatography
H4	histone 4
G	guanine
GFP	green fluorescent protein
kb	kilobase
kV	kilo Volt
L	liter
LB	Luria Bertani
μ	micro
m	milli
M	molar (mol/L)
mA	milli ampere
MAB	malic acid buffer
MBS	modified Barth solution
MEM	MOPS-DGTA-MgSO4-buffer
MEMFA	MOPS-DGTA-MgSO4-formaldehyde-buffer
min	minutes
MO	antisense morpholino oligonucleotides
MOPS	4-morpholinpropanosulfonic acid
mRNA	messenger RNA
NAD	nicotinamid-adenin-dinucleotide
NBT	nitro-blue-tetrazolium

ng	nanogram
PBS	phosphate buffered saline
PBSw	1% Tween-20 in PBS
PCR	polymerase chain reaction
pH	preponderance of hydrogen ions
%	percent
Red-gal	5-bromo-6-chloro-3-indolyl-galactopyranoside
RNA	ribonucleic acid
RNase	ribonuclease
rpm	rounds per minute
RT-PCR	reverse transcription PCR
SSC	standard saline citrate buffer
st.	stage
T	thymine
<i>Taq</i>	<i>Thermus aquaticus</i>
TAE	Tris-acetic acid-EDTA-electrophoresis buffer
TNT	<i>in vitro</i> transcription translation
Tris	trishydroxymethyl-aminomethan
U	units / uracil
UV	ultra violet light
V	Volt

Abstract

Retinoic acid (RA) is an important morphogen that regulates many biological processes, including the development of the central nervous system (CNS). Its synthesis from vitamin A (retinol) occurs in two steps, with the second reaction - catalyzed by retinal dehydrogenases (RALDHs) - long considered to be crucial for tissue-specific RA production in the embryo. Recently, the *Xenopus* homologue of retinol dehydrogenase 10 (XRDH10) was identified that mediates the first step in RA synthesis from retinol to retinal. *XRDH10* is specifically expressed in the dorsal blastopore lip and in other domains of the early embryo that partially overlap with *XRALDH2* expression. Endogenous RA suppresses *XRDH10* gene expression, suggesting negative-feedback regulation. In mRNA-injected *Xenopus* embryos, XRDH10 mimicks RA responses, influencec the gene expression of organizer markers and synergizes with XRALDH2 in posteriorizing the developing brain. Knockdown of *XRDH10* and *XRALDH2* by specific antisense morpholino oligonucleotides have the opposite effects on organizer gene expression and cause a ventralized phenotype and anteriorization of the brain. These data indicate that the conversion of retinol into retinal is a developmentally controlled step involved in specification of the dorsoventral and anteroposterior body axes as well as in pattern formation of the CNS. Combinatorial gene expression and concerted action of XRDH10 and XRALDH2 constitute a novel mechanism for the establishment of a morphogen gradient in the embryo.

1. Introduction

1.1 *Xenopus laevis* as a model organism

The African claw frog *Xenopus laevis* is an excellent model system to explore the principles that underlie embryonic development of vertebrates. Eggs can be obtained easily at any time during the year by inducing ovulation in female frogs upon injection with human chorionic gonadotropin. The fertilization of the eggs and embryogenesis take place *ex utero*, so that every developmental stage is directly accessible. Due to their large size, *Xenopus laevis* embryos are very suitable for micromanipulation experiments. Such experiments include overexpression of particular genes by injection of DNA, RNA or proteins. In loss of function studies, individual genes can be downregulated with the help of antisense morpholino oligonucleotides which specifically inhibit protein biosynthesis. Dominant negative protein constructs can impair endogenous protein function. Moreover, *Xenopus* embryos are amenable for microsurgical experiments such as explantation and transplantation. It is also possible to apply pharmacological agents to the embryos during development to alter signalling pathways. Of wide use is the animal cap assay in which the naive ectoderm located at the animal pole of the blastula embryo is extracted and cultured *in vitro* to study the effects of altered gene expression or exogenously applied proteins on cell fate determination. The cells of these animal cap explants are pluripotent and their development can be driven into certain directions dependent on the signals they are exposed to.

Gene expression in *Xenopus* can be studied by whole mount *in situ* hybridizations and immunocytochemistry at the RNA and protein level, respectively. Reverse Transcription-Polymerase Chain Reaction (RT-PCR) is a semiquantitative method to monitor transcriptional activity. In addition, proteins can be overexpressed in oocytes or embryos and used in biochemical experiments to study posttranslational modifications and protein-protein interactions. Given the high degree of conservation of genes and signalling pathways in vertebrates, the knowledge gained from studies in *Xenopus* embryos can be used to better understand human development and to learn about the molecular basis of congenital malformations and diseases.

1.2 Dorsal-ventral axis determination

Xenopus eggs are radially symmetrical. The entry of the sperm into the egg triggers a rotation of the yolk mass relative to the egg surface (Vincent et al., 1986; Vincent and Gerhart, 1987). This process, known as cortical rotation, is driven by an apparatus of parallel microtubules located on the vegetal surface of the embryo. They appear at the beginning of rotation and disappear after it is completed (Elinson and Rowning, 1988). The microtubules arise in part from the centriole of the sperm which acts as a minus-end microtubule-organizing center (Houliston and Elinson, 1991). The cortical rotation translocates vegetally localized dorsal determinants along the microtubules into the subequatorial region of the embryo where the dorsal pole is going to form. If formation of microtubules is prevented by a treatment with UV light, colchicine or inhibitory antibodies against the microtubule-associated protein XMAP230, the embryos lack dorsal-anterior structures (Scharf and Gerhart, 1983; Elinson and Rowning, 1988; Cha and Gard, 1999). The significance of the dorsal determinants can be shown by various microsurgical experiments. Depletion of the vegetal cortex and cytoplasm before cortical rotation results in embryos that do not form dorsal and neural structures (Sakai 1996; Kikkawa et al., 1996; Fuji et al., 2002). Injection of vegetal cytoplasm into these embryos restores dorsal axial development (Sakai, 1996). Transplantation of cytoplasm from a dorsal-vegetal blastomere of a 16-cell stage embryo into a ventral-vegetal blastomere of a sibling embryo results in duplication of the body axis, corroborating the presence of dorsal determinants in dorsal-vegetal blastomeres (Yuge et al., 1990). Candidates for the dorsal determinants are the Dishevelled protein (Dsh) and the Glycogen Synthase Kinase-3 (GSK-3)-binding protein GBP which directly interacts with Dsh (Yost et al., 1998; Li et al., 1999; Miller et al., 1999; Salic et al., 2000). GBP also binds to the kinesin light chain (KLC) of the kinesin motor proteins that mediate the transfer on the microtubule array (Weaver et al., 2003; Weaver and Kimelman, 2004). Upon transportation to the future dorsal side of the embryo, the dorsal determinants stabilize β -catenin. β -catenin is a Wnt pathway effector and the regulation of its stability is controlled by a complex of proteins called the β -catenin destruction complex. Central to this complex are two proteins, Axin and Adenomatous Polyposis Coli (APC) (Bienz, 1999). In the absence of a Wnt signal, β -catenin is phosphorylated within the complex by Casein Kinase 1

α (CK1 α) and GSK-3 which marks β -catenin for ubiquitination and degradation (Dominguez and Green, 2001; Polakis, 2002). β -catenin is stabilized by GBP through its binding to GSK-3 and subsequent removal from Axin leading to a degradation of GSK-3 (Dominguez and Green, 2000; Farr et al., 2000). Dsh is thought to act in part by recruiting GBP to the β -catenin-destruction complex (Salic et al., 2000). β -catenin is a multifunctional protein that can act as a nuclear transcription factor. It is a key player in the formation of the dorsal axis and experimental depletion of its transcripts results in lack of dorsal structures (Heasman et al., 1994). On the other hand, injection of exogenous β -catenin, Wnt, GBP and Dsh into early embryos produces a secondary axis (Funayama et al., 1995; Guger and Gumbiner, 1995; Sokol et al., 1995; Yost et al., 1998). β -catenin can associate with the ubiquitously expressed transcription factor 3 (Tcf3) and thereby convert Tcf3 from a transcriptional repressor to a transcriptional activator. Injection of a mutant form of Tcf3, which lacks the β -catenin-binding domain, acts in a dominant negative manner and causes loss of the dorsal axis (Molenaar et al., 1996). One of the genes that is activated by the binding of the Tcf3/ β -catenin complex to its promoter is *Siamois* (Brannon et al., 1997). Vegetal cortical cytoplasm can induce ectopic *Siamois* expression in animal cap cells (Darras et al., 1997). It is the cooperation between the homeodomain protein *Siamois* and vegetally localized paracrine factors of the TGF- β family, including Vg1 and *Xenopus* Nodal related proteins (Xnrs; Xnr1, 2, 4, 5, 6), that drives the expression of dorsal specific genes (Brannon and Kimelman, 1996; Engleka and Kessler, 2001). These include genes encoding the homeobox-containing transcription factors Goosecoid and Xlim-1 and the secreted proteins Cerberus and Frzb (Laurent et al., 1997; Engleka and Kessler, 2001). *Xnr* genes are expressed in a dorsoventral gradient across the endoderm. Their expression is driven by the synergistic action of vegetally localized VegT with dorsally localized β -catenin. Xnrs specify the mesoderm in such a way that regions with small amounts of Xnrs become ventral mesoderm and those regions with highest Xnr content become dorsal mesoderm (Agius et al., 2000). Another VegT target gene is *Derrière* which belongs to the TGF- β family. *Derrière* was shown to be essential for mesoderm patterning since a dominant-negative *Derrière* construct ablates posterior and paraxial mesoderm-specific gene expression (Sun et al., 1999).

1.3 The Spemann-Mangold organizer

In 1924, Hans Spemann and Hilde Mangold showed that transplantation of the mesodermal dorsal blastopore lip of gastrulating newt embryos (*Triturus cristatus*) into the belly skin of a sibling host embryo (*T. traeniatus*) results in the formation of a secondary body axis. Due to the different pigmentation of donor and host tissue, it was possible to conclude that the transplanted dorsal blastopore lip self-differentiates into chordamesoderm and floor plate tissue, while other structures including neural tube and somites are ectopically induced in the host embryo (Spemann and Mangold, 1924). Because of this remarkable inducing activity, the amphibian dorsal blastopore lip is referred to as the “Spemann-Mangold organizer”. Similar organizing centers are the embryonic shield in fish (Oppenheimer, 1936) and “Hensen’s node” in chick and mammalian embryos (Boettger et al., 2001).

Subsequent studies revealed that the Spemann-Mangold organizer is induced at the early blastula stage by signals from adjacent dorsal vegetal cells called the “Nieuwkoop center” (Smith, 1993; Kessler and Melton, 1994). High concentrations of mesoderm-inducing Nodal-related proteins, including *Xnr1*, 2, 4, 5 and 6, promote the formation of the organizer (Agius et al., 2000; Takahashi et al., 2000). The Nieuwkoop center itself is fated to become anterior endoderm. However, there is evidence that the establishment of the organizer does not require inductive signals from these dorsal vegetal cells. If the vegetal-most cells are removed from 32-cell stage embryos, the remaining part of the embryo can form dorsal structures (Nakamura and Takasaki, 1971). This observation can be explained by the presence of a group of cells in the dorsal animal cap, called the BCNE (Blastula Chordin and Noggin Expression) center, which further contributes to the formation of the organizer. In the BCNE center, genes including *Chordin*, *Noggin* and *Xnr3* are transcriptionally activated by β -catenin (Kuroda et al., 2004; Haramoto et al., 2004; Wessely et al., 2004). The BCNE center contains prospective neuroectodermal and organizer cells that give rise to the forebrain, most of the mid- and hindbrain, floorplate and notochord. When the BCNE center is excised from blastula embryos, brain formation fails, an effect that is rescued by transplantation of dorsal animal cap tissue (Kuroda et al., 2004). Thus, early β -catenin triggers the formation of two signalling centers at the blastula stage, the Nieuwkoop center being involved in dorsal

endoderm development and the BCNE center that is involved in neural specification (De Robertis and Kuroda, 2004).

1.4 Neural Induction

The Spemann-Mangold organizer secretes a variety of growth factor antagonists that can induce neural tissue. Bone Morphogenic proteins (BMPs), including BMP2 and BMP4, act within the ectoderm to induce epidermis. Chordin, Noggin and Xnr3 are soluble antagonists of BMP signals. Chordin and Noggin can induce dorsal ectoderm to form neural tissue and dorsalize mesodermal cells that would otherwise form ventral mesoderm (Smith et al., 1993b; Sasai et al., 1994). Chordin and Noggin bind to BMP2 and BMP4, and in this way prevent the binding to their receptors (Piccolo et al., 1996; Zimmermann et al., 1996). Knock-down of *Chordin* using specific antisense morpholino oligonucleotides (MOs) results in embryos with reduced neural tissue and an expansion of ventral mesoderm. Moreover, the dorsalizing effect of lithium chloride (LiCl) treatment which leads to a stabilization of β -catenin, can be blocked by depletion of Chordin. Organizer explants injected with *Chordin* morpholinos lose their neural-inducing activity (Oelgeschläger et al., 2003). Xnr3 lacks the mesoderm inducing capacity that is characteristic for other members of the Xnr family. Xnr3 is able to induce neural differentiation in animal caps and can antagonize BMP signalling (Hansen et al., 1997; Haramoto et al., 2004).

Beside the repression of BMP signals, neural induction requires the blockage of Wnt signalling. The organizer expresses Frzb-1/sFRP3, Crescent and sFRP2, which encode soluble Wnt antagonists of the secreted Frizzled-related protein (sFRP) family (Leyns et al., 1997; Pera and De Robertis, 2000; Chapman et al., 2004). sFRPs are homologous to the ligand-binding domain of the Wnt receptor Frizzled and sequester Wnt proteins in the extracellular space (Leyns et al., 1997; Kawano and Kypta, 2003). Dickkopf-1 (Dkk1) exhibits distinct expression in the dorsal endomesoderm of the gastrulating embryo and encodes a structurally unrelated extracellular inhibitor of Wnt signalling (Glinka et al., 1998). Dkk1 binds to the LDL receptor-related protein-5/6 (LRP5/6) that acts as a co-receptor for Wnt signals (Mao et al., 2001). Binding of Dkk1 triggers phosphorylation of the intracellular domain of LRP5/6 resulting in the

degradation of β -catenin (Tamai et al., 2004). The Dkk1-LRP5/6 complex associates with a second transmembrane protein called Kremen which promotes endocytosis and degradation of LRP5/6 (Mao et al., 2002). It could be shown that Dkk1-neutralizing antibodies inhibit head and prechordal plate formation, suggesting an important function of this Wnt inhibitor in anterior neural development (Glinka et al., 1998, Kazanskaya et al., 2000).

Cerberus is a secreted protein expressed in the anterior dorsal endoderm of gastrulating embryos and can induce ectopic head structures in the absence of trunk formation (Bouwmeester et al., 1996). Cerberus binds to and acts as a triple inhibitor of Nodal, BMP-4 and Wnt-8 ligands (Piccolo et al., 1999). Loss-of-function experiments in *Xenopus* revealed an important role of Cerberus for head induction, as specific antisense morpholino oligonucleotides inhibit head but not trunk/tail development (Kuroda et al., 2004).

Insulin-like growth factor-binding protein 5 (IGFBP-5) facilitates the neural-inducing activity of IGFs (Pera et al., 2001). Injection of *IGF2* mRNA leads to the induction of ectopic eyes and ectopic head-like structures containing brain tissue. In ectodermal explants, IGF signals can induce anterior neural markers in the absence of mesoderm formation, while injection of a dominant-negative IGF-receptor1 construct inhibits neural induction by the BMP antagonist Chordin. Thus, active IGF signals appear to be required and sufficient for anterior neural induction (Pera et al., 2001). Moreover, IGFs are inhibitors of Wnt signalling at the level of β -catenin. In *Xenopus* embryos, it could be shown that IGF-1 inhibits the β -catenin mediated activation of a luciferase reporter construct containing Tcf- binding sites, confirming that IGF-1 negatively regulates the Wnt pathway by directly preventing the β -catenin /Tcf complex from upregulating transcription of Wnt target genes (Richard-Parpaillon et al., 2002). It has been postulated that IGF-1 induces a rapid tyrosine-phosphorylation of β -catenin which may prevent interaction with its downstream effector Tcf (André et al., 1999; Richard-Papaillon et al., 2002).

Two additional inhibitors with distinct expression in the organizer are Follistatin which binds to and inhibits the mesoderm-inducer Activin, and Lefty-1/Antivin that is expressed in the anterior visceral endoderm where it inhibits Nodal signalling (Tashiro et al., 1991, Wessely et al., 2001; Perea-Gomez et al., 2002; Yamamoto et al., 2004).

On the other hand, the organizer expresses ADMP (anti-dorsalizing morphogenetic protein), which encodes a BMP3-like protein that suppresses Chordin and induces Smad1 signalling (Moos et al., 1995; Dosch and Niehrs, 2000; Reversade and De Robertis, 2005).

Several genes encoding secreted or cell-surface proteins are expressed on the ventral side of the gastrulating *Xenopus* embryos, although they play a role in neural induction. One of these factors is Crossveinless-2 (CV-2) that behaves as a BMP antagonist upon overexpression (Coffinier et al., 2002; Moser et al., 2003; Binnerts et al., 2004). The ventrally expressed factor Twisted gastrulation (Tsg) and the metalloprotease Xolloid-related (Xlr) help to maintain the proper amount of active BMPs in *Xenopus* embryos. The binding of BMP to its receptor can be prevented by the formation of a ternary complex consisting of Chordin, BMP and Tsg (Oelgeschläger et al., 2000; Chang et al., 2001, Scott et al., 2001; Ross et al., 2001; Blitz et al., 2003). Nevertheless, BMP can be released from this complex through a cleavage of Chordin by Xlr. This proteolytic cleavage can be facilitated by Tsg (Larrain et al., 2001; Oelgeschläger et al., 2003b). Tsg has a dual effect. Whether it promotes or inhibits BMP signalling depends on the abundance of Xlr, in such a way that high levels of Xlr promote BMP signalling whereas low levels repress it (Larrain et al., 2001; Oelgeschläger et al., 2003b).

The transmembrane protein Bambi resembles the type I BMP receptor, but lacks the serine-threonine kinase intracellular domain. Thereby, it functions as a cell surface inhibitor of BMP and Activin signalling (Onichtchouk et al., 1999). Another ventrally expressed inhibitor of BMP signalling is Sizzled (Salic et al., 1997). Microinjection of *Sizzled*-morpholinos (MOs) causes a ventralization of *Xenopus* embryos including an increase in ventral mesoderm and a reduction of the neural plate (Collavin and Kirschner, 2003). Sizzled is a competitive inhibitor of the proteolytic activity of Xlr.

Zebrafish embryos that carry a mutation in the *Xenopus* Sizzled homologue *ogon/mercedes* are ventralized and can be rescued by inhibition of BMP signalling (Hammerschmidt et al., 1996; Miller-Bertoglio et al., 1999; Wagner and Mullins, 2002).

Moreover, members of the Fibroblast Growth Factor (FGF) family have been shown to induce neural tissue. Targeted overexpression of FGFs in chick embryos stimulates neuronal differentiation in prospective epidermal tissue (Rodríguez-Gallardo et al., 1997). In *Xenopus*, basic FGF (bFGF) is a known mesoderm inducer that can also induce neural tissue in ectodermal explants of gastrula stage embryos (Lamb and Harland, 1995). Overexpression of *FGF8* in *Xenopus* does not only lead to an induction of ectopic neurons in ventral ectoderm, but also inhibits the expression of the early mesodermal marker *Xbra*. FGF8 signals through the FGF Receptor 4a (FGFR4a), since its effects on neurogenesis can be blocked by co-injection of a dominant negative FGFR4a (Hardcastle et al., 2000). Recently, a mechanism has been suggested to integrate various neural inducing signals based on differential phosphorylation of the transcription factor Smad1. BMP antagonists such as Chordin and Noggin prevent the phosphorylation of carboxy-terminal serines in Smad1, making it less active in inhibiting neural differentiation. IGF2 and FGF8 can trigger phosphorylation of the Smad1 linker region by MAPK. This phosphorylation further inhibits Smad1 activity and thus promotes neurogenesis (Pera et al., 2003). More recently, the Wnt signalling pathway could be integrated at the level of BMP/Smad1 phosphorylation. Coordinated phosphorylation at conserved MAPK and GSK-3 sites leads to polyubiquitination and subsequent proteosomal degradation of Smad1 at the centrosome (Fuentealba et al., 2007).

In conclusion, neural induction in *Xenopus* is triggered by a complicated network of signalling pathways that controls the expression of dorsalizing and ventralizing genes in the correct places.

1.5 Anterior-posterior patterning of the nervous system

The signals emanating from the organizer are thought to drive anterior-posterior patterning of the nervous system in *Xenopus* embryos (Yamada, 1994; Gould and Grainger, 1997; Harland and Gerhart, 1997; Sasai and De Robertis, 1997; De Robertis and Kuroda, 2004; Niehrs et al., 2001). Anterior-posterior patterning of the dorsal ectoderm takes place at early gastrula stages and occurs in a stepwise fashion with anterior fates being induced before posterior fates (Nieuwkoop et al., 1985; Sive et al., 1989; Sharpe and Gurdon, 1990; Thomas and Beddington., 1996). First, dorsal ectoderm receives a signal from the anterior dorsal mesendoderm that determines the anterior neural identity. This signal is referred to as the “activation” signal. The anterior structures include the presumptive forebrain and the non-neural cement gland. A second “transformer” signal, emanating from more posterior mesoderm, converts the neural tissue in a concentration-dependent manner into more posterior midbrain, hindbrain and spinal cord (Doniach, 1995). In addition to axial mesendoderm, lateral mesendoderm has low neural-inducing capacity and is able to induce expression of posterior markers (Kolm and Sive, 1997).

Several members of the FGF family, including FGF3, FGF4 (eFGF), FGF8 and FGF9 are expressed in the posterior dorsal, lateral and ventral mesoderm of *Xenopus* embryos (Isaacs et al., 1997). In ectoderm that is predisposed to become neural, FGFs can induce expression of posterior neural markers (Kolm and Sive, 1997). Inhibition of FGF signalling interferes with the induction of posterior fates (Holowacz and Sokol, 1999). FGFs have high affinities for glycosaminoglycan (GAG) side chains that are covalently attached to the protein core of extracellular proteoglycans, such as members of the biglycan, syndecan and glypican families. According to their sugar composition, the GAGs are classified as chondroitin sulfate, dermatan sulfate or heparan sulfate (Iozzo, 1998; Kramer and Yost, 2003). The secreted serine protease xHtrA1 triggers the cleavage of biglycan, syndecan-4 or glypican-4, thereby releasing soluble FGF-GAG complexes. In this way, FGFs are able to reach cells far away from the site of their synthesis and activate cognate receptors at distance (Hou et al., 2007).

Additional signals involved in the posteriorization of the central nervous system (CNS) are Wnt proteins (Wodarz et al., 1998). In *Xenopus*, *Xwnt3a* and *Xwnt8* are expressed in the posterior mesoderm and overexpression of both genes transforms anterior into more posterior neural tissue (McGrew et al., 1995; Fredieu et al., 1997). In contrast, blocking Wnt signalling by injection of a dominant-negative *Xwnt8* construct prevents posterior development in neuralized ectoderm (Bang et al., 1999). Consistent with this, extracellular antagonists of Wnt signals such as *Dkk1* and *Cerberus* induce expression of anterior, neural markers in naive ectoderm (Bouwmeester et al., 1996; Glinka et al., 1998; Pera et al., 2001). The actions of Wnt signals and Wnt antagonists are well conserved throughout vertebrates. Mutations in *wnt3a* and *wnt5a* cause loss of posterior structures in mouse embryos (Takada et al., 1994; Yamaguchi et al., 1999). On the other hand, mice that carry a mutation in the Wnt antagonist *Dkk1* lack head structures anterior to the midbrain (Mukhopadhyay et al., 2001). However, mouse embryos that carry a homozygous mutation in the Wnt inhibitor *Cerberus-like* (*cer-1*), resulting in null alleles, show no anterior patterning defects. This suggests that additional factors may compensate for the loss of *cer-1* in the mouse (Belo et al., 2000).

A third posteriorizing signal in the vertebrate embryo is the lipophilic molecule all-trans retinoic acid (RA). The receptors that transduce RA signals can be found in the presumptive hindbrain and more posterior in *Xenopus* gastrula embryos (Kolm and Sive, 1997). RA induces expression of posterior genes in naive ectoderm and downregulates the expression of anterior markers (Kolm and Sive, 1997). In zebrafish and mouse, exogenous RA treatment converts anterior hindbrain to a more posterior fate (Means et al., 1995). On the other hand, mutations of RA receptors in mice or retinoid deprivation in quail embryos lead to a deletion of the posterior hindbrain (Maden et al., 1996; Dupe et al., 1999).

There is evidence for a cross-talk between the three signalling pathways that lead to a posteriorization of the CNS. In *Xenopus* animal cap explants it could be shown that FGF8 induces expression of components that are involved in RA signalling and that, in turn, RA signalling is required for the correct expression of FGF8, FGFR4 and FGFR1 (Shiotsugu et al., 2004). Studies in chick embryos have revealed that FGF-signals keep cells in a stem cell like state in the tailbud by inhibiting RA synthesis

which drives differentiation of the cells. Moreover, FGF signals are sufficient and necessary for the expression of *wnt8c* in the neuroepithelium. As FGF signalling declines, *wnt8c* expression persists in the neuroepithelium and permits RA signal transduction. Once RA reaches sufficient levels, it acts to inhibit FGF signals and hence *wnt8c* expression. This mechanism mediates the transition from the proliferative undifferentiated caudal cell state to one in which differentiation and cell cycle exit are possible (Olivera-Martinez and Storey, 2007).

Anterior-posterior polarity in vertebrates is mediated by the expression of Hox genes which are homologous to the homeotic selector genes in *Drosophila*. Hox genes encode transcription factors with a conserved DNA-binding “homeodomain” sequence (Mc Ginnis et al., 1984; Scott et al., 1989). In vertebrates, up to 39 Hox genes are organized in four clusters located on four different chromosomes. Each cluster contains thirteen genes (Kessel and Gruss, 1990).

Similarly as the homeotic genes in *Drosophila*, the Hox genes located at the 3' end of a cluster are expressed first and anteriorly, while those located at the 5' end are expressed later and posteriorly (temporal and spatial colinearity; Mc Ginnis and Krumlauf, 1992). During gastrulation, Hox genes exhibit a characteristic expression profile in the trunk mesoderm and overlying neural plate with a sharp anterior boundary of gene expression and gradually decreasing transcript levels towards the posterior end of the embryo (De Robertis et al., 1991). The combinatorial gene expression of Hox genes, referred to as “Hox code”, specifies positional fate as reflected by the identity of vertebrae and embryonic hindbrain rhombomeres along the anteroposterior body axis (Kessel and Gruss, 1991; Kessel, 1992; Marshall et al., 1992). Tissue culture experiments and genetic studies in the mouse have revealed that RA induces 3'-Hox genes (Colberg-Poley et al., 1987; Breier et al., 1986, Kessel et al., 1987; Mavilio et al., 1988). In conclusion, anterior-posterior patterning of the CNS is controlled by combined actions of Wnt, FGF and RA signalling pathways. The effects of RA signals on anterior-posterior patterning are mediated by direct regulation of Hox gene expression.

1.6 Retinoids

Retinoids are small lipophilic molecules derived from vitamin A (retinol) with important roles during embryonic development and homeostasis (Ross et al., 2000). 11-cis retinal plays a major role in the visual cycle and constitutes together with the protein opsin the visual pigment rhodopsin (Lidén and Eriksson, 2006). In the developing embryo, all-trans retinoic acid (RA) is the most active naturally occurring metabolite (Thaller and Eichele, 1987; Scott et al., 1994; Horton and Maden, 1995). Excessive administration of retinoids has teratologic effects in *Xenopus* embryos, but retinol is 100-fold less efficient than RA in inducing axial defects (Durstun et al., 1989). Similarly, intraamniotic injection of retinoids cause dysmorphogenesis of rat embryos, with similar effects exerted by a 16-fold higher concentration of retinol than RA. Upon entry into the cell, RA binds to the nuclear receptors RAR and RXR which in turn act as DNA-binding transcription factors to control the activity of target genes (Thaller and Eichele, 1987; Chen et al., 1992; Scott et al. 1994; Kraft et al., 1994; Scadding and Maden, 1994; Horton and Maden, 1995; Costaridis et al., 1996). RA can act as a morphogen and specify in a concentration-dependent manner various tissue types in the developing embryo. 9-cis RA is generated from RA presumably through the action of a specific isomerase. It is present in *Xenopus* embryos and in the regenerating amphibian wound epidermis (Kraft et al., 1994; Viviano et al., 1996). Although it is undetectable endogenously in chick and mouse limb buds, it is very potent in inducing duplications of the chick wing bud (Thaller et al., 1993; Scott et al., 1994). A retinoid that is detectable in the chick limb bud is 3,4 didehydro-RA (Thaller and Eichele, 1990; Scott et al., 1994b). This retinoid is generated from 3,4-didehydro-retinol via 3,4-didehydro-retinal. It has the ability to respecify tissues in the embryo since it can induce duplications in chick wing buds (Thaller and Eichele, 1990). 4-oxo-RA is present in *Xenopus* embryos, where it has the capacity to bind to and signal through RAR β (Pijnappel et al., 1993). Eventhough it was thought to be a breakdown product of RA, it was shown to be potent in inducing neural defects in *Xenopus*. Moreover, it is a more potent teratogen during mammalian development than RA (Kraft et al., 1992).

1.7 The morphogen retinoic acid

In the mammalian embryo, the RA-precursor retinol is provided from the maternal circulation via the placenta, whereas avian, reptilian, amphibian and fish embryos use retinoid stores in the egg yolk (Lampert et al., 2003). Retinol is taken up from the nutrition as pro-vitamin A forms. The pro-vitamin A forms are retinyl esters from animal products and carotenoids from plants (Maden, 2007). These dietary components are stored in the liver and in several extrahepatic sites, including the lungs, the bone marrow and the kidneys (Blomhoff and Blomhoff, 2006). Approximately 66-75% of dietary retinoids are taken up and stored as retinyl esters in the liver (Blaner and Olson, 1994; Vogel et al., 1999). The hepatic stores of retinol can be released into the circulation via interaction with Retinol Binding Proteins (RBPs) in the plasma (Goodman, 1984). However, alternative mechanisms for the retinol transport must exist *in vivo* as RBP null mutant mice are viable and fertile (Quadro et al., 1999). Most tissues have the capacity to store retinol prior to its use (Blaner and Olson, 1994; Vogel et al., 1999; O'Byrne et al., 2005). Retinol is esterified primarily through the actions of the enzyme Lecithin:Retinol Acyll Transferase (LRAT) (Yost et al., 1988; Saari and Bredberg, 1989; Herr and Ong, 1992; Batten et al., 2004). In the event of plasma retinol deficiency, hydrolysis of retinyl esters by an enzyme called REH (Cholate-independent Retinyl-Ester Hydrolase) mobilizes stored retinyl esters (Napoli et al., 1989; Harrison et al., 1989; Harrison and Napoli, 1990). Retinol is taken up by target cells through an interaction with a membrane receptor for RBP, STRA6 (Stimulated by Retinoic Acid 6) (Kawaguchi et al., 2007). In the cytoplasm, retinol binds to RBP1 and is metabolized in a two-step process to RA. The first step is an oxidation from retinol to retinal, mediated by alcohol dehydrogenases (ADHs) and retinol dehydrogenases (RDHs). Secondly, retinal is oxidized to RA by retinal dehydrogenases (RALDHs) (Clagett-Dame and De Luca, 2002). Alternatively, pro-vitamin A carotenoids can be directly enzymatically converted into retinal, the direct precursor of RA (Olson and Hayaishi, 1965; Goodman and Huang, 1965). This conversion is mediated by a β , β -carotene-15,15'-oxygenase (bcx) (von Lintig and Vogt, 2000; von Lintig and Wyss, 2001, Lampert et al., 2003).

Recently, a member of the cytochrome p 450 family of mono-oxygenases, CYP1B1, has been identified in chick embryos that contributes to RA synthesis during embryonic patterning. This enzyme can generate both, all-trans retinal and all-trans RA, from all-trans retinol (Chambers et al., 2006).

In many cell types, two cellular RA-binding proteins, CRABP1 and CRABP2, bind to the newly synthesized RA. RA enters the nucleus with the assistance of CRABP2 (Budhu and Noy, 2002) and binds to a transcription complex that includes a dimer of the RA receptors RAR and RXR. There are three RAR genes (RAR α , β and γ) and three RXR genes (RXR α , β and γ). Each of these molecules has several splicing isoforms. RARs bind all-trans RA, while RXRs bind to 9-cis RA (Chawla et al., 2001). RARs can also bind the 9-cis isomere of RA and form heterodimers with RXRs. Upon interaction with RA, the heterodimeric receptor pair binds to a DNA sequence called the RA-Response Element (RARE). In addition to ligand binding, phosphorylation of the receptors and recruitment of co-factors are involved in modulating RA-specific gene transcription (Bastien and Rochette-Egly, 2004).

The most sensitive method for detecting RA in the organism is high performance liquid chromatography (HPLC). Analyzing mouse embryos at embryonic day 10.5 (E 10.5) and 13 revealed high levels of RA in the spinal cord and lower levels in forebrain, midbrain and hindbrain (Horten and Maden 1995). RA signalling activity was detected in transgenic RARE-*lacZ* mice, in which several RARE copies were fused to the β -*galactosidase* reporter gene (Mendelsohn et al., 1991; Reynolds et al., 1991; Rossant et al., 1991; Balkan et al., 1992; Shen et al., 1992). In late gastrula embryos, robust RA reporter gene expression was found in the posterior half with an anterior border corresponding to the anterior end of the primitive streak. At early somite stages, a sharp boundary of transgene expression demarcates the level of the first somite, at the junction between the future hindbrain and spinal cord. Later, transgene expression is apparent in the somites, developing heart, lens and neural retina, the endoderm layer of the developing gut, the mesenchyme at the base of the developing limb buds and the cervical and lumbar regions of the developing spinal cord (Reynolds et al., 1991; Balkan et al., 1992; Colbert et al., 1993; Moss et al., 1998). In *Xenopus*, HPLC-based measurements of RA have been contradictory.

Some investigators described a posterior to anterior gradient at the neural plate stage, while other studies reported a higher concentration of RA in the anterior part of the embryo (Chen et al., 1994; Creech-Kraft et al., 1994). *Xenopus* embryos, which were either injected with RARE-*lacZ* mRNA or transgenic for the RARE-*GFP* construct, show active RA signalling in the dorsal gastrula, as well as the dorsal midline and anterior head regions of neurula embryos (Yelin et al., 2005).

1.8 Vitamin A deficiency and excessive RA treatment reveal essential functions of retinoids during embryonic development

RA is an important modulator of cell survival, cellular proliferation and differentiation. Moreover, this signal plays important roles during pattern formation and organogenesis in vertebrate embryos (Glover et al., 2006; Mark et al., 2006). If vitamin A is excluded from the diet during pregnancy, congenital malformations can be observed in the offspring. These include hydrocephalus, *spina bifida*, anophthalmia, microphthalmia and patterning abnormalities of the CNS (Maden, 2002). At lower frequency cleft palate and lip, accessory external ears and arrested ascension of the kidney were reported (Hale et al., 1933). Experiments in the rat revealed additional defects in the developing genito-urinary tract, diaphragm, lung, aortic arch and heart (Wilson and Warkany, 1948; Wilson and Warkany, 1949).

Knockout experiments in mice, in which several RARs have been inactivated, phenocopy vitamin A deficiency in several aspects, but also reveal defects of the ocular and salivary glands and their ducts as well as skeletal abnormalities of forelimbs, hindlimbs and the cervical region of the axial skeleton. *RAR α* mutant mice display webbed digits on both forelimbs and hindlimbs, while *RAR γ* mutants show several congenital abnormalities including tracheal cartilage malformations and homeotic transformations along the cervical axial skeleton (Grondona et al., 1996).

On the other hand, an excess of RA in the diet of pregnant animals can cause exencephaly, *cranium bifidum*, microcephaly, microphthalmia and *spina bifida* (Cohlan, 1953; Langman and Welch, 1967). A daily oral administration of RA to pregnant pigtail monkeys (*Macaca nemestria*) results in a high frequency of craniofacial and musculoskeletal malformations. Craniofacial defects including cleft palate were reported as well as ectrodactyly, kyphosis, and muscular-joint contractures. Less frequently, transposition of the great vessels of the heart, polycystic kidney and associated urogenital anomalies occur (Fantel et al., 1977).

These studies indicate that RA plays important roles during embryonic development and that the concentration of this signalling molecule needs to be tightly regulated.

1.9 Retinoic acid signalling during organogenesis

Subsequent studies revealed that RA is involved in the formation of several embryonic structures and organs including limbs, somites, heart, pancreas, lung and the genito-urinary tract. In some cases, RA signalling acts through modulating other signalling pathways (Duester, 2008). Exogenous RA administration alters anterior-posterior patterning of the chick limb bud or proximodistal patterning of regenerating axolotl limbs (Tickle et al., 1982; Maden, 1983). Later, it was demonstrated that RA-bead implants ectopically induce *Sonic Hedgehog (Shh)* gene expression and that Shh controls limb anterior-posterior patterning (Riddle et al., 1993). Earlier studies in the chick limb bud suggest an RA morphogen gradient with highest concentration in the posterior zone of polarizing activity (Thaller and Eichele, 1987). However, studies in mouse embryos demonstrated that RA in early limb buds is distributed uniformly across the anterior-posterior axis but decreases from proximal to distal (Mic et al., 2004). In the absence of RA synthesis, forelimb buds do not develop and embryonic growth ceases prior to the stage when hindlimb buds are initiated (Niederreither et al., 2002; Mic et al., 2004). In zebrafish, the absence of RA synthesis blocks the induction of pectoral fin buds (Gilbert et al., 2006).

During somitogenesis, RA can repress caudal *Fgf8* expression in mouse embryos (Vermot et al., 2005; Sirbu and Duester, 2006). In chick embryos, it could be shown that RA attenuates Fgf8 signalling in the neuroepithelium and paraxial mesoderm, in order to control somite boundary position. (Diez del Corral et al., 2003). Experiments in mouse, chick and zebrafish embryos demonstrated that RA is required to retain bilateral symmetry of the left and right columns of somites (Kawakami et al., 2005; Vermot et al., 2005; Vermot and Pourquie, 2005, Sirbu and Duester, 2006).

RA is required for anterior-posterior patterning of the heart tube. In mice, loss of RA synthesis leads to a severe reduction of the atria/inflow tract domain. The outflow tract/ventricular domain forms an abnormal cavity that is distended medially rather than undergoing rightward looping and septation into right and left ventricles. (Niederreither et al., 2001). Analysis of cardiac-specific genes suggested that the effects of RA on early heart development are mediated through repression of *Fgf8* expression in the posterior region of the heart (Ryckebusch et al., 2008; Sirbu et al., 2008).

In the developing pancreas, studies have focused on the homeobox transcription factor *Pdx1* which is required for pancreatic specification in the posterior foregut. Evidence suggests that RA may be the signal required for *Pdx1* initiation (Stafford and Prince, 2002). Zebrafish embryos, deficient in RA, lack *Pdx1* expression and consequently fail to induce pancreas development. Similar results have been obtained in mouse and *Xenopus* embryos (Chen et al., 2004; Martin et al., 2005; Molotkov et al., 2005). In *Xenopus* embryos, an RAR antagonist induces misspecification of dorsal pancreatic tissue while ventral endodermal pancreatic tissue and the liver are not effected, demonstrating that only the dorsal pancreas requires RA activity (Chen et al., 2004). Furthermore, RA signalling influences both, mesodermal and endodermal germayers, during pancreas development (Pan et al., 2007).

In the mouse, RA has been shown to be important for stimulation of posterior foregut endoderm to acquire a lung fate (Malpel et al., 2000). Embryos that lack RA signalling in the foregut fail to develop lungs (Wang et al., 2006).

RA controls some aspects of genito-urinary tract development. Analysis of *RAR* knockout mice showed that RA plays a key role in controlling epithelial / mesenchymal interactions during kidney development (Batourina et al., 2001). RA, generated in the urogenital sinus, stimulates apoptosis in the common nephric duct that is needed for the establishment of connections between the ureters and bladder (Batourina et al., 2005).

The involvement of RA in the generation of several different embryonic structures points towards the importance of this morphogen during development and explains the diversity of malformations observed upon aberrant RA signalling.

1.10 Effects of retinoic acid on the central nervous system

Excessive RA treatment in various vertebrates, including *Xenopus*, zebrafish, mouse and rat, causes loss of anterior structures such as the forebrain and eyes and an anteriorwards expansion of hindbrain and spinal cord (Durstion et al., 1989; Maden et al., 2002; Cunningham et al., 1994; von Bubnoff et al., 1996; Simeone et al., 1995; Zhang et al., 1996; Avantaggiato et al., 1996). Consistent with this, injection of a constitutively active *RAR* α 1 construct into *Xenopus* embryos reduces anterior structures. On the other hand, injection of a dominant-negative *RAR* α 1 construct enlarges anterior structures, shortens the tail and reduces the overall length of the body axis (Blumberg et al., 1997).

More detailed analysis of RA treated embryos in various vertebrates revealed a shortened preotic hindbrain and loss of posterior rhombomere segmentation (Morriss-Kay et al., 1991; Papalopulu et al., 1991; Holder and Hill 1991; Sundin and Eichele, 1992; Wood et al., 1994; Cunningham et al., 1994; Lopez et al., 1995; Simeone et al., 1995; Lee et al., 1995; Leonard et al., 1995; Zhang et al., 1996). In mouse embryos, molecular markers suggested that excessive RA, applied before the onset of somatic segmentation, causes a loss of the anterior hindbrain rhombomeres 1-3 and formation

of a single large rhombomere presumably of rhombomere 4 identity (Wood et al., 1994; Maden et al., 2002).

In contrast, a decrease in RA signalling results in a loss of posterior hindbrain rhombomeres. In quail embryos, depriving vitamin A from the diet leads to a loss of rhombomeres 4, 5, 6 and 7. The remaining rhombomeres 1-3 expand in size (Gale et al., 1996; Maden et al., 1996). In RA deficient rat embryos, an enlarged rhombomere 4 can be found suggesting that the whole hindbrain needs adequate RA levels to develop properly (White et al., 1998; White et al., 2000). In chick embryos that have been treated with an RA antagonist at different concentrations or at various times of development, a gradual decrease of RA signalling coincides with a sequential loss of posterior rhombomeres (Dupe and Lumsden, 2001). More careful analysis showed that the sequential loss of rhombomeres is preceded by a rhombomere boundary loss. While mice deficient for a single RAR exhibit a normal hindbrain phenotype, *RAR α -RAR β* double knockouts have fused rhombomeres 6 and 7 and an expanded rhombomere 5 (Dupe et al., 1999). Compound *RAR α -RAR γ* mutants have a similar phenotype to RA deficient embryos with missing posterior rhombomeres and expanded anterior rhombomeres (Wendling et al., 2001). Interestingly, these hindbrain-specific phenotypes can be mimicked by treating mouse embryos with pan RAR antagonists. Treatment at day 7 of embryonic development (E7) phenocopies the *RAR α -RAR γ* -loss of function phenotype, while treatment at E8 phenocopies the *RAR α -RAR β* phenotype. This indicates that RAR α -RAR β function later to form the rhombomere 6/7 boundary, after the boundaries between rhombomeres 3 to 6 have been formed with the help of RAR α -RAR γ (Maden, 2002).

Data from *Xenopus*, zebrafish and mouse indicate that treatment with lower doses of RA leads to a transformation of anterior hindbrain rhombomeres into progressively more posterior ones (Holder and Hill, 1991; Marshall et al., 1992; Manns and Fritsch, 1992). In the mouse, low doses of RA lead to an anteriorwards shift of the *Hoxb1* expression domain, giving rise to two stripes, one of them corresponding to the future rhombomere 2. The nerve that emerges from this rhombomere resembles the facial nerves that usually emerge from rhombomere 4, while rhombomere 3 changes its neuronal characteristics to resemble rhombomere 5 (Marshall et al., 1992; Kessel,

1993). Further studies on *Hoxb1* in the mouse have revealed that it is regulated by a RARE sequence, located 3' to the promoter. Under normal circumstances, this element is required for early widespread induction in the posterior hindbrain up to the presumptive rhombomere 3/4 boundary (Marshall et al., 1994). Interestingly, another RARE located 5' to the promoter is required for repression of *Hoxb1* in rhombomeres 3 and 5 to limit its expression to rhombomere 4 (Studer et al., 1994). Additionally, repression of *Hoxb1* in rhombomere 5 depends on the homeodomain protein vHnf1 β which is expressed in response to RA in the posterior hindbrain up to the rhombomere 4/5 boundary (Wiellette and Sive, 2003; Sirbu et al., 2005; Hernandez et al., 2004).

RA plays a role in the dorsal-ventral specification of neurons in the spinal cord. When naive neural plate tissue from quail embryos is cultured in the presence of retinol, certain subtypes of interneurons, characterized by the expression of the homeobox genes *Dbx1*, *Dbx2*, *Evx1*, *Evx2* and *En1*, are induced (Pierani et al., 1999). In chick embryos, it could be shown that RA increases the population of caudally projecting interneurons, thus not only influencing their specification but also their axonal orientation (Shiga et al., 1995). RA seems to act on the interneuron progenitors by inducing *Dbx1* and *Dbx2* expression via suppression of *Shh* (Pierani et al., 1999). Moreover, exposure of neural plate cells to both *Shh* and RA induced *Olig2* expression which acts as a transcriptional repressor to direct the expression of downstream homeobox genes and motor neuron identity (Mizuguchi et al., 2001; Novitch et al., 2001; Scardigli et al., 2001; Rowitch et al., 2002; Novitch et al., 2003; William et al., 2003). Conversely, electroporation of a dominant-negative RAR α receptor into neural plate cells prevents the expression of *Olig2*. RA deficiency in quail embryos leads to a loss of interneuronal populations, while ventral neuronal populations have expanded at the expense of dorsal neurons. This could be shown by the downregulation of the ventral genes *Pax6*, *Irx3*, *Nkx6.2*, *Olig2* and *En1* (Diez del Corral et al., 2003; Wilson et al., 2004; Molotkova et al., 2005). In mouse and quail embryos, RA plays a role in the specification of a subset of motor neurons. The lateral motor column neurons (LMCs) are induced in regions of high RA activity in the spinal cord at branchial and lumbar somitic levels (McCaffery et al., 1994; Ensini et al., 1998). The LMC neurons can be divided into a medial group (LMCM) which projects to ventral muscles, and a lateral group (LMCL) that projects to dorsal

muscles (Maden, 2006). Chick neural tubes have decreased numbers of LMCLs when cultured in the presence of RAR antagonists (Sockanathan and Jessel, 1998). The electroporation of a dominant-negative RAR α into the branchial spinal cord inhibits LMCL production and reduces the projection of motor neurons into the limbs (Sockanathan et al., 2003).

In fish and amphibians, RA signalling is known to control the number of primary neurons. In the case of *Xenopus*, three parallel rows of motoneurons, interneurons and sensory neurons develop on each side of the trunk. These primary neurons are responsible for coordinating escape movements (Sharpe and Goldstone, 2000). Addition of RA to the embryos leads to an increase of the number of primary neurons (Papalopulu and Kintner, 1996; Franco et al., 1999; Sharpe and Goldstone, 2000). Injection of *RAR α 2* and *RXR β* mRNA into the embryo has the same effect (Sharpe and Goldstone, 1997; Sharpe and Goldstone, 2000). In contrast, administration of the RA synthesis inhibitor citral or injection of dominant-negative RAR α 2 decreases the number of primary neurons (Blumberg et al., 1997; Sharpe and Goldstone, 1997; Franco et al., 1999; Sharpe and Goldstone, 2000). Moreover, RA signals can upregulate the neuronal prepattern genes *X-ngnr-1* and *X-myl1* and downregulate genes that inhibit neurogenesis such as *Zic2* and *X-shh* (Franco et al., 1999; Maden, 2002).

Moreover, RA affects neural differentiation in other model systems. When added to murine embryonal carcinoma cells, RA induces differentiation of neurons and glia cells (Jones-Villeneuve et al., 1982; McBurney et al., 1982). RA also acts as a differentiation agent in various embryonal carcinoma cell lines, teratocarcinoma cells, stem cells and neuroblastoma cells of murine and human origin (Maden, 2001).

In conclusion, RA is involved in pattern formation of the CNS as well as in neuronal differentiation and specification.

1.11 Retinal dehydrogenases

In most tissues, RA is produced via a two-step process in which retinol is first oxidized to retinal and then in an irreversible reaction to RA. The second NAD⁺-dependent oxidation step is mediated by retinal dehydrogenases (aldehyde dehydrogenases: ALDHs). ALDHs typically consist of about 500 amino acid residues with active sites containing a catalytic cysteine residue (Perozich et al., 1999). Vertebrate ALDHs are responsible for the irreversible conversion of acetaldehyde to acetic acid, of retinal to retinoic acid and of many other physiological important aldehydes to carboxylic acids (Lindahl, 1992). The vertebrate ALDH family consists of at least 16 distinct members with RALDH1, RALDH2 and RALDH3 representing three cytosolic enzymes which are able to oxidize retinal to RA *in vitro* (Duester, 2009). RALDH2 has been shown to have a 15 fold higher catalytic efficiency than RALDH1 for retinal oxidation (Wang et al., 1996; Penzes et al., 1997).

In the mouse, *Raldh2* is the first retinal dehydrogenase to be expressed (Niederreither et al., 1997; Haselbeck et al., 1999). During gastrulation, mRNA is detected in the mesoderm adjacent to the node and primitive streak (Niederreither et al., 1997). At headfold stages, it is expressed in the trunk mesoderm anteriorly up to the level of the spinal cord / hindbrain border. Later, *Raldh2* expression localizes to a variety of tissues, including undifferentiated somites, mesenchyme surrounding the neural tube, developing gut, limb buds and distinct regions of the head. In addition, signals can be found in a subpopulation of motor neurons that innervate the limbs, in the heart, lungs, kidneys and eyes (Zhao et al., 1996).

Raldh2 knockout mice die at E10.5 due to heart failure. The embryos do not produce RA at the time when RA synthesis is normally initiated (E7.5-8.5). At E 8.5 they fail to undergo axial rotation and are shortened along the primary body axis at E 9.5. Internal defects include small somites, a lack of heart looping and chamber morphogenesis, which is the cause of lethality, a truncated frontonasal region, small otic vesicles, a lack of branchial arches 2 and 3, absent limb buds and *spina bifida* (Niederreither et al., 1999). Subsequent studies revealed a defect in hindbrain patterning. As shown by specific marker genes, including RA responsive Hox genes, rhombomeres 3 and 4 are more caudally expanded and rhombomeres 5 to 8 are reduced or lost (Niederreither et al., 2000).

The zebrafish *Raldh2* mutant called “neckless” (nls) displays truncation of the primary body axis anterior to the somites, defects in midline mesendodermal tissues and absence of pectoral fins (Begemann et al., 2001). Furthermore, the *Raldh2* mutant “no-fin” (nof) displays a lack of tissue in the branchial region and an oedema of the heart. The spinal cord marker *Hoxb6b* is reduced along the entire length of the spinal cord and the hindbrain is expanded. *Nof* embryos do not form swim bladders and die during early larval development (Grandel et al., 2002).

In *Xenopus*, *RALDH2* overexpression leads to a reduction of the forebrain territory and posteriorizes the midbrain as well as hindbrain rhombomeres 3 and 5 (Chen et al., 2001).

The other two RALDH enzymes, RALDH1 and RALDH3, appear later in development than RALDH2. In the mouse, RALDH1 protein is found from E 9 onwards in the dorsal retina, ventral mesencephalon, medial part of the otic vesicle and thymic primordium (Haselbeck et al., 1999).

Raldh1 knockout mice lack RALDH1 protein and RA in the embryonic dorsal retina and its axonal projections to the brain. However, they show no disturbance in dorsal-ventral patterning of the eye and the targeting of dorsal retinal axons to the brain still occurs. (Duester et al., 2003). It is assumed that loss of RALDH1 can be compensated by RALDH3 (Fan et al., 2003).

RALDH3 protein is first detected at E 8.5 in the rostral head and slightly later (E 9) in the surface ectoderm overlying the prospective eye field. At later stages, RALDH3 localizes to the ventral retina, dorsal pigment epithelium, lateral ganglionic eminence, dorsal margin of the otic vesicle and olfactory neuroepithelium (Li et al., 2000; Mic et al., 2000).

Chick embryos that have been injected with an ALDH inhibitor into the ectodermal site of *Raldh3* expression adjacent to the forebrain, show defects in frontonasal development (Schneider et al., 2001). *Raldh3* knockout mice exhibit eye and nasal defects. They show a shortening of the ventral retina and die at birth due to a blockage of the nasal passages (Dupé et al., 2003). The milder phenotype of RALDH1 and RALDH3 deficient mice as compared to animals with a RALDH2 deficiency, suggests that RALDH2 is the major RA-synthesizing enzyme during early embryonic development.

1.12 CYP 26 hydroxylases

A new insight into the regulation of RA signalling came with the identification of cytochrome P450 enzymes of the P26 subtype (Cyp26s) that oxidize RA to inactive products, such as 4-OH-RA, 18-OH-RA and 5,8-epoxy-RA (White et al., 1996; Fujii et al., 1997; White et al., 2000b). Due to their polar nature, these retinoid metabolites can be easily excreted from the cells. Cyp26A1, Cyp26B1, Cyp26C1 and Cyp26D1 have been cloned and analyzed in several vertebrates (Fujii et al., 1997; Hollemann et al., 1998; de Roos et al., 1999; Swindell et al., 1999; MacLean et al., 2001; Kudoh et al., 2002; Tahayato et al., 2003; Blentic et al., 2003; Reijntjes et al., 2003, 2004, 2005; Dobbs–McAuliffe et al., 2004; Emoto et al., 2005; Gu et al., 2005; Zhao et al., 2005; Hernandez et al., 2007).

In zebrafish, *Xenopus*, chick and mouse embryos, Cyp26A1 is initially expressed during gastrulation in the anterior neural plate which is fated to become the future forebrain and midbrain (Fujii et al., 1997; Hollemann et al., 1998; Swindell et al., 1999; Kudoh et al., 2002).

In *Cyp26A1*^{-/-} mice, the hindbrain and vertebrae are posteriorized and there is a severe caudal truncation with *spina bifida* and occasionally sirenomelia (Abu-Abed et al., 2001; Sakai et al., 2001). Sirenomelia, or mermaid-like phenotype, is a congenital malformation that is characterized by the fusion of the two hindlimbs into a single one. This phenotype is caused by a defect in the formation of ventral mesoderm during gastrulation (Zakin et al., 2005). In the hindbrain of *Cyp26A1* mouse mutants, rhombomere 3 is reduced and cells with rhombomere 4 identity expand into the rhombomere 2 region (Abu-Abed et al., 2001).

In *Xenopus*, ectopic expression of *CYP26A1* induces an anterior hindbrain duplication, which is reflected by a duplicated trigeminal ganglion and a posterior shift of *Krox20*, *Pax6* and *Hoxb3* expression (Hollemann et al., 1998).

Cyp26B1 mRNA shows a dynamic expression in the developing hindbrain that slightly differs between zebrafish, chick and mice (Zhao et al., 2005; Reijntjes et al., 2003; MacLean et al., 2001). Murine *Cyp26B1* is expressed distally in the limb buds. *Cyp26B1* null mutations in mice cause abnormalities in the limbs and craniofacial

skeleton as well as loss of germ cells from the testis, but no major hindbrain defects (Yashiro et al., 2004; McLean et al., 2007).

Cyp26C1 is also expressed in the hindbrain in a pattern that varies between species. *Cyp26C1* deficient mice are viable and have no obvious anatomical abnormalities (Uehara et al., 2007). In zebrafish, injection of *Cyp26C1* morpholino oligonucleotides alone or together with *Cyp26B1* morpholinos slightly shortens the hindbrain (Hernandez et al., 2007).

Cyp26D1 is expressed in the zebrafish hindbrain during early development. Overexpression of *Cyp26D1* shortens the distance between rhombomere 5 and the first somite of the injected embryos and results in left-right asymmetry of somitogenesis (Gu et al., 2006).

1.13 Retinol dehydrogenases

Several dehydrogenases, traditionally associated with alcohol metabolism have been found to participate in the oxidation of retinol to retinoic acid. Vertebrate alcohol dehydrogenases (ADHs) are responsible for the reversible conversion of ethanol to acetaldehyde, retinol to retinal and many other alcohols and aldehydes of physiological importance (Duester, 1999). They are members of the medium-chain dehydrogenase/reductase family (MDR), which mostly consists of enzymes of about 350 amino acid residues with active sites possessing catalytic zinc (Persson et al., 1994). Vertebrate ADHs consist of a family of cytosolic enzymes subdivided into eight classes with several of them being able to utilize retinoid substrates (Persson et al., 1994; Peralba et al., 1999; Duester et al., 1999). ADH1-7 are NAD(H) dependent, while ADH8 is NADP(H) dependent (Peralba et al., 1999). Genetic studies provide *in vivo* evidence that ADH1 accounts for about 90% of the oxidation of retinol when retinol is administered under supra-physiological conditions but it can also catalyze the NADH-dependent reduction of retinal to retinol (Boleda et al., 1993; Yang et al., 1994).

ADH1 is conserved across many species including teleosts, frogs, birds, rodents and humans (Duester et al., 1999). Humans possess three isoforms of ADH1, whereas rodents possess one form (Duester et al., 1999). *Adh1* exhibits restricted expression in many retinoid target tissues of the embryo such as epithelia of the genito-urinary tract, intestinal tract, liver, epidermis and lung. (Ang et al., 1996; Ang et al., 1996b). In the *Xenopus* embryo, *ADH1* expression is first localized to the pronephros anlage at the tadpole stage (st. 35) (Hoffmann et al., 1989).

ADH4 is most efficient among human ADHs for oxidation of all-trans retinol (Yang et al., 1994; Han et al., 1998). ADH4 shares 70% amino acid sequence identity with ADH1 and has been shown to efficiently catalyze oxidation of retinol to retinal in mouse, rat and human (Connor et al., 1987; Boleda et al., 1993; Yang et al., 1994; Han et al., 1998; Kedishvili et al., 1998; Duester et al., 1999). Its expression in several retinoid target tissues is suggestive of a role in retinol oxidation to produce RA. ADH4 does not play a major role in oxidation of large quantities of retinol but instead plays a role in vitamin A deficiency in maintaining sufficient metabolism of retinol (Duester, 2001). ADH4 expression is not detected in *Xenopus* embryos by whole mount *in situ* hybridization (Hoffmann et al., 1989).

In addition to cytoplasmic ADHs described above, several microsomal enzymes belonging to the short-chain dehydrogenase/reductase superfamily (SDR) exist that also participate in the metabolism of retinol to RA (Napoli, 1999; Duester, 2000). SDRs consist of approximately 250 amino acid residues. They have wide substrate specificities encompassing physiologically important alcohols and aldehydes such as hydroxysteroids and retinoids (Baker, 1996). The SDRs have been divided into five large families with different motifs in the co-factor binding site or active site and different chain lengths (Kallberg et al., 2002). Two of these five groups can be further subdivided into 7 subfamilies depending on their co-factor preference. The microsomal retinol dehydrogenases of the SDR superfamily (RDHs) generally display higher substrate specificity as compared with the ADHs (Duester, 2000). They catalyze the oxidation of different isomers of retinols as well as some steroids. The RDHs of the SDR family have an overall sequence similarity of at least 30 %. Among the conserved features is the N-terminal co-factor binding site (GXXXXGXXG, X representing any amino acid) and the catalytic site (YXXXXK). The enzymatic

reactions carried out by SDR enzymes can be grouped as mainly NAD(P)(H)-dependent oxidoreductases with a wide substrate diversity. In addition, many of the SDR RDHs display a conserved domain organization and most likely share a common folding and membrane topology (Liden and Eriksson, 2006).

The founding member of the microsomal retinol dehydrogenases is RDH5, which was identified in the retinal pigment epithelium of the bovine eye and catalyzes the oxidation of 11-cisretinol to 11-cis retinal in the visual cycle (Simon et al., 1995). Mutations in *Rdh5* are correlated with a disease called *fundus albipunctatus* which is characterized by stationary night blindness, accumulation of white spots in the retina and development of cone dystrophy (Yamamoto et al., 1999). Initial studies demonstrated that RDH5 is anchored to the ER membrane by two transmembrane domains (Simon et al., 1999). The catalytic ectodomain is facing the lumen of the ER and a short C-terminal tail of seven amino acids protrudes into the cytosol. It was shown that deletion of the cytosolic tail in RDH5 results in abolished enzymatic activity *in vivo* and mislocalizes the enzyme intracellularly (Tryggvason et al., 2001). The targeted deletion of murine *Rdh5* leads to a milder phenotype, suggesting a higher degree of redundancy in mice (Driessen et al., 2000).

RoDH1 (retinol dehydrogenase 1), RoDH2 and RoDH3 have been cloned from rat liver. Their human homologues have been shown to metabolize all-trans retinol as well as 3- α -hydroxysteroids (Chai et al., 1995, b; Chai et al., 1996; Gough et al., 1998; Kedishvili et al., 2001). RoDH1 utilizes all-trans retinol bound to CRBP1, which makes it a more specific enzyme for oxidation of all-trans retinol (Boermann and Napoli, 1995). RoDH2 has 82% sequence identity with RoDH1 and catalyzes the oxidation of all-trans retinol to all-trans retinal using NADP as a preferred co-factor (Chai et al., 1995b). RoDH2 has been shown to form stable complexes with the Cytochrome P450 CYP2D1 and this complex functions as a retinal reductase rather than the oxidation of retinal for production of RA (Imaoka et al., 1998; Duester, 2000). The microsomal SDR RoDH3 has been reported in the rat where it is only expressed in the adult liver while RoDH4 is much more efficient in oxidation of 3- α -hydroxysteroid androgens than in the oxidation of all-trans retinol (Chai et al., 1996, Gough et al., 1998).

The related enzymes cis-retinol/androgen dehydrogenase 1-3 (CRAD 1-3) metabolize 9-cis and/or all-trans retinol (Chai et al., 1997; Su et al., 1998; Zhuang et al., 2002). CRAD1 has been identified in the mouse and catalyzes NAD-dependent oxidation of cis-retinols much more efficiently than trans-retinols, while CRAD2 shows much higher activity for 11-cis retinol than for 9-cis retinol or all-trans retinol (Chai et al., 1997; Su et al., 1998). The microsomal SDR retSDR1 prefers NADPH as a co-factor and catalyzes the reduction of all-trans retinal to all-trans retinol in the mouse retina (Haeseleer et al., 1998). The reaction is essential for completion of the visual cycle.

1.14 Retinol dehydrogenase 10

An all-trans retinol dehydrogenase, denoted RDH10, has been identified in the retinal pigment epithelium in human, cow and mouse (Wu et al., 2002). RDH10 is a member of the SDR retinol dehydrogenase family. Human RDH10 recognizes all-trans retinol and cis-retinol as a substrate, indicating that it is involved in the generation of 11-cis retinal for vision and RA for differentiation and development. Silencing of endogenous *Rdh10* in human cells leads to decreased levels of retinal and RA indicating that RDH10 may function exclusively as an oxidizing enzyme (Belyaeva et al., 2008).

Recently, RDH10 has been characterized in the developing mouse embryo (Sandell et al., 2007, Cammas et al., 2007; Romand et al., 2008). A specific point mutation in the *Rdh10* locus has been obtained after treating mice with N-ethyl-N-nitrosourea (ENU; Sandell et al., 2007). These *Rdh10* mutants designated “trex” display craniofacial, organ and limb abnormalities and die at E 13.5 due to vascular defects. While the hindlimbs remain unaffected in mutant mice, the forelimbs are abnormally shaped and small. Other observed defects include misshapen optic vesicles, small otic vesicles, absent caudal pharyngeal arches, malformed cranial ganglia, and impaired neural crest cell patterning. Later in development, the cornea and the ventral half of the retina are missing, and the lens is hypoplastic (Sandell et al., 2007).

Detailed studies of *Rdh10* revealed that its expression sites correlate with regions of active retinoid signalling and *Raldh2* gene expression including the presomitic and somitic mesoderm, the cardiac region, the posterior branchial arches and the

developing kidneys (Cammass et al., 2007). Moreover, *Rdh10* shows distinct expression in the developing mouse brain, such as in the meninges, choroid plexus and striatum as well as in sensory organs like the neural retina and the inner ear (Rommand et al., 2008).

These data indicate, that the first step in RA biosynthesis, the conversion of retinol to retinal, is mediated in large part by tissue-specific expression of RDH10.

1.15 Aim of the study

The *Xenopus* homologue of the retinol dehydrogenase 10 (XRDH10) has recently been identified in a screen for secreted proteins of gastrula-stage embryos (Pera et al., 2005). The present study aims to characterize XRDH10 during early embryonic development with a focus on axis specification and patterning of the central nervous system. Topics to be addressed include the spatiotemporal gene expression of *XRDH10* and its comparison to the expression sites of *XRALDH2* and *XCYP26A1* in *Xenopus*. Then, the study aims to investigate the regulation of *XRDH10* transcription by RA signals. In mRNA microinjection experiments, the effects of XRDH10 will be studied in whole embryos and on RA target genes in embryonic explants. In gastrula embryos, effects of *XRDH10* mRNA and exogenous RA treatment will be compared during dorsal-ventral patterning. At the neurula and tailbud stage, effects on marker gene expression along the anteroposterior neuraxis will be studied and cooperative effects with *XRALDH2* investigated. A possible interaction of XRDH10 with its substrate, retinol, will be analyzed. In loss of function studies, specific antisense morpholino oligonucleotides will be microinjected to reveal the role of XRDH10 and *XRALDH2* during embryonic development, dorsoventral patterning and specification of the anteroposterior axis of the CNS. Particular emphasis will be given to the role of XRDH10 in the posteriorizing effect of retinol. Finally, a model is anticipated to explain the establishment of RA morphogen gradients in the early embryo.

2. Material and methods

2.1 Material

2.1.1 Chemicals

Basic chemicals were obtained from the companies Saveen Werner, Sigma, Roche, Applichem and Merck.

2.1.2 Solutions

AP buffer

100 mM Tris-HCl, pH 9.5, 50 mM MgCl₂, 100 mM NaCl, 0.1 % Tween-20, prepared in double distilled water (dd H₂O) just before use

Boehringer Block (BMB) 10 %

1 x MAB, 10 % BMB (Roche), dissolved at 60 °C in dd H₂O and stored at -20 °C

Citral

Citral (Sigma) stock solution (40 mM in 70 % ethanol) diluted in 0.1 x MBS

Diethylpyrocarbonate (DEPC) water

0.1 % diethylpyrocarbonate (Applichem), 500 ml dd H₂O, incubated at 37 °C for two hours and autoclaved

Disulfiram

Disulfiram (Sigma) stock solution (250 mM in DMSO) diluted in 0.1 x MBS

Ficoll 10 %

10 g Ficoll (Sigma) in 100 ml dd H₂O

Gelatine/albumine

1.1 g gelatine (Merck) in 22.5 ml 10 x PBS and 225 ml dd H₂O dissolved at 65 °C, 67.5 g albumine (Sigma) and 45 g sucrose added, stored at -20 °C in 50 ml aliquots

Human chorionic gonadotropin (Sigma)

resuspended in 5 ml autoclaved H₂O, stored in 1 ml aliquots at -20 °C

Hybridization solution

10 g Boehringer Block (Roche), 500 ml formamide, 250 ml 20 x SSC, incubated at 65 °C for 1 hour, 120 ml DEPC water, 100 ml torula RNA (10 mg/ml in water, filtered, Roche), 2 ml heparin (mg/ml in 1 x SSC, Sigma), 5 ml 20 % Tween-20, 10 ml 10 % CHAPS, 10 ml 0.5 M EDTA

Injectionbuffer

1 % Ficoll (Sigma) in 0.1 x MBS

L-cysteinhydrochloride

4 g L-cysteinhydrochloride (Applichem) in 200 ml 0.1 x MBS, pH adjusted to 8.0

Loading dye

4 ml glycerol, 2.5 ml Tris (1 M, pH 6-8), 2 ml β-mercaptoethanol, 0.8 ml SDS, 0.02 % Bromphenole Blue (VWR)

5 x MAB

500 mM maleic acid, 750 mM NaCl in dd H₂O, pH adjusted to 7.5, autoclaved

5 x MBS (Modified Barth Solution)

440 mM NaCl, 12 mM NaHCO₃, 5 mM KCl, 50 mM HEPES (pH 7.0), 4.1 mM MgSO₄, 2.05 mM CaCl₂, 1.65 mM Ca(NO₃)₂ in dd H₂O, pH adjusted to 7.4, autoclaved

10 x MEM

1 M MOPS, 20 mM EDTA, 10 mM MgSO₄ in ddH₂O

1 x MEMFA

10 ml 10 x MEM, 10 ml 37 % formaldehyde, 80 ml dd H₂O

Nile Blue

0.5 M Na₂HPO₄, 0.5 M NaH₂PO₄, adjusted to 500 ml with dd H₂O, pH adjusted to 7.8, adjusted to 1 L with dd H₂O, 0.1 g Nile Blue Chloride (Sigma) added, dissolved at 50 °C over night

10 x PBS

80 g NaCl, 2 g KCl, 14.4 g Na₂HPO₄, 2.4 g KH₂PO₄, dissolved in 800 ml dd H₂O, pH 7.4, adjusted to 1 L with dd H₂O

PBSw

1 x PBS with 0.1 % Tween-20

PBSw with proteinase K

10 µl proteinase K (0.01 mol/L, Sigma) in 20 ml PBSw

Red-gal staining solution

100 µl 0.1 M K₃Fe(CN)₆, 100 µl 0.1 M K₄Fe(CN)₆, 4 µl 0.1 M MgCl₂, 10 µl 5-bromo-6-chloro-3-indolyl-β-D-galactopyranoside (Red-gal, 40 mg/ml in DMSO Sigma) in 1.75 ml 1 x PBS

Retinal solution

All-trans retinal (Sigma) stock solution (200 mM in ethanol) diluted in 0.1 x MBS

Retinol solution

All-trans retinol (Fluka) stock solution (50 mM in DMSO) diluted in 0.1 x MBS

RA solutions

All-trans-RA stock (Sigma) solution (100 mM in DMSO) diluted in 0.1 x MBS or 1 x MBS

Staining solution for *in situ* hybridization

1.75 μ l nitro-blue-tetrazolium (NBT, Merck), 3.5 μ l 5-bromo-4-chloro-3-indolyl phosphate (BCIP, Fermentas) in 1 ml AP buffer

20 x SSC

175.3 g NaCl, 88.2 g sodium citrate dissolved in 800 ml ddH₂O, pH 7.0, adjusted to 1 L with dd H₂O, autoclaved

50 x TAE buffer

48,4 g Tris-base (Merck), 114.2 ml acetic acid, 0.5 M EDTA, pH 8.0, adjusted to 1 L with dd H₂O

TE buffer

10 mM Tris-base (Merck), 1 mM EDTA in dd H₂O

Tris buffer (pH 9.5)

121 g Tris-HCl (Merck) in 1 L dd H₂O, pH adjusted to 9.5, autoclaved

Tris buffer (pH 7.4)

121 g Tris-HCl (Merck) in 1 L dd H₂O, pH adjusted to 9.5, autoclaved

2.1.3 Media and Antibiotics

Antibiotics

Ampicillin (Sigma) was applied to liquid bacteria cultures and Luria Bertani (LB) agarplates. It was prepared as a stock solution (100 mg/ml) in dd H₂O, aliquoted and stored at -20 °C.

Luria-Bertani (LB) medium

20 g LB (Duchefa Biochemie) was dissolved into 1 L ddH₂O and autoclaved for more than 20 minutes at 121 °C. It was stored at 4°C.

Luria-Bertani (LB) agar plates

1.5 % agar (Saveen Werner) and 20 g LB (Duchefa Biochemie) were dissolved in 1 L dd H₂O and autoclaved for at least 20 minutes at 121 °C than cooled to 50 °C before ampicillin (100 µg/ml, Sigma) was added. The plates were poured in a sterile hood.

1 % agarplates

1 g agarose standart (Saveen Werner) was dissolved in 100 ml dd H₂O applying heat. The solution was poured into petridishes which were stored at 4 °C.

2.1.4 Morpholino-Oligonucleotides (all from gene Tools Inc., USA)

XRDH10-morpholino-oligonucleotides

5` - GCA TCT CTA TTT TAC TGG AAG TCA T - `3

XRALDH2-morpholino-oligonucleotides

5` - GGA AGA ACT CGA GCA CTA TGT GCA T - `3

control- morpholino-oligonucleotides

5` - CCA ACT GCT CCA GGA CCG TTT GTG G - `3

2.1.5 Constructs

pCS2+*XRDH10*

A full-length cDNA clone of *XRDH10* in pcDNA3 was obtained by secretion cloning (Pera et al., 2005). The *XRDH10* cDNA was subcloned into the *XhoI* restriction sites of the pCS2+ vector. For sense RNA synthesis, the construct was linearized with *NotI* and RNA transcribed with SP6 RNA polymerase.

pBluescript II KS-*XRDH10*

Full-length cDNA of *XRDH10* was excised from pCS2+*XRDH10* and cloned into the *XbaI* and *HindIII* restriction sites of the pBluescript II KS-vector. For antisense RNA synthesis, the construct was linearized with *BamHI* and transcribed with T7 RNA polymerase.

pCS2+*XRDH10**

To generate the rescue construct pCS2+*XRDH10**, the wobbled nucleotides in codons 2-8 were exchanged via a two-step PCR-mutagenesis from pCS2+*XRDH10*, using the primers *XRDH10*-wob-F-1st (ATG CAT ATA GTC CTC GAA TTC TTT CTG GTC), *XRDH10*-wob-F-2nd (GCA TCG ATA TGC ATA TCG TCG TGG AAT TTT TTG TGG TC) and *XRDH10*-R (GCC TCG AGT TAA AAT TCC ATT TTT TGT TTC ATT G) and *Pfu*-polymerase (Stratagene). The final PCR products were inserted into the *ClaI* and *XhoI* restriction sites of the pCS2+ vector. To prepare sense RNA, the construct was linearized with *NotI* and transcribed with SP6 RNA polymerase.

pCS2+*XRALDH2*

A full-length cDNA clone of *XRALDH2* in pcDNA3 was obtained by secretion cloning (Pera et al., 2005). The *XALDH2* cDNA was subcloned into the *EcoRI* and *XhoI* restriction sites of the pCS2+ vector. For sense RNA synthesis, the construct was linearized with *NotI* and RNA transcribed with SP6 RNA polymerase.

pBluescript II KS-*XRALDH2*

Full-length cDNA of *XRALDH2* was excised from pCS2+*XRALDH2* and cloned into the restriction sites for *XbaI* and *HindIII* of the pBluescript II KS-vector. For antisense RNA synthesis, the construct was linearized with *BamHI* and transcribed with T7 RNA polymerase.

pCS2+m*RALDH2*

pCS2+m*RALDH2* was generated from pCMV-Sport6-*Aldh1a2* (Imagenes GmbH, Germany; IMAGE ID, 30471325) by subcloning the insert into the *EcoRI* and *XbaI* sites of pCS2+. To prepare sense RNA, the construct was linearized with *NotI* and transcribed with SP6 RNA polymerase.

pCS2+*XCYP26A1*

The construct was a kind gift from Prof. Tomas Pieler (Göttingen University, Germany). It was linearized with *NotI* and transcribed with SP6 polymerase to generate sense RNA. To generate antisense RNA, the construct was linearized with *EcoRI* and transcribed with T7 RNA polymerase.

pXEX-*βgal*

The construct was a kind gift from Prof. Richard Harland (UC Berkeley, CA, USA). To generate sense RNA, it was linearized with *XbaI* and transcribed with T7 RNA polymerase.

pCS2+*FoxG1*

For antisense RNA synthesis, the construct was linearized with *XhoI* and transcribed with SP6 RNA polymerase.

pGEM-T-*Rx2a*

For antisense RNA synthesis, the construct was linearized with *XhoI* and transcribed with SP6 RNA polymerase.

pGEM-*Krox20*

For antisense RNA synthesis, the construct was linearized with *XhoI* and transcribed with SP6 RNA polymerase.

pBluescript II KS-*En2*

For antisense RNA synthesis, the construct was linearized with *XbaI* and transcribed with T3 RNA polymerase.

pBluescript II KS-*Xlim-1*

For antisense RNA synthesis, the construct was linearized with *XhoI* and transcribed with T7 RNA polymerase.

pBluescript II KS-*Chordin*

For antisense RNA synthesis, the construct was linearized with *EcoRI* and transcribed with T7 RNA polymerase.

Goosecoid

For antisense RNA synthesis, the construct was linearized with *XhoI* and transcribed with T7 RNA polymerase.

pCS2+*ADMP*

For antisense RNA synthesis, the construct was linearized with *EcoRI* and transcribed with T7 RNA polymerase.

HoxD1

For antisense RNA synthesis, the construct was linearized with *EcoRI* and transcribed with T7 RNA polymerase.

pGEM1-*HoxC6*

For antisense RNA synthesis, the construct was linearized with *BamHI* and transcribed with T7 RNA polymerase.

pGEM3Z+*HoxB3*

For antisense RNA synthesis, the construct was linearized with *Hind III* and transcribed with T7 RNA polymerase.

pcDNA3-*Noggin*

For antisense RNA synthesis, the construct was linearized with *KpnI* and transcribed with SP6 RNA polymerase.

pCS2+*Frzb1*

For antisense RNA synthesis, the construct was linearized with *NotI* and transcribed with SP6 RNA polymerase.

pcDNA3-*sFRP2*

For antisense RNA synthesis, the construct was linearized with *NotI* and transcribed with SP6 RNA polymerase.

pcDNA3-*Crescent*

For antisense RNA synthesis, the construct was linearized with *NotI* and transcribed with SP6 RNA polymerase.

pGEM3Z+*XCRABP*

For antisense RNA synthesis, the construct was linearized with *EcoRI* and transcribed with SP6 RNA polymerase.

2.1.6 Enzymes

Proteinase K (Merck, 0.01 mol/L)

Pfu-Polymerase (Stratagene, 2.5 U/ μ l)

Restriction enzymes (Fermentas and NEB/Promega)

Reverse Transcriptase (Roche, 50 U/ml)

RNase A (Fermentas)

RNase T1 (Fermentas, 1000 U/ μ l)

RNase out (Invitrogen, 40 U/ μ l)

RNase free DNaseI (Fermentas, 1 U/ μ l)

SP6 RNA Polymerase (Fermentas, 20 U/ μ l)

Taq-Polymerase (Perkin Elmer, 5U/ μ l)

T4 DNA Ligase (NEB/Promega, 3 U/ μ l)

T3 RNA Polymerase (Fermentas, 200 U/ μ l)

T7 RNA Polymerase (Fermentas, 200 U/ μ l)

2.1.7 Reaction-kits

The following kits were used in this study according to the manufacturer's instructions.

QIAquick PCR Purification Kit (Qiagen)

QIAquick Gel Extraction Kit (Qiagen)

QIAGEN Plasmid Midi Kit (Qiagen)

Rneasy Mini Kit (Qiagen)

QIAprep Spin Miniprep Kit (Qiagen)

SP6 Message Machine in vitro transcription Kit (Ambion)

TNT Coupled Reticulocyte Lysate Systems (Promega)

2.1.8 Equipment

Centrifuges

Centrifuge 5415D (Eppendorf)

Sorvall RC-5B PLUS Superspeed Centrifuge (Kendro Laboratory Products)

Cooling Centrifuge 5417R (Eppendorf)

Computerhardware

Mac OS X

PC HP Compaq DC 5800

Computersoftware

Adobe Photoshop 5.0/6.0 (Adobe Systems Europe, Lt., Edinburgh, Scotland)

Multalin (<http://www.bioinfo.genotoul.fr/multalin/multalin.html>)

SignalP (<http://www.cbs.dtu.dk/services/SignalP>)

Gene Jockey (Biosoft, Cambridge)

Electroporator

E. coli pulser (Bio Rad Laboratories)

Electroporationcuvettes (Eurogentec)

Embryo manipulations

Gastromaster (XENOTEK)

Microinjecter (Eppendorf)

Pneumatic Pico Pump PV 820 (World Precision Instruments)

Flaming/Brown Micropipette Puller Model P-97 (Sutter Instrument Co.)

Glasscapillaries (Clark)

Gel documentation Unit Herolab UVT-20 M (Techtum Lab)

Histology

Vibratome type VT1200S (Leica)

Incubators

Bacteria culture incubator AK82 (INFO-RS AG)

Economy Incubator with fan, size 2 (Gallenkamp/Labassco)

Incubator WB 22 K (Mytrom)

Microliterpipets

Precision microliter pipettes Pipetman (Gilson)

Photometer Nanodrop-1000 (Saveen Werner)

Optic equipment

Stereomicroscope (H. Saur)

Microscope SMZ 1500 (Nikon)

Microscope MC 80 (Zeiss)

Camera Digital Sight DS-2 Mv (Nikon)

Euromex Fiber Optic Light Source EK-1 (H. Saur)

PCR-Cycler

T3 Thermocycler (Biometra)

pH-meter

MA 235 pH/Ion analyzer (Mettler Toledo)

Shaker/Stirrer

Shaker Polymax 1040 (Heidolph)

Vortex Genie (Scientific Industries)

Stirrer RET Basic (KIKA Werke)

Thermoblock

Thermomixer Compact (Eppendorf)

2.1.9 Experimental organism

The African clawed frog *Xenopus laevis* was used as experimental organism during this study. Frogs were purchased from Nasco (Ft. Atkinson, USA). The embryonic staging was done according to Nieuwkoop and Faber (1994).

2.2 Methods

2.2.1 Comparison of RDH10 protein sequences

The 5'-end of the isolated *XRDH10* cDNA clone was sequenced and the translated protein sequence was used in a BLAST (Basic Local Alignment Search Tool) search to find orthologues (<http://www.ncbi.nlm.nih.gov/>). The program Multalign was used to compare the sequences (<http://www.bioinfo.genotoul.fr/multalin/multalin.html>). The signalpeptide was identified with the help of the program SignalP (<http://www.cbs.dtu.dk/services/SignalP>).

2.2.2 Restriction digest of plasmid DNA

Plasmid DNA (5 µg) was digested with the suitable restriction enzymes (Fermentas/NEB, Promega). Linearized products were used for *in vitro* transcription for either sense RNA to be used for microinjections, or antisense RNA labeled with digoxigenin for *in situ* hybridizations. The digest was performed, using 2 to 5 units of restriction enzymes per µg DNA.

In order to analyze the linearized DNA fragments, gel electrophoresis was performed. Agarose gels were prepared (0.8 %) in 1 x TAE buffer and 0.6 µg/ml ethidiumbromide. As running buffer, 1 x TAE buffer was used. A 1 kb molecular marker (0.1 µg/µl, Fermentas) was used to determine the size of the bands. The DNA bands were visualized with the help of UV-transillumination (Gel documentation unit Herolab UVT-20 M; Techtum Lab). Linearized plasmid DNA was purified using the QIAquick PCR Purification Kit (Qiagen) according to the manufacturer's instructions. After purification, the DNA was eluted in 30 µl DEPC water and stored at -20 °C.

2.2.3 *In vitro* transcription of sense RNA for microinjections

In order to transcribe sense RNAs for microinjections, the SP6 Message Machine *in vitro* transcription Kit (Ambion) was used according to the manufacturer's instructions.

The reaction mix was incubated at 37 °C for 2 hours. Afterwards, 4 µl of RNase free DNaseI (1 U/µl, Fermentas) were added. After an additional incubation at 37 °C for 30 minutes to digest the DNA template, the transcribed RNA was purified using the Rneasy Mini Kit (Qiagen). The RNA concentration was measured with the help of the Nanodrop-1000 (Saveen Werner).

2.2.4 *In vitro* transcription of antisense RNA for *in situ* hybridizations

Antisense RNA probes were transcribed *in vitro* and labeled with digoxigenin. The reaction mix contained 1500 ng of linearized plasmid DNA, 5 µl of 5 x transcription buffer (Fermentas), 4 µl of digoxigenin-NTP-mix (10 mM ATP, 10 mM GTP, 10 mM CTP, 6.5 mM UTP, 3.5 mM digoxigenin-11-UTP, Fermentas), 2 µl DTT (Fermentas), 0.5 µl RNase out (40 U/µl, Invitrogen), 1 µl polymerase (Fermentas), 0.5 µl pyrophosphatase (0.1 U/µl, Fermentas), DEPC water (up to 25 µl). After incubation for 2.5 hours at 37 °C, 4 µl DNaseI (1 U/µl, Fermentas) were added and the mix was incubated for additional 30 minutes to digest the DNA template. The transcribed RNA was purified using the Rneasy Mini Kit (Qiagen) according to the manufacturer's instructions. The RNA was eluted with 35 µl DEPC water into 30 µl formamide in an incubation step of 5 minutes at 65 °C and analyzed with gel electrophoresis using a 1 % agarose gel. The RNA was diluted in 1 ml hybridization mix and stored at -20 °C.

2.2.5 Preparation of antisense morpholino oligonucleotides

2 μ l of the concentrated morpholino oligonucleotide solutions (Gene Tools Inc.) were incubated at 65 °C for 5 minutes, spinned down and diluted with DEPC water to be used for microinjections.

2.2.6 TNT-assay

In order to test the specificity of the morpholinos, an *in vitro* transcription translation (TNT) assay was performed. 0.3 μ g of pCS2+ plasmids, containing either *XRDH10* or *XRALDH2* as inserts, were mixed with the concentrated morpholino solutions up to a volume of 5 μ l. A TNT mix was prepared that contained 6.25 μ l TNT lysate, 0.5 μ l TNT buffer, 0.25 μ l methionine, 0.25 μ l RNase out (40 U/ μ l, Invitrogen) and 0.25 μ l SP6 polymerase (20 U/ μ l, Fermentas). 0.8 μ l radioactive methionine were added to the mix. Of this mix, 8 μ l were added to the plasmid-morpholino mixture. The probes were incubated at 30 °C for 90 minutes and frozen over night at -80 °C. An SDS gel was prepared containing 5.93 ml dd H₂O, 3.75 ml 1.5 M Tris (pH 8.8), 5 ml Gel-30, 150 μ l 10 % SDS, 75 μ l 10 % APS and 15 μ l TEMED. The stacking gel contained 6.1 ml dd H₂O, 2.5 ml 0.5 M Tris (pH6.8), 1.33 ml Gel-30, 100 μ l 10 % SDS, 50 μ l 10 % APS and 10 μ l TEMED.

After polymerization of the gel, the probes were thawed and 1.25 μ l non-radioactive methionine (100 mM) were added. The probes were incubated for 5 minutes at 4 °C and mixed with 4 μ l of loading dye. After 5 minutes incubation at 95 °C the probes were mixed with loading buffer and together with a protein ladder (Fermentas) loaded onto the gel. Electrophoresis was performed at 110 mA and 120 V. After 1 hour the gel was fixed in 7 % acetic acid, 7 % methanol and 1 % glycerol in dd H₂O for 5 minutes. Then, the gel was placed between a Whatman Paper and plastic foil and dried over night at 70 °C. The dried gel was then exposed to an X-ray film (Hyperfilm ECL, Amersham Biosciences) over night.

2.2.7 Digest and purification of the pCS2-vector using gel extraction to generate pCS2+XRDH10*

4 µg of the recombinant pCS2-vector were digested with 3 µl *ClaI* (5000 U/ml, NEB Promega) and *XhoI* (20000 U/ml, NEB Promega). 10 µl Tango buffer (Fermentas) and 32 µl DEPC water were added to the mix. The reaction was incubated at 37 °C for 3 hours and analyzed on a 0.8 % agarose gel. Through UV-transillumination (365 nm) a 4 kb large band, representing the vector, was identified. This vector band was cut from the gel using a scapel blade and purified with the QIAquick Gel Extraction Kit (Qiagen) according to the manufacturer's instructions.

2.2.8 Ligation

The purified PCR product (see 2.1.5, pCS2+XRDH10*) was inserted into the pCS2+vector. Insert and vector DNA were quantified visually through gel electrophoresis using an ethidiumbromide-stained 0.8 % gel. For the ligation reaction, 1 µl of 10 x T4 buffer (NEB Promega), 0.4 µl (ca. 50 ng) of the empty vector, 2.5 µl (ca. 50 ng) of the PCR product, 1 µl of T4 ligase (3 U/µl; NEB Promega) and 5.1 µl of dd H₂O were mixed. The reaction was incubated at 16 °C for 3 hours. The product was analyzed on a 1.5 % agarose gel, followed by a control digest with *ClaI* and *XhoI*.

2.2.9 DNA transformation

For the electrotransformation, competent *E. coli* bacteria from the strain XL1 Blue were used. All steps until the application of the electric shock were performed on ice. A 40 µl aliquot of the competent bacteria was thawed on ice and carefully mixed with 1 µl of the ligation product. The mixture was applied to an electroporation cuvette (Eurogentec). The electroporation was performed with an electric pulse of 2.4 kV. Afterwards, 0.5 ml of LB medium were added to the electroporation cuvette. The bacteria suspension was transferred to a 15 ml tube and incubated for 30 minutes at 37 °C, shaking at a rate of 220 rpm. The bacteria suspension was poured onto an LB-agar

plate containing ampicillin (50 µg/ml, Sigma) and distributed with the help of sterile glass beads. This was followed by an incubation at 37 °C over night.

2.2.10 Colony PCR

From the agar plates, 9 different clones were picked and incubated for 4 hours in 100 µl LB-medium supplied with 50 µg/ml ampicillin (Sigma) at 37 °C. PCR reactions were performed as described under 2.2.21. The PCR mix contained 2.5 µl 10 x PCR buffer with MgCl₂ (Fermentas), 0.5 µl 10 mM dNTP-mix (Qbiogene), 2 µl primer (*XRDH10-wob-F-2nd* and *XRDH10-R*), 1 µl of bacteria culture, 0.5 µl *Taq*-polymerase (5 U/µl, Perkin Elmer) and 18.5 µl dd H₂O. The PCR products were analyzed on a 1.8 % agarose gel and one clone was found to contain pCS2+*XRDH10**.

2.2.11 Plasmid DNA preparation

50 µl of the bacteria suspension originating from the clone containing pCS2+*XRDH10** were added to 4 ml LB-medium with 50 µg/ml ampicillin (Sigma). The suspension was incubated over night at 37 °C. The plasmids were purified using the QIAprep Spin Miniprep Kit (Qiagen).

2.2.12 *In vitro* fertilization

Male *Xenopus laevis* were sacrificed to obtain the testes. The testes were rinsed in 1 x MBS, macerated and stored on ice. To induce ovulation, female frogs were injected with 1000 U of human chorionic gonadotropin (Sigma) into the dorsal lymph sac and kept at 16 °C over night. Ovulation occurred ca. 10 hours after the injection. The eggs were collected in glass petridishes. 100 µl of the testis-suspension were diluted 1:10 with H₂O in the petridish and dropped onto the eggs. After 10 minutes, 0.1 x MBS was added to the eggs to prevent them from drying out. After additional 35 minutes, the jelly coat surrounding the eggs was removed incubating them in a 2 % L-cystein

hydrochloride solution prepared in 0.1 x MBS (pH8.0). After several washing steps in 0.1x MBS, albino embryos were stained with the vital dye solution Nile Blue for 3 minutes to better visualize the developmental stages and facilitate the orientation of the embryos during the injection. Embryos were cultured in 0.1 x MBS. The determination of the developmental stage was performed according to Nieuwkoop and Faber (1994).

2.2.13 Microinjection of *Xenopus laevis* embryos

Microinjection needles were prepared from glass capillaries (Clark) using the Flaming/Brown Micropipette Puller Model P-97 (Sutter Instrument Co.). Sense RNA and morpholino-oligonucleotide solutions were back-filled into the needles using microloaders (Eppendorf). The microinjection apparatus (H. Saur) was connected to a Pneumatic Pico Pump model PV 820 (World Precision Instruments) and an N₂ gas supply. For the injections, embryos were transferred to injection buffer and placed onto glass slides in the correct positions.

2.2.14 Chemical treatments

All-trans retinoic acid (Sigma), all-trans retinol (Fluka) and disulfiram (Sigma) were dissolved in DMSO as 10 mM, 50 mM and 250 mM stock solutions. All-trans retinal (Sigma) and citral (Sigma) were dissolved in 70 % ethanol as 5 mM and 40 mM stock solutions. The stock solutions were diluted to the final concentrations in 0.1 x MBS for treatment of whole embryos and in 1 x MBS for treatment of animal cap explants.

2.2.15 Fixation of embryos

The embryos were fixed in MEMFA at 4 °C over night. Afterwards, they were rinsed 3 times in 1 x PBS and dehydrated in an ethanol series (25 % , 50 %, 75 % in 1 x PBS, 100 %). The embryos were stored in 100 % ethanol at -20 °C.

2.2.16 Red-gal staining

After a short fixation in MEMFA (45 minutes) at room temperature, the embryos were washed 3 times in 1 x PBS and stained with Red-gal staining solution over night at 4 °C to visualize the activity of the co-injected lineage tracer β -galactosidase. Afterwards, the embryos were fixed in MEMFA at 4 °C for several hours. After three washing steps with 1 x PBS they were dehydrated in an ethanol series and stored at -20 °C.

2.2.17 Whole mount *in situ* hybridization

The whole mount *in situ* hybridization was performed as described (Hollemann et al., 1998) over a period of three days.

Day 1:

Embryos were rehydrated through an ethanol series (75 %, 50 %, 25 % in 1 x PBS, 1 x PBS). Afterwards, they were washed with Ptw (4 x 5 minutes). The embryos were treated with 0.5 μ l/ml Proteinase K (0.01 mol/L, Sigma) diluted in Ptw for 3 minutes at room temperature. Washing steps in 0.1 M triethanolamine in dd H₂O (pH 7.5, 2 x 5 minutes) followed. Acetic anhydrid (12.5 μ l/4 ml triethanolamin) was added to the embryos (2 x 5 min). The embryos were washed in Ptw (2 x 5 min) and refixed in 4 % formaldehyde in 1 x Ptw for 20 minutes at room temperature. Afterwards, the embryos underwent 5 washing steps in 1 x Ptw (5 minutes each), and one washing step in hybridization mix (5 hours, 65 °C). The embryos were hybridized over night at 65 °C in hybridization mix containing the antisense RNA probes.

Day 2:

The antisense probes were removed and stored at -20 °C, to be reused, and replaced with hybridization mix. After an incubation step at 65 °C for 10 minutes, the embryos were washed three times in 2 x SSC, pH 7.0 (each step 5 minutes) at 60 °C. Unspecifically bound antisense RNA was digested by incubating the embryos in 2 μ l/ml RNase A (10 mg/ml diluted in TE buffer, Fermentas) and 0.1 μ l/ml RNase T1

(1000 U/ μ l, Fermentas), diluted in 2 x SSC for 60 minutes at 37 °C. Afterwards, the embryos underwent the following washing steps: 2 x SSC (10 minutes), 0.2 x SSC (2 x 30 minutes at 60 °C), 1 x MAB (2 x 15 minutes), 2 % BMB in 1 x MAB (20 minutes) and 2 % BMB, 20 % horse serum in 1 x MAB (40 minutes). The embryos were incubated with an anti-digoxigenin-alkaline-phosphatase conjugated antibody (Sigma), diluted 1:5000 in 2 % BMB, 20 % horse serum and 1 x MAB for 4 hours. Afterwards, they were washed in 1 x MAB for three times (10 minutes each step) and kept in 1 x MAB over night at 4 °C.

Day 3:

The embryos were washed 5 times in 1 x MAB for 5 minutes and 2 times in AP buffer for 5 minutes. For the staining reaction, AP buffer was substituted with an NBT/BCIP solution (1.75 μ l/ml NBT, Fermentas; 3.5 μ l/ml BCIP, Fermentas in APB). The embryos were incubated on ice under dark conditions, until the desired staining was obtained. The staining reaction was stopped by exchanging the staining solution with 100 % methanol. The embryos were then transferred through a methanol series (100 %, 75 %, 50 %, 25 %), dehydrated through an ethanol series and stored in 100 % ethanol at -20 °C.

2.2.18 Histological sections

The embryos were rehydrated through an ethanol series, transferred to 1 x PBS and subsequently to gelatine/albumine. They were placed into the embedding medium consisting of 1.5 ml gelatine/albumine supplied with 105 μ l glutaraldehyde. After complete polymerization of the medium, the embryos were sections using the Vibratome type VT1200S (Leica).

2.2.19 Animal cap explants

The embryos were cultured in 0.1 x MBS until they had reached mid-blastula stage (st. 8). The animal caps were excised with the help of a Gastromaster (XENOTEK) and cultured in 1 x MBS in petridishes coated with 1 % agarose. When embryos from the same fertilizations reached the late gastrula stage (st. 12), 8 to 10 animal caps were collected in 400 µl Trizol (Invitrogen) in a 1.5 ml microfuge tube and vortexed for 30 seconds. The tubes were frozen in liquid nitrogen and stored at -80 °C.

2.2.20 RNA extraction

The tissue, that was frozen in Trizol, was thawed and the tubes were vortexed for additional 30 seconds. This was repeated after addition of 80 µl chloroform. The probes were centrifuged for 15 minutes at 4 °C at 13000 rpm and the supernatant was transferred into new microfuge tubes to which 200 µl chloroform were added. An additional vortex step of 30 seconds was performed, followed by a centrifugation of 5 minutes at 4 °C, 13000 rpm. The supernatant was transferred into a new reaction tube and 200 µl of isopropanol were added. The probes were mixed well and incubated for at least 30 minutes at -20 °C. Afterwards, they were centrifuged for 30 minutes at 13000 rpm and 4 °C. The RNA pellets were washed with 400 µl 75 % ethanol in DEPC water by centrifugation for 5 minutes at 4°C and 1300 rpm. The supernatant was discarded and the RNA pellets were semi-dried at 56 °C. The pellet was resuspended in 30 µl DEPC water and heated to 55 °C for 10 minutes to facilitate the dissolving of the RNA.

2.2.21 Reverse transcription PCR

In order to quantify the expression levels of different genes in whole embryos and animal cap explants, the isolated RNA was reverse transcribed to cDNA followed by PCR reactions with gene specific primers. The reaction mix for the reverse transcription contained 2 μ l 25 mM MgCl₂ (Qbiogene), 1 μ l incubation mix without MgCl₂ (Qbiogene), 1 μ l dNTPs (10 mM dATP, 10 mM dGTP, 10 mM dCTP, 10 mM dTTP; Qbiogene), 0.5 μ l random hexamers (50 ng/ μ l; Invitrogen), 0.4 μ l reverse transcriptase (50 U/ml; Roche), 0.2 μ l RNase out (40 U/ μ l; Invitrogen), 1.5 μ l RNA (30 ng/ μ l) and 3.4 μ l DEPC water. The program for the reverse transcription consisted of the following steps:

22 °C for 10 minutes, 42 °C for 50 minutes and 99 °C for 5 minutes. The transcribed cDNA was used for PCR reactions using gene specific primers. The PCR reaction mix contained 5 μ l cDNA, 0.5 μ l 25 mM MgCl₂ (Qbiogen), 2 μ l incubation mix without MgCl₂ (Qbiogene), 0.75 μ l gene specific primer (forward and reverse primer, 7.5 μ M each, Invitrogen), 0.1 μ l *Taq*-polymerase (5 U/ μ l, Perkin Elmer) and 16.75 μ l dd H₂O. The PCR program consisted of the following steps: Predenaturing at 94 °C for 2 minutes, denaturing at 94 °C for 45 °C, annealing of the primers at temperatures between 56 °C and 60 °C, depending on the primers, for 45 seconds, elongation of the complementary DNA strands at 72 °C for 45 seconds and a final elongation step of 5 minutes at 72 °C. This program was repeated for 25 to 30 cycles depending on the primers. Annealing temperatures and cycle numbers for the different primers are shown in the table below.

Gene	Forward	Reverse	Annealing temperature	Cycles
<i>H4</i>	CGGGATAACATT CAG GGTATCACT	ACTCATGGCGGT AACTGTTCTTCC	56°C	25
<i>HoxD1</i>	CAGCCCCGATTA CGATTATTATGG	CCGGGGGAG GCA GTTTTG	56°C	30
<i>Gbx-2</i>	CCCCCAAAA CTC AAACCCTTC TAA	TGGCTCGCGTAT GGCAAACCTATT	56°C	30
<i>Meis3</i>	CAGCACGGGGGA TGATGATAGTC	ACCTCCTTGCCC TGTGCGATTAGA	56°C	30
<i>Xcad-3</i>	GGATCACCGAGG GAGGAATG	TAAGAGCGCTGG GTGAGT	56°C	28
<i>XRDH10</i>	CTCAATAATGCC GGGGTGGTCTCA	GATCGCTCTCAT GGCCTGGTT CA	60°C	28
<i>XRALDH2</i>	ACTTCCCCCTGC TGATGTTTG	TAGTCTGGGGTC CTTGCTCTGTAG	56°C	28
<i>XCYP26</i>	GCTGCCACGTCC CTCACCTCTTTT	GCCGATGCAGCA CCTCACTCC A	60°C	28

Tab.1. Primers for RT-PCR

3. Results

3.1 Protein structure of *Xenopus* RDH10

XRDH10 was isolated as a full-length cDNA clone by secretion cloning from lithiumchloride (LiCl)-dorsalized *Xenopus* embryos at gastrula stages (Pera et al., 2005). *XRDH10* encodes a 341 amino acid protein and contains an aminoterminal signal peptide. As a member of the short-chain dehydrogenase/reductase (SDR) superfamily, *XRDH10* contains the characteristic NAD⁺ binding site (sequence motif: TGXXXGXXG). The sequence motifs NNAG and YXXXXK display the active site of *XRDH10* and are conserved among the members of the SDR superfamily (Fig. 1 A).

The protein sequence of *XRDH10* was compared to RDH10 protein sequences in other species using a genetic database (<http://www.ncbi.nlm.nih.gov/>).

The *XRDH10* protein displays 95% identity to *XRDH10-b* (gene bank accession number: AAH77913).

XRDH10 has considerable identity to human and mouse (88 %), chick (87 %) and zebrafish RDH10 (77 %) (Fig1 B, C).

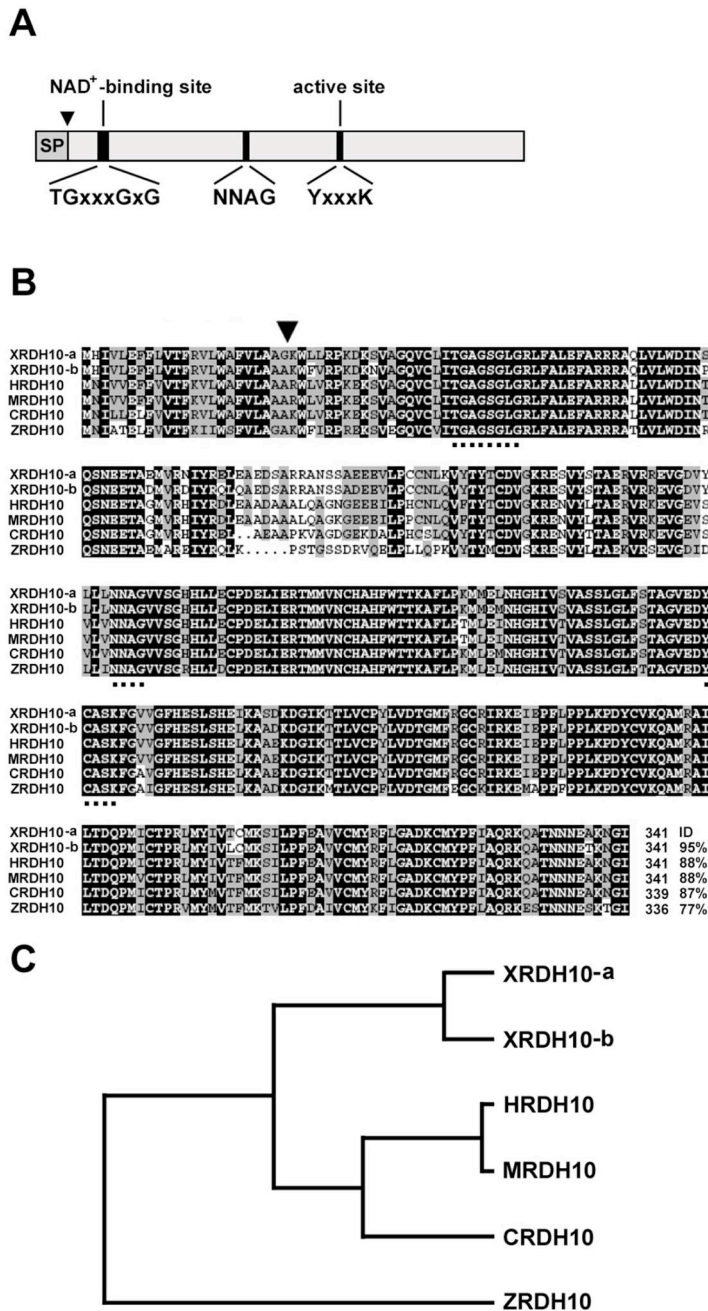


Fig. 1. *Xenopus* retinol dehydrogenase 10

(A) Protein structure of XRDH10. The invariant sequences TGXXXGxG (co-factor binding; X indicates amino acid residue), NNAG and YXXXX (active site) are characteristic for members of the short-chain dehydrogenase/reductase family (Persson et al., 2003). SP, signal peptide.

(B) Sequence alignment of *Xenopus*, human, mouse, chick and zebrafish proteins. Two *X. laevis* RDH10 isoforms (XRDH10-a and XRDH10-b) are shown. The arrowhead indicates the predicted signal peptide cleavage site. The dotted underline labels conserved sequences. Modified from Strate, 2005.

(C) Evolutionary relationship of RDH10 sequences.

3.2 *XRDH10* is dynamically expressed during early embryogenesis

In order to study the temporal expression of *XRDH10*, reverse transcription PCR (RT-PCR), using RNA from whole embryos was performed. *XRDH10* transcripts can be detected throughout all the stages examined with elevated expression levels at the late gastrula (st. 12), neurula (st. 14-18) and in the early tadpole stages (st. 32, 40) (Fig. 2 A).

Whole mount *in situ* hybridizations show abundant transcripts in 4-cell and blastula stage embryos (Fig. 2 B, C). RT-PCR reveals equivalent levels of *XRDH10* mRNA in the animal and vegetal pole in late blastula stage embryos (st. 9) (Fig. 2 D). *XRDH10* transcripts can be visualized by *in situ* hybridization only in the animal hemisphere of the 4-cell and blastula stage embryos, presumably because the signals are quenched in the vegetal hemisphere due to the yolk. At the midgastrula stage (st. 11) *XRDH10* transcripts are detected in the dorsal blastopore lip (Fig. 2 E). A mid-sagittal section showed that the *XRDH10*-expression in the dorsal blastopore lip is restricted to the involuted mesoderm (Fig. 2 F). The signals are embedded in the periblastoporal expression domain of *XRALDH2* (Fig. 2 G) and complementary to two *XCYP26A1* expression domains in the dorsal animal cap and in the ventrolateral blastopore lip (Fig. 2 H) (Hollemann et al., 1998; Chen et al., 2001). At the late gastrula stage (st. 12), *XRDH10* transcripts can be detected in the head process, the anterior lateral plate, the presomitic mesoderm and the ventral blastopore lip (Fig. 2 I).

In early neurula stage embryos, *XRDH10* shows additional expression in the presomitic mesoderm and cardiac crescent (Fig. 2 J and inset). *XRDH10* signals in the anterior trunk mesoderm are embedded in those of *XRALDH2*, with *XRDH10* being more anteriorly expressed than *XRALDH2* (Fig. 2 J, K) (Chen et al., 2001). These sites of expression are flanked by non-overlapping *XCYP26A1* expression domains in the posterior head and posterior trunk ectoderm (Fig. 2 L) (Hollemann et al., 1998). In early tailbud stage embryos (st. 22), *XRDH10* transcripts overlap with *XRALDH2* expression in the eyefield (Fig. 2 M, N) (Chen et al., 2001). These domains are surrounded by *XCYP26A1* expression (Fig. 2 O) (Hollemann et al., 1998). At a more advanced stage (st. 24), further *XRDH10* expression can be detected in the anterior lateral plate, the pronephros, the trunk neural crest, posterior mesoderm and the proctodeum (Fig. 2 P, Q).

In early tadpole embryos (st. 32), *XRDH10* expression is found in the olfactory system, the telencephalon, the midbrain, the eyes, the midbrain-hindbrain boundary the ear placodes and in the posterior branchial arches. Transcripts can be detected in the anterior lateral plate, the spinal cord, the neural crest, the pronephros and the posterior mesoderm (Fig. 2 R, RI-RVI). *XRDH10* transcripts overlap with the expression of *XRALDH2* in the telencephalon, eyes, ears, anterior lateral plate, pronephros and spinal cord (Fig 2 R, S) (Chen et al., 2001). *XCYP26A1* is expressed in a non-overlapping manner in the periocular region, in tissues that flank the pronephros and in the tip of the tailbud, more posterior than *XRDH10* expression (Fig. 2 R, T) (Hollemann et al., 1998).

In conclusion, *XRDH10* displays a dynamic expression pattern during development. *XRDH10* transcripts are embedded in *XRALDH2* expression domains at several sites and complementary to *XCYP26A1* expression.

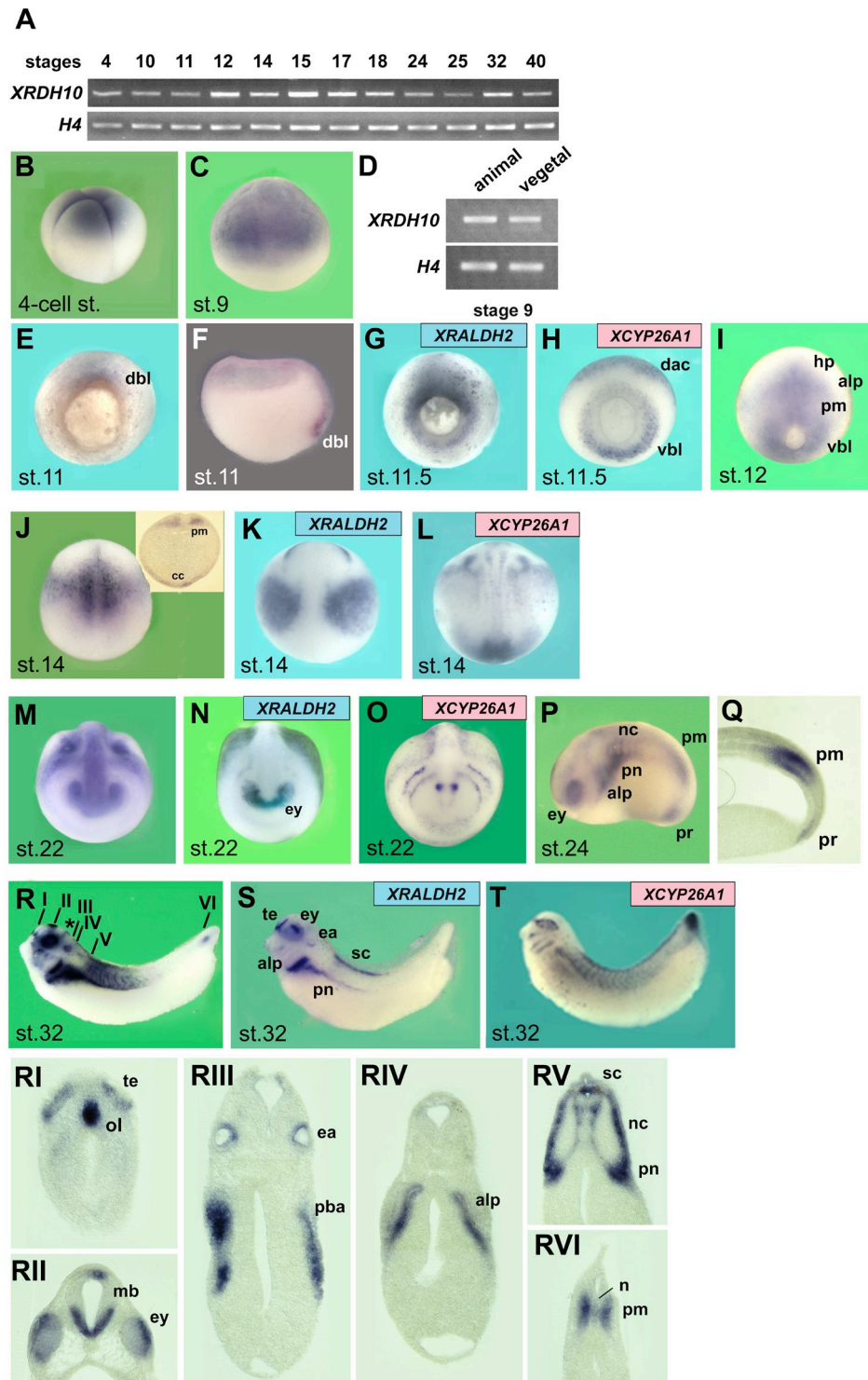


Fig. 2. Gene expression of *XRDH10* in early *Xenopus*

(A, D) RT-PCR analysis of whole embryos (A, see also: Strate, 2005) and animal or vegetal explants from late blastula stage embryos (st. 9) (D). H4 was used as a loading control. The developmental stages refer to Nieuwkoop and Faber, 1994. Expression of *XRDH10* is upregulated during the late gastrula stage (st.12), neurula stages (st. 15-18) and early tadpole stages (st, 32, 40) (A). At the late blastula stage (st. 9) an equal distribution of *XRDH10* mRNA can be found in the animal and vegetal hemisphere (D).

(B, C, E-T and RI-RVI) Whole mount *in situ* hybridizations.

(B, C) At the 4-cell stage and the late blastula stage (st. 9) *XRDH10* seems to be enriched in the animal hemisphere. The signal is quenched in the vegetal hemisphere due to the high yolk content.

(E-H) Gastrula stage embryos (st.11/11.5) shown in vegetal view and sagittally sectioned (F). *XRDH10* expression can be detected in the mesoderm of the dorsal blastopore lip, see also: Strate, 2005 (E, F). *XRALDH2* is co-expressed in the dorsal blastopore lip but is encircling the blastoporus, see: Strate, 2005 (G). *XCYP26A1* is expressed complementary in the ventral blastopore lip and in the dorsal animal cap (H; Strate, 2005).

(I-L) Dorsal views of whole mount *in situ* hybridized embryos in late gastrula/early neurula stages. At st.12, *XRDH10* is expressed in the ventral blastopore lip, presomitic mesoderm, anterior lateral plate and head process (I). Later in development (st. 14), *XRDH10* expression persists in the presomitic mesoderm (J). A transverse section reveals *XRDH10* expression in the cardiac crescent (inset). *XRALDH2* is co-expressed in the presomitic mesoderm, while *XCYP26A1* transcripts can be found complementary in anterior and posterior regions (K, L; Strate, 2005).

(M-O) Embryos at tailbud stage (st.22) in anterior view. *XRDH10* and *XRALDH2* are expressed in the eyefield and encircled by *XCYP26A1* expression.

(P, Q) Lateral view of a tailbud stage embryo (st. 24) and sagittal section (Q). *XRDH10* expression can be found in distinct expression domains. Transcripts can be detected in the eye, the anterior lateral plate, the pronephros, the neural crest, the presomitic mesoderm and the proctodeum.

(R-T) Lateral views of early tadpole stage embryos (st. 32). *XRDH10* and *XRALDH2* are co-expressed in the telencephalon, the eye, the ear, the anterior lateral plate, the pronephros and the spinal cord. Exclusive *XRDH10* expression domains can be found in the midbrain, the midbrain-hindbrain boundary (*), the posterior branchial arches and the presomitic mesoderm. The expression domain in the eye, the pronephros and the tail tip is flanked by *XCYP26A1* expression. T: Strate, 2005

(RI-RVI) Transversal sections of (R). alp: anterior lateral plate, cc: cardiac crescent, dac: dorsal animal cap, dbl: dorsal blastopore lip, ea: ear, ey: eye, hp: head process, mb: midbrain, n: notochord, nc: neural crest, ol: olfactory system, pba: posterior branchial arch, pm: presomitic mesoderm, pn: pronephros, pr: proctodeum, sc: spinal cord, te: telencephalon, vbl: ventral blastopore lip.

3.3 Retinoic acid suppresses *XRDH10* gene expression

The overlap of *RDH10* expression with several sites of active RA signalling as previously described in the mouse (Sandell et al., 2007; Cammas et al., 2007) and supported by findings in *Xenopus* (Fig. 2) suggested a possible regulation of this gene by RA. *Xenopus* embryos were cultured in different concentrations of RA or RA inhibitors and the gene expression of *XRDH10* was analyzed by whole mount *in situ* hybridization.

Treatment of embryos with 5 μ M RA from midgastrula to late neurula stages (st. 11 - st. 18) leads to an overall reduction of *XRDH10* expression compared to DMSO-treated control embryos (Fig 3 A, B and insets). Embryos were then treated with 5 μ M RA from stage 16 to stage 28, to minimize developmental defects induced by the RA-treatment.

At the tailbud stage a specific block of *XRDH10* expression can be observed in the head structures and in the mesoderm. *XRDH10* is strongly reduced in the olfactory system, the eyes and the ear placodes as well as in brain regions, such as the telencephalon and the midbrain-hindbrain boundary. *XRDH10* expression is suppressed in the pronephros and in the somitic mesoderm of the trunk and the tailtip (Fig. 3 C, D).

Injection of 2 ng *XRALDH2* mRNA into the marginal zone and subsequent treatment with 5 μ M retinal from st. 11 onwards leads to a robust reduction of *XRDH10* expression, suggesting the suppression of *XRDH10* by endogenous RA (Fig. 3 E, F).

In contrast, three different approaches showed that lowering of endogenous RA levels in the embryo upregulates *XRDH10* gene expression. Exposure to the RA synthesis inhibitors disulfiram (10 μ M, Vermot and Pourquié, 2005) from stage 11 onwards increases transcript levels of *XRDH10* at the neurula stage (Fig 3 G, H). The RA synthesis inhibitor citral (3,7-dimethyl-2,6-octadienal, Schuh et al., 1993) applied at a concentration of 20 μ M has a similar effect (Fig 3I, J).

XCYP26A1 mRNA, microinjected at the 4-cell stage into the marginal zone, causes a local upregulation of *XRDH10* expression in injected cells (Fig 3 K, L and insets).

In conclusion, endogenous RA suppresses *XRDH10* gene expression and thereby controls the first enzymatic step of RA biosynthesis (Fig 3 M).

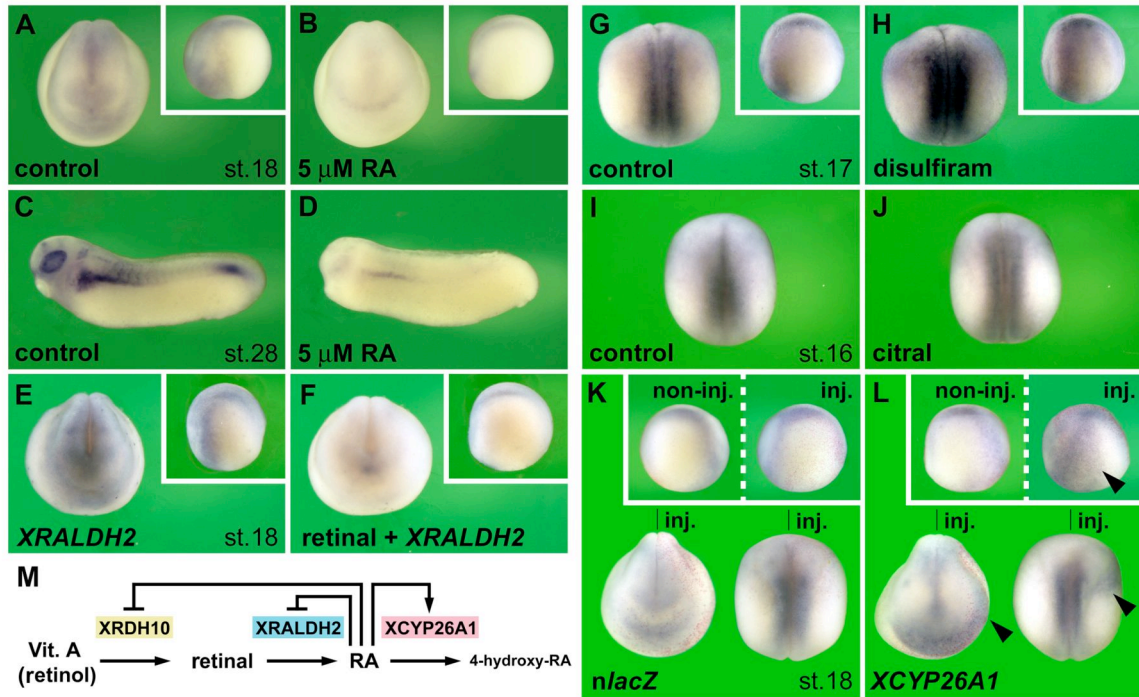


Fig. 3. Retinoic acid downregulates *XRDH10* gene expression.

Whole mount *in situ* hybridization analysis of *XRDH10* transcription at neurula (A,B,E-L) and tailbud stage (C,D). Embryos are shown in anterior (A,B,E,F,K,L), lateral (C,D, insets) and dorsal views (G-L).

(A-D) Embryos were treated from stage 11 (A,B) or stage 16 (C,D) onwards with 0.05% DMSO (A, C) as control or with 5 μ M RA. Note that RA induces significant reduction of *XRDH10* expression.

(E,F) Embryos were microinjected into the animal pole at the 4-cell stage with 2 ng *XRALDH2* mRNA and treated from stage 11 onwards with 0.05% ethanol as control (E) or 5 μ M retinal (F).

(G-J) Treatment from stage 11 onwards with the RA inhibitors disulfiram (10 μ M) or citral (20 μ M) causes elevation of *XRDH10* expression.

(K, L) Embryos were anically injected into a single blastomere at the 4-cell stage with 300 pg *n lacZ* mRNA as lineage tracer (red nuclei) alone (K) or with 2 ng *XCYP26A1* mRNA (L). Note that *XCYP26A1* induces an upregulation of *XRDH10* expression on the injected side (arrowhead).

(M) Negative feedback regulation of RA biosynthesis.

Indicated gene expression patterns were obtained in A, 55/55; B, 22/31; C, 30/30; D, 37/37; E, 11/11; F, 16/17; G, 29/29; H, 49/49; I, 31/31; J, 54/57; K, 36/36; L, 48/53.

3.4 XRDH10 has retinoic acid-like activity

In order to investigate the activity of XRDH10, mRNA microinjections into the animal pole at the 4-cell stage were performed.

At the tadpole stage, overexpression of *XRDH10* causes moderate reduction of head structures and shortening of the anteroposterior body axis (Fig 4 A, B). This effect is reminiscent of the microcephaly and shortened tails obtained by treating embryos with 0.1 μM RA during late blastula and gastrula stages (st. 9-12) (Fig. 4 C) (Durstion et al., 1989). The phenotype obtained by *XRDH10* mRNA injection can be rescued by coinjecting *XCYP26A1* mRNA or by treating injected embryos with 4 μM citral during late blastula and gastrula (st. 9-12) stages (Fig. 4D,E), suggesting that XRDH10 may act through the RA signalling pathway.

To test whether overexpression of *XRDH10* leads to increased RA signalling, several RA target genes were analyzed in an animal cap assay (Fig. 4 F). To this end, mRNA injected animal cap tissue was isolated at late blastula stage (st. 9), and the explants were cultured until late gastrula stage (st. 12.5). RT-PCR analysis revealed, that the RA target genes *Xgbx-2*, *Xcad-3*, *Meis3* and *HoxD1* (von Bubnoff et al., 1996; Kolm et al., 1997, Dibner et al., 2004; Shiotsugu et al., 2004) are upregulated upon *XRDH10* mRNA injection (Fig. 4 F, lane 3). These effects can also be obtained after treating animal caps with 5 μM RA from stages 9 to 12 (Fig 4F, lane 4).

The results show that XRDH10 and RA have common activities and that XRDH10 activates RA signalling in *Xenopus* embryos.

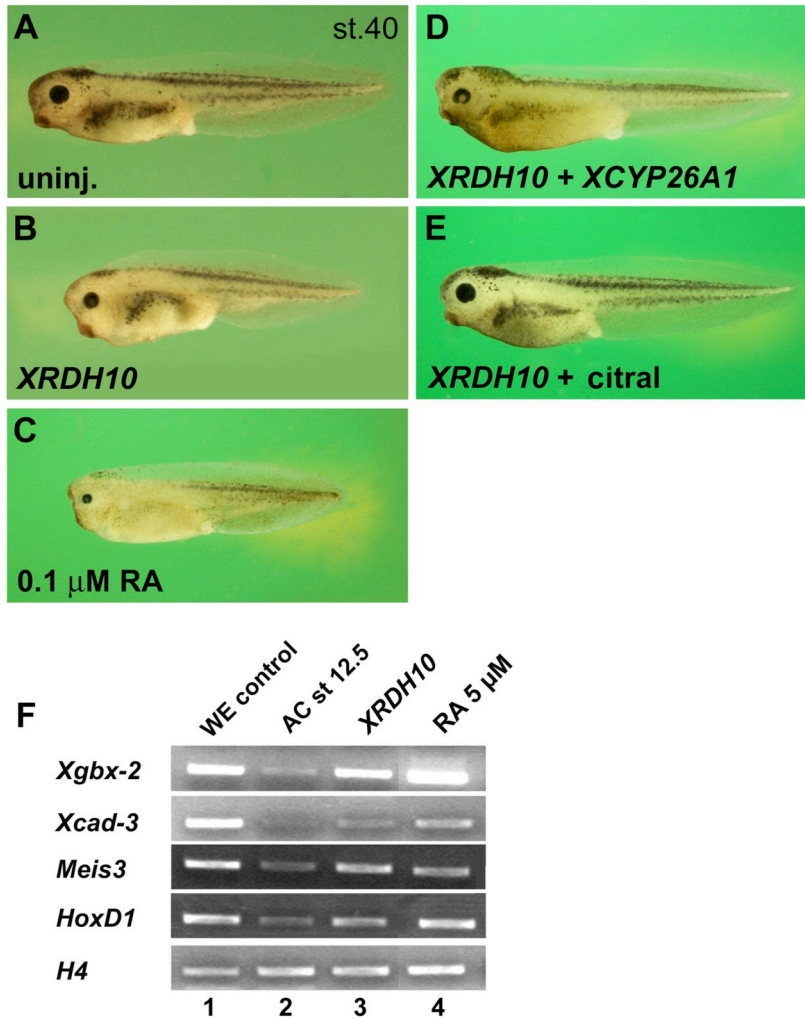


Fig. 4. XRDH10 induces RA signalling.

(A) Uninjected tadpole embryo.

(B) Animal injection of 4 ng *XRDH10* mRNA at the 4-cell stage induces slight reduction of head structures and shortening of the tail.

(C) Treatment with 0.1 μM RA between stages 9 and 12 induces microcephaly and tail shortening.

(D) Co-injection of 0.5 ng *XCYP26A1* mRNA reverts the effect of *XRDH10* mRNA and restores normal head and tail development.

(E) Treatment with 4 μM citral at stages 9-12 abrogates the activity of *XRDH10* mRNA.

(F) RT-PCR analysis of animal caps explanted from stage 8 embryos and cultured until stage 12.5; see: Strate, 2005. Embryos were injected with 4 ng *XRDH10* mRNA (lane 3) and animal caps treated with 5 μM RA (lane 4). Note that *XRDH10* stimulates the transcription of the RA target genes *Xgbx-2*, *Xcad-3*, *Meis3* and *HoxD1*. *H4* was used as a loading control. Frequency of embryos with the indicated phenotypes was: B, 30/39; C, 25/25; D, 30/40; E29/39.

3.5 XRDH10 modulates organizer-specific gene expression

Since *XRDH10* is expressed in the dorsal blastopore lip (Fig. 2 E, F), the effects of *XRDH10* mRNA injection on genes demarcating the Spemann-Mangold organizer were examined by whole mount *in situ* hybridizations (Figs. 5, 6).

XRDH10 mRNA was injected radially at the 4-cell stage. Embryos were first analyzed for the expression of *Chordin* at the late blastula stage (st.9) (Fig 5 A-D). At this stage, *Chordin* is expressed in the BCNE (Blastula Chordin and Noggin Expression) center, a region in the dorsal animal cap that gives rise to the CNS and the Spemann-Mangold organizer (Fig. 5A, Wessely et al., 2001).

XRDH10 overexpression leads to a moderate upregulation of *Chordin* expression in the BCNE center (Fig. 5 B). Similarly, treatment of embryos with 5 μ M RA between stages 7 and 9 slightly elevates *Chordin* transcripts in this region (Fig. 5D).

Next, the effects of XRDH10 and RA on *Chordin* expression after the onset of gastrulation were analyzed (Fig 5 E-H). At stage 10.5 *Chordin* signals are restricted to the dorsal blastopore lip (Fig. 5E; Sasai et al., 1994). *XRDH10* mRNA injection causes an expansion of the *Chordin* expression domain (Fig. 5F). A similar effect can be observed upon RA treatment between stages 8 and 10.5 (Fig. 5 H). Another gene, that is activated in organizer, is *Xlim-1* (Fig. 5 I, Taira et al., 1992). *Xlim-1* expression is laterally expanded in embryos injected with *XRDH10* mRNA (Fig. 5J). Notably, treatment with RA leads, in addition to increased levels in the blastopore lip, to ectopic *Xlim-1* expression in the animal cap (Fig. 5L, inset, Taira et al., 1994). Hence, *Chordin* and *Xlim-1* expression are positively regulated by XRDH10 and RA signals.

Additional genes with distinct expression in the dorsal blastopore lip are *Gooseoid* and *ADMP* (Fig. 5 M, Q; Cho et al., 1991; Moos et al., 1995).

XRDH10 overexpression leads to a downregulation of these genes (Fig. 5 N, R), similarly as exogenous RA downregulates *Gooseoid* and *ADMP* (Fig. 5P, T; Yelin et al., 2005). The results indicate that *Gooseoid* and *ADMP* are negatively regulated by XRDH10 and RA.

Additionally, the expression patterns of the organizer markers *Noggin*, *Frzb*, *sFRP2* and *Crescent* were examined after *XRDH10* overexpression or RA treatment. These markers are not affected (Fig. 6 A-P).

In conclusion, *XRDH10* overexpression differentially affects gene expression in the Spemann-Mangold organizer.

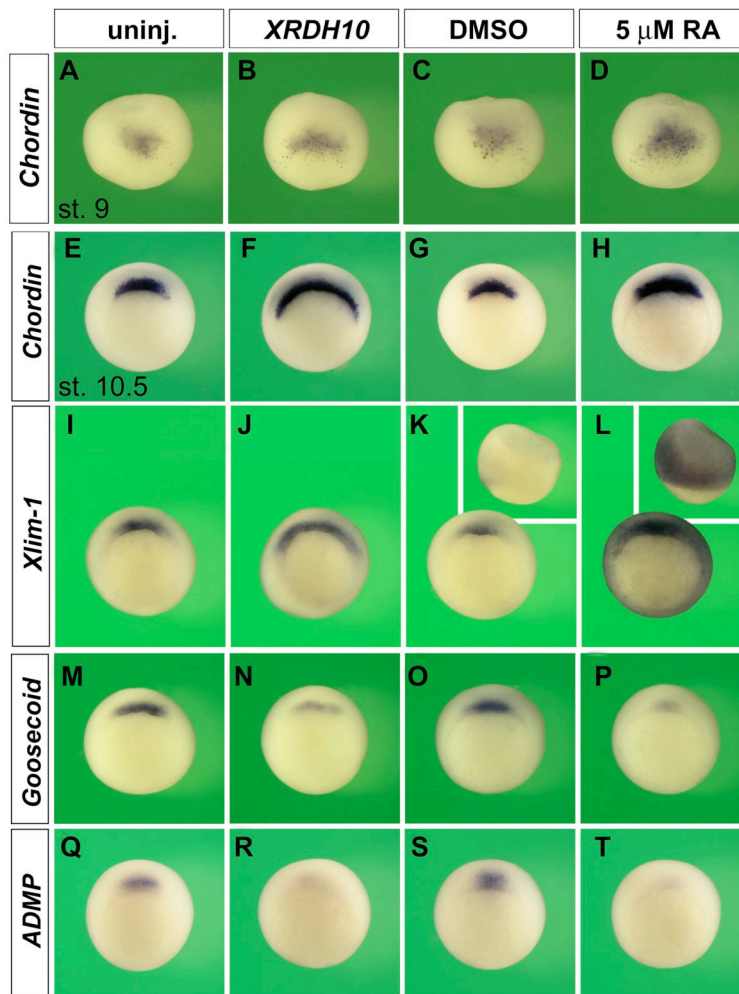


Fig. 5. *XRDH10* upregulates *Chordin* and *Xlim-1* and downregulates *Goosecoid* and *ADMP* expression in the dorsal blastopore lip.

Whole mount *in situ* hybridization of gastrula embryos in dorsal view (A-D) and vegetal view (E-T). Insets depict lateral views. Embryos were injected into the margin of each blastomere at the 4-cell stage with 1 ng *XRDH10* mRNA (B, F, J, N, R). Others were treated with DMSO as a control (C, G, K, O, S) or 5 μ M RA from stage 8 onwards (D, H, L, P, T). *XRDH10* mRNA and RA expand the expression of *Chordin* and *Xlim-1* (B, D, F, H, J, L). *Goosecoid* and *ADMP* are downregulated upon *XRDH10* mRNA injection or RA treatment (N, P, R, T). Frequency of embryos with the indicated phenotypes was: A, 10/11; B, 11/11; C, 31/38; D, 47/47; E, 45/45; F, 19/39; G, 31/31; H, 41/41; I, 38/38; J, 29/43; K, 30/36; L, 16/29; M, 6/8; N, 4/6; O, 22/28; P, 15/24; Q, 14/14; R, 9/13; S, 64/69; T, 38/50

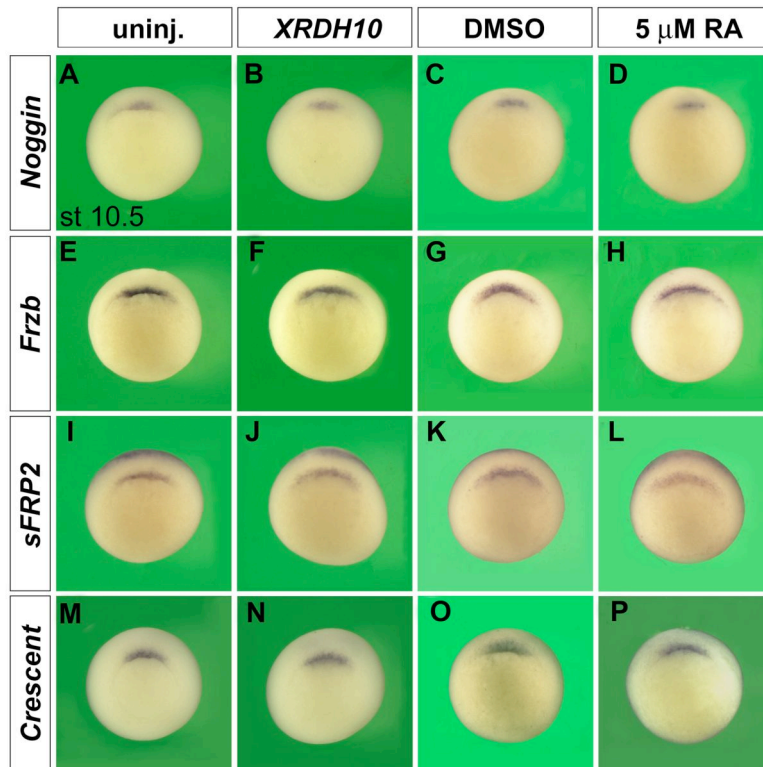


Fig. 6. *XRDH10* does not affect the organizer genes *Noggin*, *Frzb*, *sFRP2* and *Crescent*.

Whole mount *in situ* hybridized embryos shown in vegetal view. Embryos were injected at the 4-cell stage into the marginal zone of each blastomere with 1 ng *XRDH10* mRNA (B, F, J, N) or treated with DMSO as a control (C, G, K, O) or 5 μ M RA from stage 8 onwards (D, H, L, P). The organizer markers *Noggin*, *Frzb*, *sFRP2* and *Crescent* were not affected by mRNA injections or RA treatments. Frequency of embryos with the indicated phenotypes was: A, 16/16; B, 24/28; C, 53/53; D, 45/45; E, 12/12; F, 27/27; G, 12/12; H, 20/20; I, 16/16; J, 25/25; K, 24/24; L, 28/28; M, 15/15; N, 28/28; O, 62/62; P, 42/46.

3.6 XRDH10 co-operates with XRALDH2 during axis development and central nervous system patterning

In order to study the effects of XRDH10 on patterning of the CNS, mRNA was injected animally into one blastomere of the 4-cell stage embryo (Fig. 7). Nuclear *lacZ* (*nlacZ*) mRNA was co-injected as a lineage tracer, to visualize the injected cells.

At the late gastrula stage (st.12.5) *HoxD1* is expressed in the trunk mesoderm and overlying ectoderm with the anterior boundary at the level of the hindbrain rhombomere 4 (Fig. 7 A; Kolm and Sive, 1997).

Microinjection of *XRDH10* mRNA leads to an upregulation and anteriorwards expansion of the *HoxD1* expression domain (Fig. 7 B). Overexpression of *XRALDH2* or a combination of *XRDH10* and *XRALDH2* causes a similar phenotype (Fig. 7 C, D). Co-injection of *XRDH10* and *XCYP26A1* mRNA reverts the effects of *XRDH10* overexpression, leading to a reduction of *HoxD1* expression and a posteriorwards retraction of the *HoxD1* expression domain (Fig. 7E).

At the early neurula stage (stage 14) *XLim-1* is expressed in the notochord, distinct stripes demarcating neurons in the open neural plate and in the lateral mesodermal regions (Fig. 7 F; Taira et al., 1994). Microinjection of *XRDH10*, *XRALDH2* or a combination of both mRNAs causes an anteriorwards shift of the *XLim-1* expression domains in the neurons and lateral mesoderm (Fig. 7G-I). A combination of *XRDH10* and *XRALDH2* causes an expansion of the neuronal *XLim-1* expression domain (Fig. 7 I). In contrast, co-injection of *XRDH10* and *XCYP26A1* mRNAs leads to a complete repression of *XLim-1* signals on the injected site (Fig. 7J)

Next, the effects on the developing brain using the hindbrain marker Krox20 (rhombomeres 3 and 5; Nieto et al., 1991) the midbrain-hindbrain marker En2 (Hemmati-Brivanlou et al., 1991), the eyefield marker Rx2A (Mathers et al., 1997) and the telencephalic marker FoxG1 (*XBF1*; Bourguignon et al., 1998) were analyzed (Fig. 7 K-U). Previous studies have shown, that overexpression of *XRALDH2* posteriorizes the neural tube, whereas *XCYP26A1* has the opposite effect (Hollemann et al., 1998; Chen et al., 2001).

At the tailbud stage (st. 23), *XRDH10* mRNA shows little effect when injected alone (Fig. 7 L, Q). However, *XRDH10* mRNA enhances the posteriorizing effect of *XRALDH2* and causes a robust anterior shift of the *Krox20*, *En2* and *Rx2A* expression domains upon co-injection of both mRNAs (Fig. 7 M, N, R, S). In contrast, a combination of *XRDH10* and *XCYP26A1* mRNA results in a pronounced posterior shift of *Krox20* and *En2* expression (Fig. 7 O, T). This supports that the effects of *XRDH10* overexpression are due to elevated RA signalling. The location of the telencephalic marker *FoxG1* is not affected by any of the injections (Fig. 7 Q-T). Analysis of *Krox 20* expression shows that the frequency of rhombomeric shifts induced by a combination of *XRDH10* and *XRALDH2* exceeds the sum of effects induced by each mRNA alone (Fig. 7 U), suggesting that the two enzymes cooperate during pattern formation of the CNS.

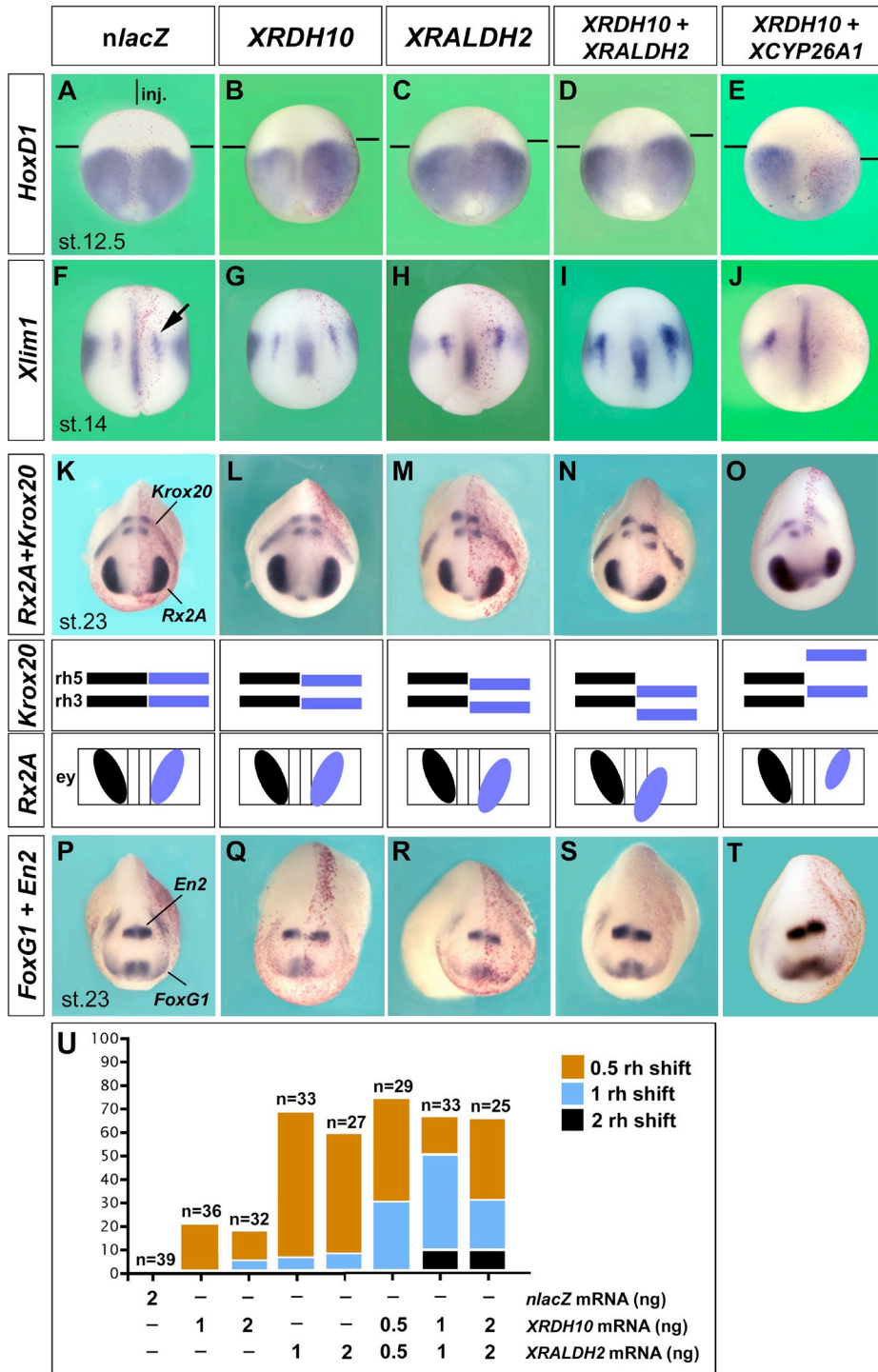


Fig. 7. Overexpression of *XRDH10* and *XRALDH2* results in an anteriorwards shift of neural markers, while *XCYP26A1* has the opposite effect.

Whole mount *in situ* hybridizations of embryos after microinjection of mRNA into the animal pole of one dorsal blastomere at the 4-cell stage. The lineage tracer *nlacZ* (red nuclei) labels the injected right side.

(A-E) Late gastrula embryos in dorsal view (anterior to the top). *HoxD1* demarcates the ectoderm and mesoderm in the trunk with an anterior expression boundary at the level of rhombomere 4 (horizontal line). Microinjection of *XRDH10*, *XRALDH2* or a combination leads to an anteriorwards shift of the *HoxD1* expression domain (A-D) that can be reverted by co-injecting *XCYP26A1* (E).

(F-J) Early neurula embryos in dorsal view showing *Xlim-1* expression in two lines of neural cells (arrow). Injection of *XRDH10* or *XRALDH2* leads to an anteriorwards shift of the neuronal *XLim-1* expression domain (G, H). A combination of *XRDH10* and *XRALDH2* leads to an expansion of the *XLim-1* positive neuronal domain.

(K-O) Early tailbud embryos in anterior view (posterior to the top) and schematic overviews demarcating *Rx2A* expression in the eyes and *Krox20* expression in rhombomeres 3 and 5 of the hindbrain. The anteriorwards shift of the rhombomeres upon *XRALDH2* injection is enhanced upon co-injection of *XRDH10* (M, N). See also Strate, 2005.

(P-T) *FoxG1* labels the telencephalon, and *En2* the mid-hindbrain boundary in early tailbud embryos. The mid-hindbrain boundary is shifted anteriorwards upon overexpression of *XRALDH2* or a combination of *XRALDH2* and *XRDH10* (R,S). See also Strate, 2005

(U) Synergistic effects of *XRDH10* and *XRALDH2* on hindbrain patterning. The anteriorward shift of *Krox20* expression is shown in response to mRNA injections at the indicated doses. Note that *XRDH10* has little effect on its own, but strongly enhances the posteriorizing effect of *XRALDH2*. *nlacZ* mRNA was injected as control.

Injected RNA amounts were, if not otherwise noted: *nlacZ* (300 pg), *XRDH10* (1 ng), *XRALDH2* (1 ng) and *XCYP26A1* (0.5 ng). ey: eye; rh: rhombomere.

Indicated changes of gene expression were observed in B, 35/78; C, 43/59; D, 18/29; E, 9/9; G, 24/96; H, 45/95; I, 30/51; J, 13/13; L, 7/36; M, 22/33; N, 22/33; O, 15/15; Q, 6/56 (*En2*); R, 7/19 (*En2*); S, 8/20 (*En2*); T, 25/25 (*En2*) embryos.

3.7 Retinol is a limiting factor for XRDH10 activity

The relatively mild phenotype observed in *XRDH10* mRNA-injected embryos raised the question of whether XRDH10 activity may be restricted by insufficient amounts of endogenous retinol. Therefore, the effects of *XRDH10* overexpression in the presence of excessive retinol were examined (Fig. 8).

Embryos that were treated with 50 μ M retinol during gastrula and neurula stages (stages 9-12) show a reduction of head structures, in particular of the eyes and the cement gland tissue (Fig. 8 A, B). In retinol-treated embryos that were anally injected with 1 ng *XRDH10* mRNA, a complete loss of head structures can be observed (Fig. 8 C). Co-injection of *XCYP26A1* mRNA partially rescues the loss of head structures (Fig. 7 D). *XCYP26A1* is able to revert the loss of eyes in a dose-dependent manner (Fig. 8D, E).

In order to study the effects on CNS patterning, whole mount *in situ* hybridizations using *Rx2A* and *Krox20* antisense probes were performed (Fig. 8 F-I).

Embryos, treated with 25 μ M retinol, show a reduction of the eyefield compared to DMSO treated control embryos (Fig 8 F, G). Unilateral injection of *XRDH10* mRNA causes a much stronger reduction of the eyefield on the injected site in retinol-treated embryos (Fig. 8 H). The effect on the eyefield can be rescued upon co-injection of *XCYP26A1* mRNA (Fig 8 I).

Together the results suggest that the supply of retinol is limiting for XRDH10 activity during head development and eye formation.

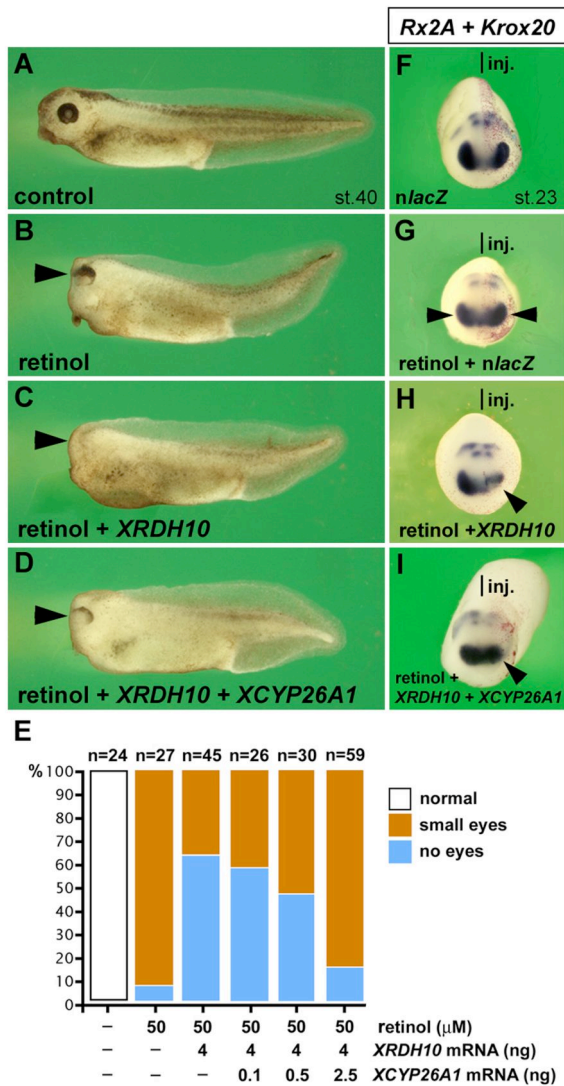


Fig. 8. XRDH10 co-operates with retinol during head development.

Embryos were injected into the animal pole at the 4-cell stage with the indicated mRNAs and treated with DMSO or retinol at stages 9 - 12.

(A) DMSO-treated control embryo at tadpole stage.

(B) Retinol (50 μM) induces microcephaly at the tadpole stage.

(C) Injection of *XRDH10* mRNA (1 ng into four blastomeres) and subsequent retinol treatment causes anencephaly.

(D) *XCYP26A1* mRNA (2.5 ng) partially restores eye and head structures in retinol/*XRDH10*-treated embryos.

(E) Eye deficiencies induced by retinol and *XRDH10* and dose-dependent rescue by *XCYP26A1* mRNA in stage 40 embryos.

(F-I) Retinol (25 μM) leads to a slight reduction of the *Rx2A*-positive eye field at the tail bud stage (arrowhead in G). In the retinol-treated embryos, *XRDH10* mRNA (1 ng in one dorsal blastomere) causes a unilateral collapse of *Rx2A* expression (arrowhead in H), which is rescued by co-injection of 2.5 ng *XCYP26A1* mRNA (arrowhead in I).

Indicated phenotypes were observed in A, 24/24; B, 25/27; C, 28/45; D, 51/59; G, 13/15; H, 20/35; I, 10/13 embryos.

3.8 Loss of XRDH10 and XRALDH2 affects the anterior-posterior and dorsal-ventral axis of the embryo

In order to study the function of XRDH10 and XRALDH2, morpholino oligonucleotides targeted against the translation initiation sites of *XRDH10* and *XRALDH2* were injected into embryos (*XRDH10*-MO and *XRALDH2*-MO) (Fig. 9 A, B). An *in vitro* transcription-translation assay revealed, that the morpholino oligonucleotides block the protein biosynthesis of *XRDH10* and *XRALDH2* efficiently (Fig. 9 C, D).

Embryos were injected marginally with 5.2 pmol of *XRDH10*-MO or *XRALDH2*-MO. At the late tailbud-stage (stage 28), morphant embryos exhibit small heads and enlarged ventroposterior structures (Fig. 9 E-G). At the tadpole-stage (stage 40) MO-injected embryos exhibited reduced eyes and head structures and a shortening of the tail (Fig. 9 H-J). Importantly, the phenotypes can be rescued by co-injecting *XRDH10* or *XRALDH2* mRNA-constructs that are not targeted by the morpholino oligonucleotides (*XRDH10** and *mRALDH2*), indicating that the observed effects are specific (insets).

In conclusion, depletion of XRDH10 and XRALDH2 affects the anterior-posterior and dorsal-ventral axis of the embryo.

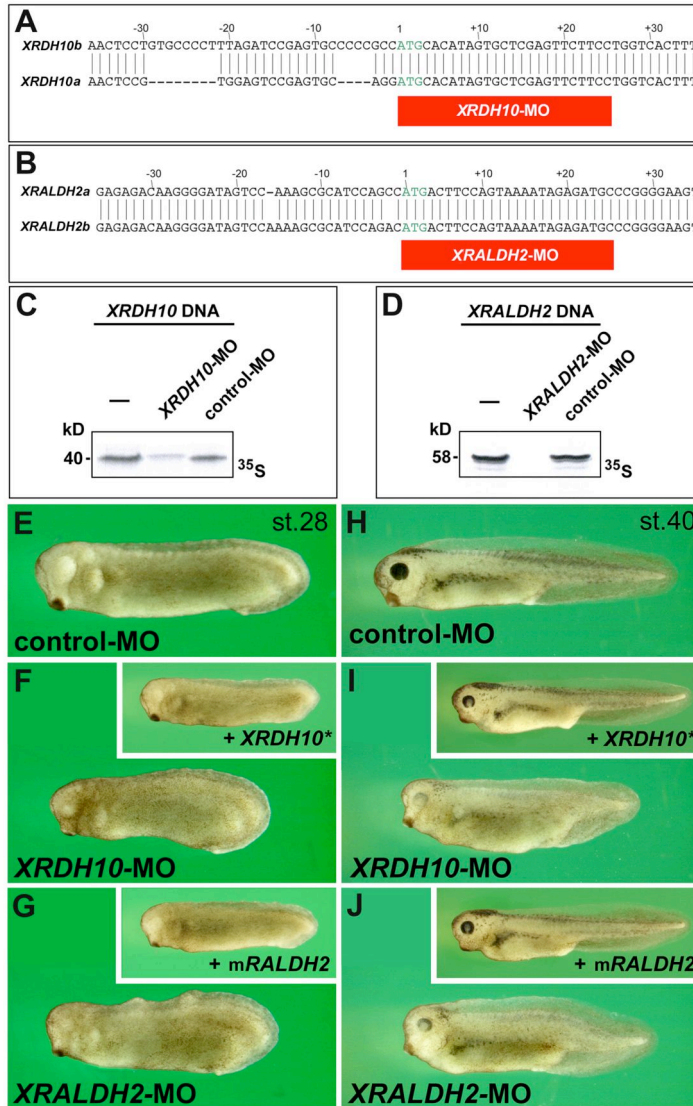


Fig. 9. Knockdown of *XRDH10* and *XRALDH2* induces ventralization.

Antisense morpholino oligonucleotides (MOs) were injected marginally at the 2-cell stage (5.2 pmol per blastomere), followed by injection of non-targeted mRNA constructs (*XRDH10** and m*RALDH2*) at the 4-cell stage (1 ng per blastomere).

(A,B) MOs target the translation initiation sites of two pseudoalleles of *Xenopus laevis* *RDH10* and *RALDH2*.

(C,D) Protein synthesis of *XRDH10* and *XRALDH2* is specifically inhibited by *XRDH10-MO* and *XRALDH2-MO*, but not by control-MO of random sequence.

(E-J) Microinjection of *XRDH10-MO* and *XRALDH2-MO* leads to microcephaly and enlarged ventroposterior structures in tailbud embryos (E-G) and to reduced eye structures and shortened tails in tadpoles (H-J). Normal development is restored by *XRDH10** and m*XRALDH2* mRNAs, respectively (insets).

Indicated phenotypes were observed in E, 101/117; F, 62/84 (inset: 73/98); G, 44/67 (inset: 80/84); H, 74/79; I, 39/50 (inset: 56/68); J, 18/48 (inset: 58/64).

3.9 Loss of XRDH10 and XRALDH2 affects the expression of early organizer markers and early mesodermal markers

In order to study the effects of XRDH10 and XRALDH2 depletion on early organizer markers, morpholino oligonucleotides were injected radially into the marginal zone.

When the embryos reached gastrula stages (st. 10.5) it could be observed, that *XRDH10*-MO or *XRALDH2*-MO cause a reduction of *Chordin* gene expression, an effect that can be rescued by co-injecting *XRDH10** or m*XRALDH2* (Fig 10 A-C and insets). On the contrary, depletion of XRDH10 or XRALDH2 leads to an upregulation of the organizer markers Goosecoid and ADMP (Fig. 10 D-I).

While *XRDH10*-MO or *XRALDH2*-MO have no apparent effects on *Xlim-1* expression in gastrula embryos (data not shown), specific effects on this gene can be observed later in development. At the advanced neurula stage (stage 18) *Xlim-1* demarcates the pronephros anlage in the lateral mesoderm (arrowhead in Fig. 10 J). Unilateral injection of *XRDH10*-MO or *XRALDH2*-MO into one site of the embryo causes a posteriorwards retraction of this expression domain (Fig. 10 K,L) This effect can be rescued by co-injecting *XRDH10** or m*RALDH2* (insets in Fig. 10 K, L).

The results show that XRDH10 and XRALDH2 are required for the correct expression of the early organizer markers Chordin, ADMP and Goosecoid and of the lateral mesoderm marker *Xlim-1*.

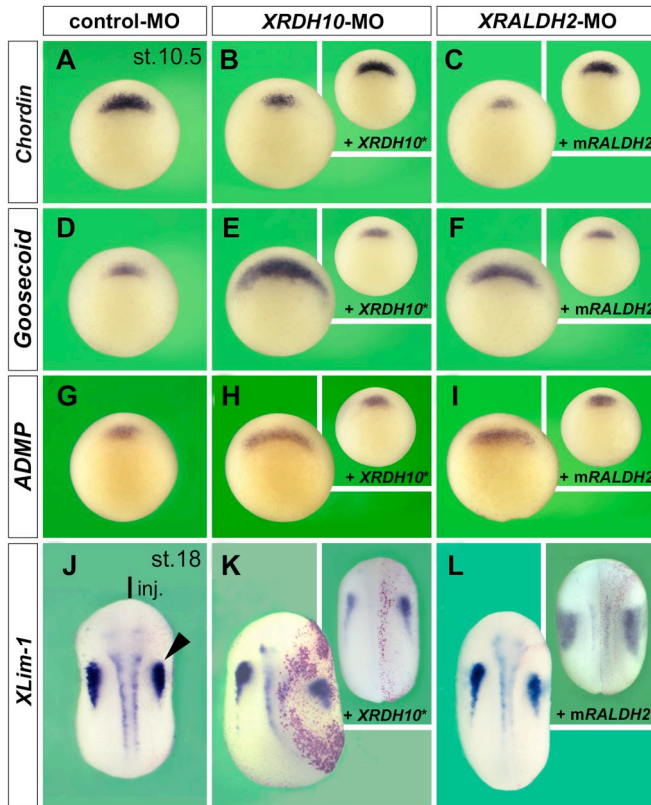


Fig. 10. Knockdown of *XRDH10* and *XRALDH2* influences organizer markers and mesodermal gene expression.

Antisense morpholino oligonucleotides (MOs) were injected marginally at the 2-cell stage (5.2 pmol per blastomere). Insets show embryos co-injected with rescue constructs that cannot be targeted by the morpholinos (*XRDH10** and m*RALDH2*)

(A-I) Gastrula embryos in dorsal view. *XRDH10*- and *XRALDH2*-morphants have reduced *Chordin* expression (A-C) and expanded expression domains of *Goosecoid* (D-F) and *ADMP* (G-I).

(J-L) Neurula embryos in dorsal view (anterior to the top) after a single injection of MOs with the lineage tracer *nlacZ* mRNA (red nuclei). *XRDH10*-MO and *XRALDH2*-MO reduce *Xlim-1* expression in the pronephros (arrowhead).

Indicated phenotypes were observed in A, 33/33; B, 21/36 (inset: 19/27); C, 28/36 (inset: 20/28); D, 51/56; E, 28/38 (inset: 46/53); F, 37/49 (inset: 34/44); G, 52/52; H, 14/26 (inset: 51/62); I, 51/62 (inset: 23/32); J, 11/15; K, 14/20 (inset: 28/32); L, 16/24 (inset: 50/51) embryos.

3.10 Loss of XRDH10 and XRALDH2 affects anterior-posterior patterning of the nervous system

In order to investigate the effects of XRDH10 and XRALDH2 depletion on the anterior-posterior patterning of the nervous system, *RDH10*-MO or *RALDH2*-MO were injected unilaterally into the marginal zones of 4-cell stage embryos and the effects were examined by whole mount *in situ* hybridizations (Fig. 11).

At the advanced gastrula stage (st. 12), injection of *XRDH10*-MO causes a reduction of *HoxD1* transcript levels and a posteriorwards retraction of the expression domain (Fig. 11 A, B). The *XRALDH2*-MO or a combination of *XRDH10*-MO and *XRALDH2*-MO causes a similar phenotype (Fig. 11 C, D). The posteriorwards retraction of *HoxD1* expression by ablation of XRDH10 or XRALDH2 can be rescued by co-injecting the specific rescue mRNAs *XRDH10** and *mRALDH2* (Fig. 10 E, F).

In late neurula stages and early tailbud embryos (stages 18 and 22) the effects on several region-specific CNS markers were tested, including *Rx2A* (eyes), *En2* (midbrain-hindbrain boundary), *Krox20* (Rhombomeres 3 and 5), *HoxB3* (rhombomeres 5/6), *xCRABP* (hindbrain) and *HoxC6* (spinal cord) (Fig. 11 G-Y). Upon ablation of XRDH10 or XRALDH2, a posteriorwards shift of *En2*, *Krox20*, *HoxB3* and *xCRABP* can be observed (Fig. 11 H, I, N, N', O, O', T, U). The effects on these markers are more severe upon co-injection of both MOs (Fig. 11 J, P, P', V). Co-injection of the MOs with the non-targeted mRNA constructs restores normal expression of the examined genes, supporting the specificity of the MO phenotypes (Fig. 11 K, L, Q, Q', R, R', W, X). The *Rx2A* and *HoxC6* expression domains remain unaffected (Fig. 11 H-J, T-V). The results suggest that XRDH10 and XRALDH2 depletion affects posterior midbrain and hindbrain patterning, but not the eye anlage and spinal cord at the analyzed stages.

Notably, the extent of the rhombomeric shift induced by 2.6 pmol *XRDH10*-MO is similar to that of an equimolar amount of *XRALDH2*-MO (Fig. 10 T, U, Y). The rhombomeric shift is not significantly increased when both MOs are injected together (Fig. 10 V, Y).

These results support an important role for XRDH10 and XRALDH2 in positioning hindbrain rhombomeres along the anterior-posterior neuraxis in *Xenopus*

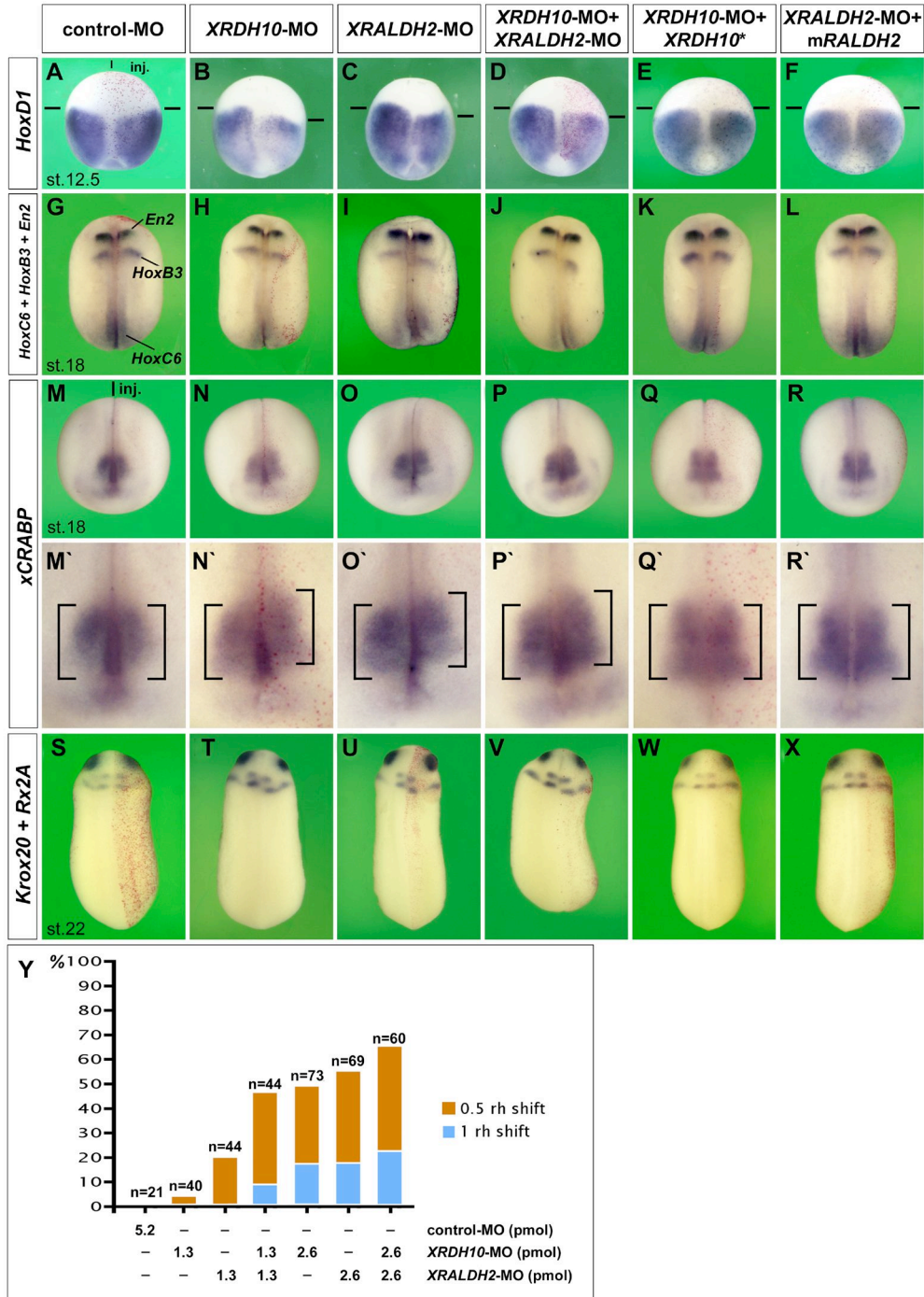


Fig. 11. *XRDH10* is critical for CNS patterning.

Morpholino oligonucleotides (MOs; each 2.6 pmol per embryo) were injected into the margin of one blastomere at the 2-cell stage. The non-targeted mRNA constructs *XRDH10** and *mRALDH2* (each 1 ng) and the lineage tracer *nlacZ* mRNA were co-injected. Embryos are shown in dorsal view (anterior to the top: A-L, S-X) or anterior-dorsal view (posterior to the top: M-R, M'-R').

(A-F) Late gastrula embryos. *XRDH10*-MO, *XRALDH2*-MO, or a combination of both morpholinos, causes a reduction and posteriorwards retraction of *HoxD1* expression, which is reverted by *XRDH10** and m*RALDH2* mRNA.

(G-L) Neurula embryos showing expression of *En2* (mid-/hindbrain boundary), *HoxB3* (hindbrain rhombomeres 5 and 6) and *HoxC6* (anterior spinal cord). The midbrain-hindbrain boundary and the hindbrain rhombomeres 5/6 are shifted posteriorwards upon ablation of *XRDH10* or *XRALDH2* (H, I). Strongest effects can be observed after depleting both enzymes (J). The position of the anterior spinal cord is not affected by any of the injections.

(M-R) Embryos at the advanced neurala stage. The panels M'-R' are magnifications of the embryos shown in M-R. Embryos show expression of *xCRABP* (cellular retinoic acid binding protein) that demarcates the presumptive hindbrain (square brackets). *XRDH10*-MO, *XRALDH2*-MO or a combination of both morpholinos cause a posteriorwards shift of the *xCRABP*-expression domain (M-P, M'-P'). The effects are neutralized by *XRDH10** and m*RALDH2* mRNA, respectively.

(S-X) Tailbud embryos depicting expression of *Rx2A* (eyes) and *Krox20* (rhombomeres 3 and 5). The anteriorwards shift of the rhombomeres and the eyefield that could be observed after injection of *XRALDH2*-MO is enhanced by co-injecting *XRDH10*-MO (T-V).

(Y) Effects of *XRDH10* and *XRALDH2* knockdown on hindbrain patterning. The posteriorwards shift of *Krox20* expression is shown in response to MO injections at the indicated doses.

Frequencies of embryos with indicated phenotypes were:

A, 77/88; B, 55/105; C, 30/68; D, 54/88; E, 19/21; F, 23/25; G, 34/35; H, 17/31 (*En2*); H, 30/31 (*HoxB3*); H, 27/31 (*HoxC6*); I, 15/33 (*En2*); I, 31/33 (*HoxB3*); I, 32/33 (*HoxC6*); J, 6/9 (*En2*); J, 8/9 (*HoxB3*); J, 5/9 (*HoxC6*); K, 20/23; L, 39/39
M, 9/11; N, 10/11; O, 18/19; P, 12/12; Q, 11/11; R, 17/19; S, 10/10; T, 35/73; U, 37/69; V, 38/60; W, 10/10; X, 13/14

3.11 XRDH10 is required for the posteriorizing effect of retinol

In order to underline the important function of XRDH10 in RA metabolism, it was investigated whether retinol can exert its posteriorizing effect on embryos in the absence of XRDH10 (Fig. 12).

Embryos that were treated with 100 μ M retinol during blastula and gastrula stages (stages 9-12) show an anteriorwards expansion of the *HoxD1* expression domain (Fig. 12 C). In embryos that were unilaterally injected with *XRDH10*-MO before the retinol-treatment, the *HoxD1* expression domain does not expand anteriorwards on the injected site (Fig 12 D).

This suggests that XRDH10 is required for the first step of RA biosynthesis.

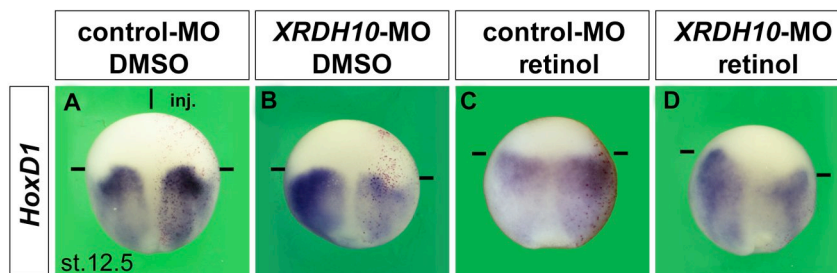


Fig. 12. XRDH10 is critical for the posteriorizing effect of retinol.

(A-D) Treatment with 100 μ M retinol at stages 9 -12 induces a robust anterior expansion of *HoxD1* expression in late gastrula embryos (C). *XRDH10*-MO reverses the effect of retinol on the injected right side (D).

Frequency of embryos with the indicated phenotype was A, 9/9; B, 7/13; C, 9/9; D, 20/33.

4. Discussion

The *Xenopus* homologue of retinol dehydrogenase 10 (*XRDH10*) mediates the first step in RA synthesis from retinol to retinal. *XRDH10* is expressed in the dorsal blastopore lip and in other domains of the embryo that partially overlap with *XRALDH2* expression and are complementary to *XCYP26A1* expression domains. Endogenous RA suppresses endogenous *XRDH10* gene expression, suggesting a negative feedback regulation. Embryos, injected with *XRDH10* mRNA resemble embryos that were treated with low doses of exogenous RA. Upon *XRDH10* mRNA injection, RA target genes are upregulated and the gene expression of early organizer markers is influenced. *XRDH10* synergizes with *XRALDH2* in posteriorizing the developing hindbrain. Knockdown of *XRDH10* and *XRALDH2* by injection of specific morpholino oligonucleotides has the opposite effect on organizer gene expression and causes a ventralized phenotype as well as anteriorization of the brain. The data indicate that the conversion from retinol to retinal by *XRDH10* is involved in the specification of the dorsal-ventral and anterior-posterior body axes as well as in pattern formation of the central nervous system. The combinatorial gene expression and concerted action of *XRDH10* and *XRALDH2* constitutes a new mechanism for the establishment of a morphogen gradient in the embryo.

4.1 Comparison of *RDH10* gene expression in *Xenopus* and mouse embryonic development

RDH10 has been cloned in several vertebrate species, including mouse, rat and human, but its gene expression during embryogenesis has so far only been described in the mouse (Wu et al., 2004; Sandell et al., 2007; Cammas et al., 2007; Belyaeva et al., 2008; Romand et al., 2008). Here, the first report of *RDH10* gene expression in a non-mammalian species is presented (Fig. 2). The analysis of *XRDH10* reveals several similarities with mouse *Rdh10* gene expression. At the open neural plate stage, common expression domains can be found in the lateral mesoderm, cardiac crescent and the ventral neural groove. With the closure of the neural tube, *RDH10* demarcates the roofplate of the midbrain, the midbrain-hindbrain boundary, the ear

and the olfactory system in both species. In addition, *XRDH10* expression in the pronephros correlates to the mouse *Rdh10* expression in the nephric system. However, differences in the *RDH10* gene activities in the two species can be detected. Most importantly, *RDH10* gene expression appears to start earlier in *Xenopus* than in the mouse. Maternal *XRDH10* transcripts can be detected already at the 4-cell stage and in embryos preceding mid-blastula transition. During gastrulation, distinct expression of *XRDH10* is observed first in the dorsal blastopore lip and then in the ventral blastopore lip, paraxial mesoderm and head process. In contrast, mouse *Rdh10* transcripts are not detected before the head fold stage, consistent with an apparent absence of RA signals in RARE-*lacZ* transgenic mice (Rossant et al., 1991). In earlier egg cylinder stage, the precursor all-trans retinal is present and expression of RDH5 and ADH4 can be detected, suggesting that other enzymes could convert retinol into retinal before the onset of *Rdh10* expression in the early mouse embryo (Ulven et al., 2000). In view of the generally lower RNA content in the mouse compared to *Xenopus* embryos, it is possible that murine *Rdh10* may be present earlier and has escaped attention due to limitations of detection by whole mount *in situ* hybridization. In more advanced embryos, there are additional differences in gene expression patterns. *XRDH10* is abundant in the presomitic mesoderm, while this tissue is free of *Rdh10* expression in the mouse. Later, *XRDH10* demarcates neural crest cells between the somites, while murine *Rdh10* is expressed in the somites. Along the developing neural tube, *XRDH10* is robustly expressed in the ventral midbrain, while murine *Rdh10* transcripts are confined to the ventral hindbrain and spinal cord anlage. In conclusion, there is extensive overlap between *RDH10* gene expression in *Xenopus* and mouse, suggesting an important and evolutionary conserved role of this enzyme in both species. Some differences with respect to the temporal and spatial expression patterns exist that may reflect divergent strategies in supplying RA in lower vertebrates and mammals.

4.2 *XRDH10* gene expression demarcates sites of RA signalling in the developing embryo

In this study, it could be shown that *XRDH10* overlaps with *XRALDH2* expression in several domains. These regions are the dorsal blastopore lip at gastrula stages, the paraxial trunk mesoderm at neurula stages, the eye field in early tailbud stages and the telencephalon, spinal cord, eyes, ears, anterior lateral plate and pronephros in late tailbud stages. (Fig. 2 E, G, J, K, M, N, R, S see also Chen et al., 2001 for *XRALDH2*). Of note is, that *XRDH10* is expressed in more restricted areas than *XRALDH2*, being frequently embedded in the *XRALDH2* expression domains. Moreover, *XCYP26A1* is expressed adjacent to *XRDH10* and *XRALDH2* in the ventral blastopore lip, the anterior and posterior parts of the neural plate, around the eye anlage and in advanced tailbud stages in the periocular region, in tissue flanking the pronephros and in the tip of the tailbud (Fig 2 H, L, O, T, see also Hollemann et al., 1999 for *XCYP26A1*). Thus, *XCYP26A1* is expressed complementary to *XRDH10* and *XRALDH2*, suggesting a fine-regulated supply of RA in the embryo.

Previous studies aimed at directly measuring the spatial distribution of RA in *Xenopus* embryos, using High Performance Liquid Chromatography (HPLC; Chen et al., 1994; Creech-Kraft et al., 1994). Elevated RA levels have been found in the dorsal part of gastrula embryos and in the anterior portion of neurula embryos (Chen et al., 1994). These results are in accordance with the robust *XRDH10* and *XRALDH2* expression in the dorsal blastopore lip and anterior trunk mesoderm (Fig 2 E, G, J, K). *Xenopus* embryos that have been ubiquitously injected with the RARE- β -galactosidase fusion construct reveal distinct sites of active RA-signalling, including the dorsal blastopore lip at the mid-gastrula stage, the dorsal midline at early neurula stage and late tailbud stages, as well as anterior head structures (Yelin et al., 2007). Together, the expression of *XRDH10* and *XRALDH2* matches reported sites of RA abundance and RA signalling in the early *Xenopus* embryo.

In the mouse, the *Rdh10* expression pattern also overlaps at several sites with that of *Raldh2* (Niederreither et al., 1997; Moss et al., 1998; Sandell et al., 2007). At the headfold stage, *Rdh10* and *Raldh2* are expressed in the paraxial mesoderm. Similar as in *Xenopus*, the anterior border of *Rdh10* expression is located slightly more anterior than the *Raldh2* expression border. During early somitogenesis, both genes are expressed in the somites and in the adjacent lateral plate mesoderm with a sharp

anterior and posterior boundary. Later, *Rdh10* and *Raldh2* are co-expressed in the posterior branchial arch region, the developing cochlear system and the posteriormost segment of the heart tube. In the developing limb buds, murine *Rdh10* transcripts are concentrated in the zone of polarizing activity (ZPA), while *Raldh2* expression is confined to the proximal margin of the limb bud without extending into the future limb (Niederreither et al., 1997; Mic et al., 2004). This suggests that *Rdh10* provides an enriched source of retinal within the ZPA that can be converted into RA in the posterior, proximal region. During limb development, *Rdh10* and *Raldh2* are co-expressed in the interdigital mesenchyme (Cammass et al., 2007; Niederreither et al., 2002). In early somite stages, murine *Cyp26A1* is expressed in the caudal neural plate, tailbud mesoderm and hindgut endoderm, as well as in anterior regions, which is complementary to the *Rdh10* and *Raldh2* expression in the somites and in the adjacent lateral plate mesoderm at early somite stages (Fujii et al., 1997; Niederreither et al., 1997; Sandell et al., 2007). *Cyp26A1* expression can be found in the distal epithelium of fore- and hindlimb buds, complementary to the proximal location of *Rdh10* and *Raldh2* expression (Fujii et al., 1997; Niederreither et al., 1997; Sandell et al., 2007). This suggests, that also in the mouse RA is generated in distinct areas by the combined actions of *Rdh10* and *Raldh2* and restricted by *Cyp26A1*, which is expressed in adjacent but non-overlapping regions. It needs to be pointed out that, during early embryogenesis in several vertebrates including zebrafish, *Xenopus*, chick and mouse, RALDH2 and CYP26A1 are the main RA metabolizing enzymes. RALDH1 and RALDH3 as well as CYP26B1, CYP26C1 and CYP26D1 metabolize RA later in development (Haselbeck et al., 1999; Li et al., 2000; Mic et al., 2000, Zhao et al., 2005; Reijntjes et al., 2003; MacLean et al., 2001, Uehara et al., 2007, Gu et al., 2006). However, RDH10 is the only retinol-converting enzyme that is expressed in a tissue-specific manner in the early embryo (Sandell et al., 2007; Cammass et al., 2007; Romand et al., 2008; this study).

Several sites in which *Rdh10* and *Raldh2* expression in the mouse overlap display active RA signalling. These regions include the paraxial mesoderm at head fold stages, the somites at the onset of somitogenesis, the lateral plate, the developing heart and the developing limb buds (Sandell et al., 2007; Niederreither et al., 1997; Rossant et al., 1991). *Rdh10* and *Raldh2* are co-expressed in the developing ear and in the olfactory system, where RA signalling can be detected.. While *Rdh10* and *Raldh2*

expression can be detected in the paraxial mesoderm at head fold stages, mouse embryos that are transgenic for the RARE-*lacZ* reporter gene show RA activity in all three germ layers in this area, suggesting a diffusion of RA (Rossant et al, 1991; Niederreither et al., 1997; Rommand et al. 2008). Interestingly, the anterior border of RA transgene activity at early somite stages protrudes into the hindbrain up to rhombomere 2, while *Raldh2* expression has an anterior limit at the level of the hindbrain-spinal cord boundary, suggesting a diffusion of RA along the hindbrain territory (Sirbu et al., 2005).

Taken together, *Rdh10* gene expression demarcates sites of RA signalling activity in both *Xenopus* and the mouse, suggesting that *Rdh10* may have an important role in supplying RA in the developing embryo.

4.3 *XRDH10* gene expression is regulated by retinoic acid

An important observation in this study is that RA downregulates transcript levels of *XRDH10* (Fig 3 A-D). Importantly, a low dosis of RA was chosen and added to embryos during an advanced period of development to avoid teratologic side effects. The observed reduction of *XRDH10* gene expression is therefore not due to malformation or loss of morphological structures, but to specific loss of gene expression domains. At taibud stages, expression of *XRDH10* upon RA treatment is strongly reduced in the pronephros and lost in the eyes, ears, olfactory system, mid-hindbrain boundary, branchial arches, anterior lateral plate, neural crest cells and presomitic mesoderm. The failure to completely suppress *XRDH10* in the pronephros might be due to a later onset of gene expression in this domain after the time when RA is administered. In contrast, lowering of RA levels by administration of the pharmacological inhibitors disulfiram and citral or overexpression of *XCYP26A1* elevates *XRDH10* expression, suggesting that endogenous RA suppresses *XRDH10* gene activity.

Previous studies have shown that RA downregulates *RALDH2* expression in *Xenopus* and other vertebrate species (Chen et al., 2001, Niderreither et al., 1997; Dobbs-McAuliffe et al., 2004). *Xenopus* embryos that have been treated with RA during blastula and early gastrula stages show downregulation of *XRALDH2*. Analysis of

early neurula embryos suggested that the anterior region, including the stomodeal-hypophyseal, olfactory and eye anlagen, is most sensitive to RA treatment and shows loss of *XRALDH2* expression. In tailbud and tadpole embryos, the *XRALDH2* expression in the otic vesicle is lost upon RA treatment, whereas *XRALDH2* expression in the pronephric ducts and the spinal cord does not seem to be affected (Chen et al., 2001). These results reveal a negative feedback regulation of RA biosynthesis in distinct anterior areas that are particularly sensitive to elevated RA levels. However, the early treatment with RA (blastula stages) might have led to a general loss of anterior structures which would reveal the loss of gene expression as a secondary effect. The failure to suppress *XRALDH2* in the pronephric duct and spinal cord might be due to a later onset of gene expression in these domains after the time when RA is administered.

In the mouse, administration of RA to pregnant mice at E 8.5 results in a downregulation of *Raldh2* transcripts in the caudal somites, the coelomic wall and the cloacal region (Niederreither et al., 1997). The most conclusive experiment for the regulation of *RALDH2* by RA was obtained in zebrafish embryonic and adult fibroblast cells which were co-transfected with a construct containing the *RALDH2* promoter region fused to the firefly luciferase reporter gene and a cDNA encoding the ligand-dependent transcription factor *RAR α* . It was shown that treatment of the cells with RA leads to a downregulation of *RALDH2* promoter activity, suggesting that RA directly suppresses *RALDH2* transcriptional activity (Dobbs-McAuliffe et al., 2004). Moreover RA can positively regulate the transcription of the degrading enzyme CYP26A1 (Hollemann et al., 1998; Reijntjes et al., 2003; White et al., 2007). In *Xenopus*, RA treatment increases *XCYP26A1* transcription in animal cap cells. However, *XCYP26A1* transcripts are reduced in the marginal zone of gastrula stage embryos upon RA treatment which suggests that *XCYP26A1* can also be negatively regulated by RA in distinct regions of the embryo (Hollemann et al., 1998). Expression of *Cyp26a1* was examined in zebrafish embryos that had been treated with an inhibitor of RALDHs, diethylaminobenzaldehyde (DEAB), in order to abolish RA signalling. DEAB-treated embryos lack *Cyp26a1* expression in the somites, suggesting that RA is required for *Cyp26a1* to be properly expressed (Dobbs-McAuliffe, et al., 2004).

The results point to an intricate regulatory network, in which RA suppresses anabolic and stimulates catabolic enzymes.

Despite the regulation of anabolic and catabolic enzymes, RA also influences the expression of other components that are involved in RA signalling. It can control the availability of retinol by positively regulating lecithin:retinol acyltransferase which esterifies and thus stores retinol, making it unavailable for synthesis of RA (Matsuura and Ross, 1993). Furthermore, RA positively regulates *CRABP2* expression in F9 teratocarcinoma cells with RA (Giguere et al., 1990). In the murine *CRBP1* gene a RARE was identified and characterized as a binding site for RAR β 2. *CRBP1* expression can be induced upon RA treatment (Smith et al., 1991). Finally, RA is able to induce expression of different isoforms of RARs. The murine *RAR α 2* gene contains a RARE to which all RARs can bind and *RAR α 2* can be induced upon RA treatment in murine embryonic stem cells (Leroy et al., 1991).

Thus, RA can control its own synthesis, degradation and signalling activity, providing a fine-tuned feedback control that provides protection against exogenous retinoid fluctuations and allows the stabilization of local RA distribution and signalling in the embryo. Here, it is shown for the first time that *RDH10* is negatively regulated by endogenous RA, suggesting negative feedback regulation at the level of vitamin A conversion into retinal. It remains to be shown whether *RDH10* is a direct RA target gene. Promoter reporter gene studies as described for *Raldh2* in the zebrafish could be done to reveal if whether *XRDH10* is directly regulated by RA signals. The feedback-regulated blockage of the first step of RA biosynthesis provides a very efficient way to adjust the RA production to the actual need of this signalling molecule. A fine-tuned feedback regulatory mechanism protects against RA fluctuations and contributes to a robust temporally and spatially regulated distribution of this morphogen in the embryo.

4.4 The role of *XRDH10* in dorsal-ventral patterning

The dorsal blastopore lip, or organizer, plays an important role in establishing the dorsal-ventral body axis of the embryo (De Robertis and Kuroda, 2004). In this study, a distinct expression of *XRDH10* could be observed in the organizer of early gastrula embryos (Fig. 2 E). Within the blastopore lip, *XRDH10* signals are embedded in the

dorsolateral expression domain of *XRALDH2* and complementary to *XCYP26A1* expression that is confined to the ventrolateral domain (Hollemann et al., 1998; Chen et al., 2001). *XRDH10* expression also coincides with sites of active RA signalling in the dorsal blastopore lip, as observed in RARE-*lacZ* mRNA-injected and RARE-*GFP* transgenic *Xenopus* embryos (Yelin et al., 2005). It was shown in this study that microinjection of *XRDH10* mRNA or treatment with exogenous RA leads to upregulation of *Chordin* and *Xlim-1* expression, while *Gooseoid* (*Gsc*) and *ADMP* expression are downregulated (Fig. 5). This is a specific effect, as other organizer markers including *Noggin*, *Frzb1*, *sFRP2*, and *Crescent* are not affected (Fig. 6). In contrast, morpholino oligonucleotide-mediated downregulation of *XRDH10* or *XRALDH2* leads to a suppression of *Chordin*, and upregulation of *Gsc* and *ADMP* expression in the dorsal blastopore lip (Fig. 10 I-K), suggesting that RA signals may play an important role in regulating the transcription of these organizer-specific genes.

It has previously been shown that, in accordance with the findings presented in this study, RA suppresses *Gsc* expression and that the RA-synthesis inhibitor citral stimulates *Gsc* expression during gastrulation (Yelin et al., 2005). Hence, the results from this study support a role of RA as a negative regulator of *Gsc* and reveal an essential role of both, *XRDH10* and *XRALDH2*, in suppressing this transcription factor.

Xlim-1 expression is known to be upregulated by excessive RA treatment and was found to be a direct target gene of RA (Taira et al., 1992, 1994; Blumberg et al., 1997; Cartry et al., 2006). In this study, it was observed that *XRDH10* mRNA stimulates expression of this gene in the blastopore lip, supporting a positive effect of RA on *Xlim-1* expression. However, a downregulation of *Xlim-1* expression after injection of *XRDH10* or *XRALDH2* morpholino oligonucleotides can only be observed in the lateral plate mesoderm of neurula embryos (Fig. 10 J-L), while expression of this gene in the blastopore lip at the gastrula stage is unaffected (data not shown). This suggests that RA may be dispensable for inducing this transcription factor in the dorsal blastopore lip.

This study presents, for the first time, *ADMP* as an RA-regulated gene. *XRDH10* mRNA and RA downregulate *ADMP* expression, whereas morpholino oligonucleotides against *XRDH10* and *XRALDH2* cause the opposite effect,

suggesting that RA may act as an endogenous negative regulator of *ADMP* expression.

While the gain- and loss of function studies presented here support a role of RA as a positive regulator of *Chordin* expression, previous work by others has come to the opposite conclusion. Yelin and co-workers reported that treatment of embryos between stages 8.5 and 10.5 with 1 μ M RA downregulates *Chordin* transcription, whereas 60 μ M citral or injection of *CYP26A1* mRNA causes the opposite effect (Yelin et al., 2005). The discrepancy may be explained by different protocols, i.e. treatment of RA at a five-fold higher dosis (5 μ M) and for a shorter period (stage 9 to 10.5). Negative feedback regulatortory mechanisms may contribute to the observed discrepancies. Indeed, treatment of embryos with citral, disulfiram or injection of *CYP26A1* leads to an upregulation of *XRDH10* (Fig. 3 G-K) which could in turn elevate the RA level and upregulate *Chordin* expression. This study showed that injection of *XRDH10* mRNA leads to a more dramatic and more frequent expansion of the *Chordin* expression domain than external treatment with RA (Fig. 5 F, H). Moreover, an upregulation of *Chordin* following RA treatment or *XRDH10* mRNA injection could be observed already at late blastula stages, supporting the positive effect of RA signalling on *Chordin* expression (Fig. 5 A-D).

ADMP is a homologue of BMP3 and induces BMP/Smad1 signalling via the ALK2 receptor (Reversade and De Robertis, 2005). In contrast, *Chordin* acts as a secreted BMP antagonist that binds to BMPs and prevents them from signalling (Sasai et al., 1994; Piccolo et al., 1996). The ventralized phenotype observed in *XRDH10* or *XRALDH2* depleted embryos (Fig. 9) is reminscent of elevated BMP/Smad1 signalling (e.g. Pera et al., 2003; Fuentealba et al., 2007) that may result from elevating protein levels of *ADMP* and lowering *Chordin* levels in the organizer. Thus, the opposite transcriptional regulation of *ADMP* and *Chordin* genes by RA in the dorsal blastopore lip provides a possible mechanism for the observed roles of two biosynthetic enzymes in the regulation of dorsoventral patterning in the embryo.

4.5 The role of XRDH10 in anterior-posterior patterning

In this study, it could be shown that XRDH10 affects patterning of the anterior-posterior body axis. Injection of *XRDH10* mRNA leads to a moderate reduction of head structures and a shortening of the anterior-posterior body axis (Fig. 4 A, B). This effect is reminiscent of the microcephaly and shortened tails obtained by treating embryos with 0.1 μ M RA (Durstun et al., 1989). Moreover, *XRDH10* mRNA increases the posteriorizing effect of retinol, causing a loss of head structures (anencephaly) and collapse of the eye field (Fig. 8 C, H). In early embryos, *XRDH10* mRNA causes an upregulation and anteriorwards expansion of the markers *HoxD1* (expressed in trunk mesoderm and overlying ectoderm) and *Xlim-1* (expressed in lateral plate mesoderm, notochord and neurons). These effects were reverted by co-injection of *XCYP26A1* mRNA, suggesting that XRDH10 promotes posterior development in an RA-dependent manner (Fig. 7). It could be shown that *XRDH10* morpholino oligonucleotides cause the opposite phenotypes, resulting in reduction and posteriorwards retraction of *HoxD1* and *Xlim-1* expression (Fig. 10 J-L, 11 A-F). Within the developing brain, overexpression of *XRDH10* causes a slight anteriorward shift *En2* (demarcating the midbrain-hindbrain boundary), and *Krox20* (expressed in rhombomeres 3 and 5) (Fig. 7 K-T). In contrast, knockdown of *XRDH10* results in a robust posteriorwards shift of these markers as well as of *HoxB3* (rhombomeres 5 and 6) and *XCRABP* (hindbrain) (Fig. 11 G-X). Previous studies showed that microinjection of *XRALDH2* mRNA results in an anteriorward shift of *Otx2* (forebrain, midbrain), *En2* and *Krox20* expression (Chen et al., 2001). The study presented here supports this important function of *XRALDH2* in brain patterning in *Xenopus* (Fig. 11 C, I, O, O', U). Moreover, a caudal expansion of rhombomeres 3 and 4 and a reduction of rhombomeres 5 to 8 was observed in *Raldh2* knockout mice (Niederreither et al., 2000).

Consistent with this, in the mouse, low doses of RA lead to an anteriorwards shift of the rhombomere specific *Hoxb1* expression domain (Marshall et al., 1992).

It has been reported that, in vitamin A-deficient quail embryos, a decrease in RA signalling leads to an expansion of the rhombomeres 1-3 and a loss of the posteriormost rhombomeres 4-7 (Maden et al., 1996). Similar changes in rhombomeric patterning were observed in mouse embryos deficient of $RAR\alpha$ and

RAR γ (Wendling et al., 2001). It is interesting to note that *XRDH10* and *XRALDH2* morphant *Xenopus* embryos do not show a loss of posterior hindbrain rhombomeres, as the analyzed markers Krox20 and HoxB3 are not reduced, but only posteriorly shifted. In accordance with these results, microinjection of *XCYP26A1* or dominant negative *RAR β* mRNA leads to a posterior shift, but not loss of hindbrain-specific markers in *Xenopus* embryos (Hollemann et al., 1998; van der Wees et al., 1998). The experiments suggest that species-specific differences may exist among vertebrates in the response of the developing hindbrain to changed levels of RA.

In this study, it was demonstrated that overexpression of *XRDH10* and *XRALDH2* together results in a pronounced anteriorwards shift of the hindbrain rhombomeres 3 and 5 (Fig. 7 N, U). The extent of the rhombomeric shift induced by a combination of *XRDH10* and *XRALDH2* exceeds the sum of effects induced by each mRNA alone, suggesting that the two enzymes act synergistically during the patterning of the embryonic hindbrain. However, loss of function experiments revealed that knockdown of *XRDH10* by a high dosis of morpholino oligonucleotide (2.6 pmol) results in a posteriorwards shift of rhombomeres 3 and 5 that is not further exacerbated by concomitant knockdown of *XRALDH2* (Fig. 11 Y). In addition, analysis of the expression of the RA target gene *HoxD1* revealed that the posteriorizing effect of retinol is blocked by morpholino oligonucleotide-mediated depletion of *XRDH10* (Fig. 12). This result strengthens the importance of *XRDH10* during patterning of the nervous system and suggests that this enzyme is indispensable for the conversion of retinol into RA in the early embryo.

4.6 Model for the establishment of the retinoic acid morphogen gradient

Along the anterior-posterior neuraxis concentration gradients of RA specify positional values through the activation of Hox genes. This has been postulated for the developing hindbrain and spinal cord (Gould et al., 1998; Muhr et al., 1999; Dupé and Lumsden, 2001; Liu et al., 2001). Retinoid deficiency in quail embryos is associated with alterations of Hox gene expression in the caudal hindbrain (Maden et al., 1996). Conversely, the addition of exogenous RA can result in ectopic Hox expression and

concomitant posterior transformations of rhombomere identity in several species (Papalopulu et al., 1991; Marshall et al., 1992; Kessel, 1993; Conlon, 1995; Hill et al., 1995; Gale et al., 1996). Furthermore, expression of constitutively active or dominant negative *RAR α* in *Xenopus* embryos causes alterations in normal Hox gene expression (Sharpe and Goldstone, 1997; Blumberg et al., 1997; Kolm et al., 1997). For 3 Hox genes it has been demonstrated that they contain RAREs, making them direct target genes of RA (Dupé et al., 1997; Qian et al., 2000). Eventhough a gradient for RA has never been directly visualized, there is evidence that such a gradient might exist. In frog and chick embryos exogenous RA treatment causes concentration-dependent effects on hindbrain patterning (Durstun et al., 1989; Sive et al., 1990; Marshall et al., 1992; Godsave et al. 1998). Different concentrations of a pharmacological blocker of Raldh2 causes a graded anteriorization of the hindbrain, indicating that posterior rhombomeres require higher concentrations of RA (Begemann et al., 2004; Maves and Kimmel, 2005). *In situ* hybridization studies showed that expression of Hox genes occurs in a graded ditribution. The maximum corresponds to the anterior border of expression with levels diminishing posteriorwards which reflects the gradual distribution of RA (De Robertis et al., 1991).

Previous models have suggested that RA gradients arise as a result of local RA supply by RALDH2 in the paraxial trunk mesoderm, diffusion of RA and CYP26A1-mediated RA decay at the anterior and posterior ends of the neural plate (Maden, 1999; Maden, 2002; Sirbu et al., 2005; Hernandez et al., 2007; White et al., 2007). Such a gradient has been postulated for the hindbrain which falls within a gap between *RALDH2* and *CYP26A1* expressing cells in the trunk and anterior head regions, respectively (Swindell et al., 1999). In RARE-*nlacZ* mouse embryos, RA signalling takes place in the neural tube including the hindbrain region, eventhough *Raldh2* is expressed in the somites and mesenchyme surrounding the neural tube with an anterior limit at the spinal cord-hindbrain border (Rossant et al., 1991; Niederreither et al., 1997; Sirbu et al., 2005). This points towards a diffusion of newly synthesized RA.

The data presented in this study suggest an alternative model for RA gradient formation that postulates the generation of an initial RA gradient already during the RA synthesis step. The model is based on the expression patterns and coordinated action of XRDH10 and XRALDH2. At early neurula stage, XRDH10 is abundant in anterior trunk mesoderm cells that produce retinal. The secreted retinal is thought to

diffuse into posterior cells which contain XRALDH2 and further oxidize retinal into RA. As a consequence, highest levels of RA are produced in the anterior trunk mesoderm where *XRALDH2* and *XRDH10* are co-expressed, with decreasing concentrations towards the posterior end. The newly synthesized RA can diffuse into the overlying neural plate ectoderm. Degradation of RA at the anterior and posterior poles by the action of CYP26A1 further refine the RA gradients in the hindbrain and spinal cord (Fig. 13). This mechanism may not only apply to the establishment of RA gradients along the primary neuraxis, but also to other areas where *XRDH10* and *XRALDH2* are co-expressed and complementary to *XCYP26A1* expression, such as in the dorsal blastopore lip, the pronephros anlage, the eye field and the ear placode. The mechanism of nested gene expression and combinatorial action has initially been found in the Hox genes, the most prominent targets of RA signalling in vertebrates (Kessel and Gruss, 1991). This suggests a common principle for the generation and downstream signalling events of this morphogen.

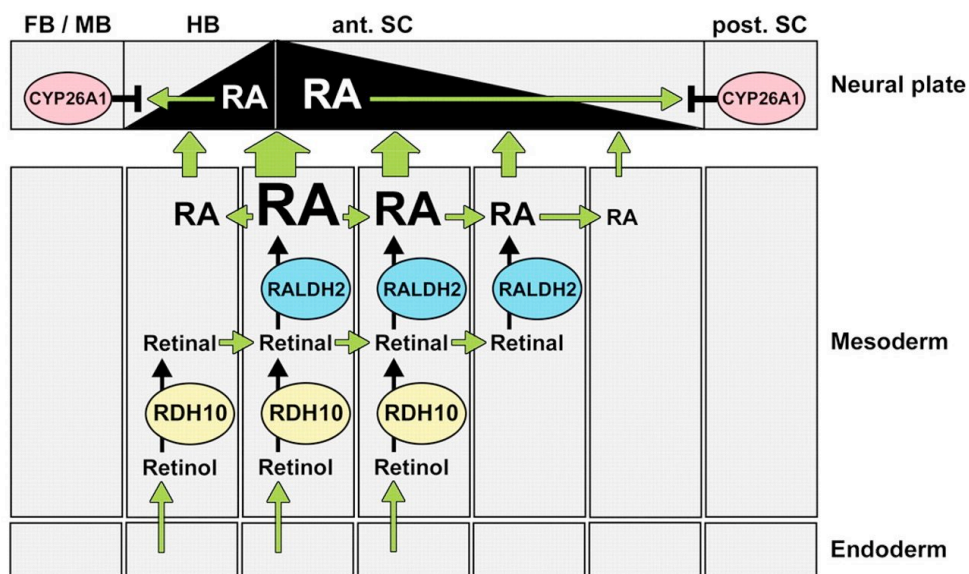


Fig.13. Model for the establishment of RA morphogen gradients in the early embryo. The nested gene expression and combinatorial action of *RDH10* and *RALDH2* causes a posteriorward flow of retinal that generates an initial RA gradient in the trunk mesoderm with a peak at the level of the hindbrain-spinal cord boundary. Subsequent diffusion of RA creates two gradients across the hindbrain and spinal cord, which acquire their final shape through CYP26A1-mediated RA degradation at the anterior (ant.) and posterior (post.) ends of the neural plate. FB, forebrain; MB, midbrain; HB, hindbrain; SC, spinal cord.

5. Conclusion

In this study, the recently identified *Xenopus* homologue of retinol dehydrogenase 10 (XRDH10) was characterized. XRDH10 is a member of the short-chain dehydrogenase/reductase (SDR) family and mediates the first step in RA synthesis, the oxidation from retinol to retinal.

During early development in *Xenopus*, *XRDH10* is dynamically expressed. Transcripts can be detected within *XRALDH2* expression domains and complementary to *XCYP26A1* expression. *XRDH10* and *XRALDH2* expression demarcate areas in the embryo, where active RA signalling takes place.

XRDH10 expression is suppressed by RA, suggesting a negative-feedback regulation. Microinjection of *XRDH10* mRNA into *Xenopus* embryos causes microcephaly and shortened tails, a phenotype that can be observed after treating embryos with low RA concentrations. Moreover, XRDH10 can upregulate a set of RA target genes, suggesting that XRDH10 and RA have common activities.

XRDH10 and RA influence the expression of early organizer markers. Microinjection of *XRDH10* mRNA or treatment with exogenous RA leads to upregulation of the organizer markers *Chordin* and *XLim-1*, while *Gooseoid (Gsc)* and *ADMP* expression are downregulated, suggesting that RA signals may influence the transcription of these organizer-specific genes. In tailbud stage embryos, XRDH10 synergizes with *XRALDH2* in posteriorizing the developing brain, indicating that XRDH10 co-operates with *XRALDH2* in stimulating RA signalling.

Morpholino-mediated knockdown of *XRDH10* causes a reduction of head structures and enlargement of ventroposterior structures. In gastrula embryos, downregulation of *XRDH10* or *XRALDH2* leads to a suppression of *Chordin*, and upregulation of *Gsc* and *ADMP* expression in the dorsal blastopore lip, providing a possible role of the two RA biosynthetic enzymes in the regulation of dorsoventral patterning in the embryo. Microinjection of XRDH10-MOs leads to an anteriorization of the developing brain as observed in *XRALDH2* morphant embryos, demonstrating an involvement of XRDH10 in RA biosynthesis during axis formation and brain patterning.

The data, obtained in this study, indicate that the conversion of retinol into retinal is a developmentally controlled step, involved in the specification of the dorsoventral and anteroposterior body axes as well as in pattern formation of the CNS. The combinatorial gene expression and concerted action of XRDH10 and XRALDH2 may constitute a 'biosynthetic enzyme code' for the establishment of a morphogen gradient in the embryo.

6. References

- Abu-Abed S, Dollé P, Metzger D, Beckett B, Chambon P, Petkovich M. (2001) The retinoic acid-metabolizing enzyme, CYP26A1, is essential for normal hindbrain patterning, vertebral identity, and development of posterior structures. *Genes Dev*, 15, 226-40
- Agius E, Oelgeschläger M, Wessely O, Kemp C, De Robertis EM. (2000) Endodermal Nodal-related signals and mesoderm induction in *Xenopus*. *Development*, 127, 1173-83
- André F, Rigot V, Thimonier J, Montixi C, Parat F, Pommier G, Marvaldi J, Luis J. (1999) Integrins and E-cadherin cooperate with IGF-I to induce migration of epithelial colonic cells. In *J Cancer*, 83, 497-505
- Ang HL, Deltour L, Zgombić-Knight M, Wagner MA, Duester G. (1996) Expression patterns of class I and class IV alcohol dehydrogenase genes in developing epithelia suggest a role for alcohol dehydrogenase in local retinoic acid synthesis. *Alcohol Clin Exp Res.*, 20, 1050-64
- Ang HL, Deltour L, Hayamizu TF, Zgombić-Knight M, Duester G. (1996b) Retinoic acid synthesis in mouse embryos during gastrulation and craniofacial development linked to class IV alcohol dehydrogenase gene expression. *J Biol Chem*, 271, 9526-34
- Avantaggiato V, Acampora D, Tuorto F, Simeone A. (1996) Retinoic acid induces stage-specific repatterning of the rostral central nervous system. *Dev Biol*, 175, 347-57
- Baker ME. (1996) Unusual evolution of 11 β - and 17 β -hydroxysteroid and retinol dehydrogenases. *Bioessays*, 18, 63-70
- Balkan W, Colbert M, Bock C, Linney E. (1992) Transgenic indicator mice for studying activated retinoic acid receptors during development. *Proc Natl Acad Sci U S A*, 89, 3347-51
- Bang AG, Papalopulu N, Goulding MD, Kintner C. (1999) Expression of Pax-3 in the lateral neural plate is dependent on a Wnt-mediated signal from posterior nonaxial mesoderm. *Dev Biol*, 212, 366-80
- Bastien J, Rochette-Egly C. (2004) Nuclear retinoid receptors and the transcription of retinoid-target genes. *Gene*, 328, 1-16
- Batourina E, Gim S, Bello N, Shy M, Clagett-Dame M, Srinivas S, Costantini F, Mendelsohn C. (2001) Vitamin A controls epithelial/mesenchymal interactions through Ret expression. *Nat Genet*, 27, 74-8

- Batourina E, Tsai S, Lambert S, Sprengle P, Viana R, Dutta S, Hensle T, Wang F, Niederreither K, McMahon AP, Carroll TJ, Mendelsohn CL. (2005) Apoptosis induced by vitamin A signaling is crucial for connecting the ureters to the bladder. *Nat Genet*, 37, 1082-9
- Batten ML, Imanishi Y, Maeda T, Tu DC, Moise AR, Bronson D, Possin D, Van Gelder RN, Baehr W, Palczewski K. (2004) Lecithin-retinol acyltransferase is essential for accumulation of all-trans-retinyl esters in the eye and in the liver. *J Biol Chem*, 279, 10422-32
- Begemann G, Schilling TF, Rauch GJ, Geisler R, Ingham PW. (2001) The zebrafish neckless mutation reveals a requirement for raldh2 in mesodermal signals that pattern the hindbrain. *Development*, 128, 3081-94
- Begemann G, Marx M, Mebus K, Meyer A, Bastmeyer M. (2004) Beyond the neckless phenotype: influence of reduced retinoic acid signaling on motor neuron development in the zebrafish hindbrain. *Dev Biol*, 271, 119-29
- Belo JA, Bachiller D, Agius E, Kemp C, Borges AC, Marques S, Piccolo S, De Robertis EM. (2000) Cerberus-like is a secreted BMP and nodal antagonist not essential for mouse development. *Genesis*, 26, 265-70
- Belyaeva OV, Johnson MP, Kedishvili NY. (2008) Kinetic analysis of human enzyme RDH10 defines the characteristics of a physiologically relevant retinol dehydrogenase. *J Biol Chem*, 283, 20299-308
- Bienz M.(1999) APC: the plot thickens. *Curr Opin Genet Dev*, 9, 595-603
- Binnerts ME, Wen X, Canté-Barrett K, Bright J, Chen HT, Asundi V, Sattari P, Tang T, Boyle B, Funk W, Rupp F. (2004) Human Crossveinless-2 is a novel inhibitor of bone morphogenetic proteins. *Biochem Biophys Res Commun* 315, 272-80
- Blaner and Olson (1994)
In *The retinoids, Biology, Chemistry and Medicine* (Sporn M B, Roberts A B, and Goodman D S) 2nd Ed., pp. 229-256, Raven Press, Ltd., New York
- Blentic A, Gale E, Maden M. (2003) Retinoic acid signalling centres in the avian embryo identified by sites of expression of synthesising and catabolising enzymes. *Dev Dyn*, 227, 114-27
- Blitz IL, Cho KW, Chang C. (2003) Twisted gastrulation loss-of-function analyses support its role as a BMP inhibitor during early *Xenopus* embryogenesis. *Development*, 130, 4975-88
- Blomhoff R, Blomhoff HK. (2006) Overview of retinoid metabolism and function. *J Neurobiol*, 66, 606-30

- Blumberg B, Bolado J Jr, Moreno TA, Kintner C, Evans RM, Papalopulu N. (1997) An essential role for retinoid signaling in anteroposterior neural patterning. *Development*, 124, 373-9
- Boerman MH, Napoli JL. (1995) Effects of sulfhydryl reagents, retinoids, and solubilization on the activity of microsomal retinol dehydrogenase. *Arch Biochem Biophys*, 321, 434-41
- Boettger T, Knoetgen H, Wittler L, Kessel M. (2001) The avian organizer. *Int J Dev Biol*, 45, 281-7
- Boleda MD, Saubi N, Farrés J, Parés X. (1993) Physiological substrates for rat alcohol dehydrogenase classes: aldehydes of lipid peroxidation, omega-hydroxyfatty acids, and retinoids. *Arch Biochem Biophys*, 307, 85-90
- Bourguignon C, Li J, Papalopulu N. (1998) XBF-1, a winged helix transcription factor with dual activity, has a role in positioning neurogenesis in *Xenopus* competent ectoderm. *Development*, 125, 4889-900
- Bouwmeester T, Kim S, Sasai Y, Lu B, De Robertis EM. (1996) Cerberus is a head-inducing secreted factor expressed in the anterior endoderm of Spemann's organizer. *Nature*, 382, 595-601
- Brannon M, Gomperts M, Sumoy L, Moon RT, Kimelman D. (1997) A beta-catenin/XTcf-3 complex binds to the siamois promoter to regulate dorsal axis specification in *Xenopus*. *Genes Dev*, 11, 2359-70
- Brannon M, Kimelman D. (1996) Activation of Siamois by the Wnt pathway. *Dev Biol*, 180, 344-7
- Breier G, Bućan M, Francke U, Colberg-Poley AM, Gruss P. (1986) Sequential expression of murine homeo box genes during F9 EC cell differentiation. *EMBO*, 5, 2209-15
- Cammas L, Romand R, Fraulob V, Mura C, Dollé P. (2007) Expression of the murine retinol dehydrogenase 10 (Rdh10) gene correlates with many sites of retinoid signalling during embryogenesis and organ differentiation. *Dev Dyn*, 236, 2899-908
- Cartry J, Nichane M, Ribes V, Colas A, Riou JF, Pieler T, Dollé P, Bellefroid EJ, Umbhauer M. (2006) Retinoic acid signalling is required for specification of pronephric cell fate. *Dev Biol*, 299, 35-51
- Cha BJ, Gard DL. (1999) XMAP230 is required for the organization of cortical microtubules and patterning of the dorsoventral axis in fertilized *Xenopus* eggs. *Dev Biol*, 205, 275-86

- Chai X, Zhai Y, Popescu G, Napoli JL. (1995b) Cloning of a cDNA for a second retinol dehydrogenase type II. Expression of its mRNA relative to type I. *J Biol Chem*, 270, 28408-12
- Chai X, Zhai Y, Napoli JL. (1996) Cloning of a rat cDNA encoding retinol dehydrogenase isozyme type III. *Gene*, 169, 219-22
- Chai X, Zhai Y, Napoli JL. (1997) cDNA cloning and characterization of a cis-retinol/3alpha-hydroxysterol short-chain dehydrogenase. *Chem*, 272, 33125-31
- Chambers D, Wilson L, Maden M, Lumsden A. (2006) RALDH-independent generation of retinoic acid during vertebrate embryogenesis by CYP1B1. *Development*, 134, 1369-83
- Chang C, Holtzman DA, Chau S, Chickering T, Woolf EA, Holmgren LM, Bodorova J, Gearing DP, Holmes WE, Brivanlou AH. (2001) Twisted gastrulation can function as a BMP antagonist. *Nature*, 410, 483-7
- Chapman SC, Brown R, Lees L, Schoenwolf GC, Lumsden A. (2004) Expression analysis of chick Wnt and frizzled genes and selected inhibitors in early chick patterning. *Dev Dyn*, 229, 668-76
- Chawla A, Repa JJ, Evans RM, Mangelsdorf DJ. (2001) Nuclear receptors and lipid physiology: opening the X-files. *Science*, 294, 1866-70
- Chen Y, Huang L, Russo AF, Solursh M. (1992) Retinoic acid is enriched in Hensen's node and is developmentally regulated in the early chicken embryo. *Proc Natl Acad Sci U S A*. 89, 10056-9
- Chen Y, Huang L, Solursh M. (1994) A concentration gradient of retinoids in the early *Xenopus laevis* embryo. *Dev Biol*, 161, 70-6
- Chen Y, Pollet N, Niehrs C, Pieler T. (2001) Increased XRALDH2 activity has a posteriorizing effect on the central nervous system of *Xenopus* embryos. *Mech Dev*, 101, 91-103
- Chen Y, Pan FC, Brandes N, Afelik S, Sölter M, Pieler T. (2004) Retinoic acid signaling is essential for pancreas development and promotes endocrine at the expense of exocrine cell differentiation in *Xenopus*. *Dev Biol*, 271, 144-60
- Cho, KW, Blumberg, B, Steinbeisser, H and De Robertis, E. M.(1991) Molecular nature of Spemann's organizer: the role of the *Xenopus* homeobox gene goosecoid. *Cell* 67, 1111-1120
- Clagett-Dame M, DeLuca HF. (2002) The role of vitamin A in mammalian reproduction and embryonic development. *Annu Rev Nutr*, 22, 347-81

- Coffinier C, Ketpura N, Tran U, Geissert D, De Robertis EM. (2002) Mouse Crossveinless-2 is the vertebrate homolog of a *Drosophila* extracellular regulator of BMP signaling., *Mech Dev.* 119, 179-84
- Cohlan SQ. (1953) Excessive intake of vitamin A during pregnancy as a cause of congenital anomalies in the rat. *Am J Dis Child*, 86, 348-9
- Colberg-Poley AM, Püschel AW, Dony C, Voss SD, Gruss P. (1987) Post-transcriptional regulation of a murine homeobox gene transcript in F9 embryonal carcinoma cells. *Differentiation*, 35, 206-11
- Colbert MC, Linney E, LaMantia AS. (1993) Local sources of retinoic acid coincide with retinoid-mediated transgene activity during embryonic development. *Proc Natl Acad Sci U S A*, 90, 6572-6
- Collavin L, Kirschner MW. (2003) The secreted Frizzled-related protein Sizzled functions as a negative feedback regulator of extreme ventral mesoderm. *Development*, 130, 805-16
- Conlon RA. (1995) Retinoic acid and pattern formation in vertebrates. *Trends Genet*, 11, 314-9
- Connor MJ, Smit MH. (1987) Terminal-group oxidation of retinol by mouse epidermis. Inhibition in vitro and in vivo. *Biochem J*, 244, 489-92
- Creech Kraft J, Schuh T, Juchau MR, Kimelman D. (1994) Temporal distribution, localization and metabolism of all-trans-retinol, didehydroretinol and all-trans-retinal during *Xenopus* development. *Biochem J*, 301, 111-9
- Cunningham ML, Mac Auley A, Mirkes PE. (1994) From gastrulation to neurulation: transition in retinoic acid sensitivity identifies distinct stages of neural patterning in the rat. *Dev Dyn*, 200, 227-41
- Darras S, Marikawa Y, Elinson RP, Lemaire P. (1997) Animal and vegetal pole cells of early *Xenopus* embryos respond differently to maternal dorsal determinants: implications for the patterning of the organiser. *Development*, 124, 4275-86
- De Robertis EM, Morita EA, Cho KW. (1991) Gradient fields and homeobox genes. *Development*, 112, 669-78
- De Robertis EM, Kuroda H. (2004) Dorsal-ventral patterning and neural induction in *Xenopus* embryos. *Annu Rev Cell Dev Biol.* 20, 285-308
- de Roos K, Sonneveld E, Compaan B, ten Berge D, Durston AJ, van der Saag PT. (1999) Expression of retinoic acid 4-hydroxylase (CYP26) during mouse and *Xenopus laevis* embryogenesis., *Mech Dev*, 82, 205-11

- Diez del Corral R, Olivera-Martinez I, Goriely A, Gale E, Maden M, Storey K. (2003) Opposing FGF and retinoid pathways control ventral neural pattern, neuronal differentiation, and segmentation during body axis extension. *Neuron*, 40, 65-79
- Dobbs-McAuliffe B, Zhao Q, Linney E. (2004) Feedback mechanisms regulate retinoic acid production and degradation in the zebrafish embryo. *Mech Dev*, 121, 339-50
- Dominguez I, Green JB. (2000) Dorsal downregulation of GSK3beta by a non-Wnt-like mechanism is an early molecular consequence of cortical rotation in early *Xenopus* embryos. *Development*, 127, 861-8
- Dominguez I, Green JB. (2001) Missing links in GSK3 regulation. *Dev Biol*, 235, 303-13
- Doniach T. (1995) Basic FGF as an inducer of anteroposterior neural pattern. *Cell*, 83, 1067-70
- Dosch R, Niehrs C. (2000) Requirement for anti-dorsalizing morphogenetic protein in organizer patterning. *Mech Dev*, 90, 195-203
- Driessen CA, Winkens HJ, Hoffmann K, Kuhlmann LD, Janssen BP, Van Vugt AH, Van Hooser JP, Wieringa BE, Deutman AF, Palczewski K, Ruether K, Janssen JJ. (2000) Disruption of the 11-cis-retinol dehydrogenase gene leads to accumulation of cis-retinols and cis-retinyl esters. *Mol Cell Biol*, 20, 4275-87
- Duester G. (1999) Function of alcohol dehydrogenase and aldehyde dehydrogenase gene families in retinoid signaling. *Adv Exp Med Biol*, 463, 311-9
- Duester G. (2000) Families of retinoid dehydrogenases regulating vitamin A function: production of visual pigment and retinoic acid. *Eur J Biochem.*, 267, 4315-24
- Duester G. (2001) Genetic dissection of retinoid dehydrogenases. *Chem Biol Interact*, 130-132, 469-80
- Duester G, Mic FA, Molotkov A. (2003) Cytosolic retinoid dehydrogenases govern ubiquitous metabolism of retinol to retinaldehyde followed by tissue-specific metabolism to retinoic acid. *Chem Biol Interact*, 143-144, 201-10
- Duester G. (2008) Retinoic acid synthesis and signaling during early organogenesis. *Cell*, 134, 921-31
- Duester G. (2009) Keeping an eye on retinoic acid signaling during eye development. *Chem Biol Interact.*, 178, 178-81

- Dupé V, Davenne M, Brocard J, Dollé P, Mark M, Dierich A, Chambon P, Rijli FM. (1997) In vivo functional analysis of the Hoxa-1 3' retinoic acid response element (3'RARE). *Development*, 124, 399-410
- Dupé V, Ghyselinck NB, Wendling O, Chambon P, Mark M. (1999) Key roles of retinoic acid receptors alpha and beta in the patterning of the caudal hindbrain, pharyngeal arches and otocyst in the mouse. *Development*, 126, 5051-9
- Dupé V, Lumsden A. (2001) Hindbrain patterning involves graded responses to retinoic acid signalling. *Development*, 128, 2199-208
- Dupé V, Matt N, Garnier JM, Chambon P, Mark M, Ghyselinck NB. (2003) A newborn lethal defect due to inactivation of retinaldehyde dehydrogenase type 3 is prevented by maternal retinoic acid treatment. *Proc Natl Acad Sci U S A*, 100, 14036-41
- Durstun AJ, Timmermans JP, Hage WJ, Hendriks HF, de Vries NJ, Heideveld M, Nieuwkoop PD. (1989) Retinoic acid causes an anteroposterior transformation in the developing central nervous system. *Nature*, 340, 140-4
- Elinson RP, Rowning B. (1988) A transient array of parallel microtubules in frog eggs: potential tracks for a cytoplasmic rotation that specifies the dorso-ventral axis. *Dev Biol*, 128, 185-97
- Emoto Y, Wada H, Okamoto H, Kudo A, Imai Y. (2005) Retinoic acid-metabolizing enzyme Cyp26a1 is essential for determining territories of hindbrain and spinal cord in zebrafish. *Dev Biol*, 278, 415-27
- Engleka MJ, Kessler DS. (2001) Siamese cooperates with TGFbeta signals to induce the complete function of the Spemann-Mangold organizer. *Int J Dev Biol*, 45, 241-50
- Ensini M, Tsuchida TN, Belting HG, Jessell TM. (1998) The control of rostrocaudal pattern in the developing spinal cord: specification of motor neuron subtype identity is initiated by signals from paraxial mesoderm. *Development*, 125, 969-82
- Fan X, Molotkov A, Manabe S, Donmoyer CM, Deltour L, Foglio MH, Cuenca AE, Blaner WS, Lipton SA, Duester G. (2003) Targeted disruption of Aldh1a1 (Raldh1) provides evidence for a complex mechanism of retinoic acid synthesis in the developing retina. *Mol Cell Biol*, 23, 4637-48
- Fantel AG, Shepard TH, Newell-Morris LL, Moffett BC. (1977) Teratogenic effects of retinoic acid in pigtail monkeys (*Macaca nemestrina*). I. General features. *Teratology*, 15, 65-71
- Farr GH 3rd, Ferkey DM, Yost C, Pierce SB, Weaver C, Kimelman D. (2000) Interaction among GSK-3, GBP, axin, and APC in *Xenopus* axis specification. *J Cell Biol*, 148, 691-702

- Franco PG, Paganelli AR, López SL, Carrasco AE. (1999) Functional association of retinoic acid and hedgehog signaling in *Xenopus* primary neurogenesis. *Development*, 126, 4257-65
- Fredieu JR, Cui Y, Maier D, Danilchik MV, Christian JL. (1997) Xwnt-8 and lithium can act upon either dorsal mesodermal or neurectodermal cells to cause a loss of forebrain in *Xenopus* embryos. *Dev Bio*, 186, 100-14
- Fuentealba LC, Eivers E, Ikeda A, Hurtado C, Kuroda H, Pera EM, De Robertis EM. (2007) Integrating patterning signals: Wnt/GSK3 regulates the duration of the BMP/Smad1 signal. *Cell*, 131, 980-93
- Fujii H, Sato T, Kaneko S, Gotoh O, Fujii-Kuriyama Y, Osawa K, Kato S, Hamada H. (1997) Metabolic inactivation of retinoic acid by a novel P450 differentially expressed in developing mouse embryos. *EMBO*, 16, 4163-73
- Fujii H, Nagai T, Shirasawa H, Doi JY, Yasui K, Nishimatsu S, Takeda H, Sakai M. (2002) Anteroposterior patterning in *Xenopus* embryos: egg fragment assay system reveals a synergy of dorsalizing and posteriorizing embryonic domains. *Dev Biol*, 252, 15-30
- Funayama N, Fagotto F, McCrea P, Gumbiner BM. (1995) Embryonic axis induction by the armadillo repeat domain of beta-catenin: evidence for intracellular signaling. *J Cell Biol*, 128, 959-68
- Gale E, Prince V, Lumsden A, Clarke J, Holder N, Maden M. (1996) Late effects of retinoic acid on neural crest and aspects of rhombomere. *Development*, 122, 783-93
- Gibert Y, Gajewski A, Meyer A, Begemann G. (2006) Induction and prepatterning of the zebrafish pectoral fin bud requires axial retinoic acid signaling. *Development*, 133, 2649-59
- Giguère V, Lyn S, Yip P, Siu CH, Amin S. (1990) Molecular cloning of cDNA encoding a second cellular retinoic acid-binding protein. *Proc Natl Acad Sci*, 87, 6233-7
- Glinka A, Wu W, Delius H, Monaghan AP, Blumenstock C, Niehrs C. (1998) Dickkopf-1 is a member of a new family of secreted proteins and functions in head induction. *Nature*, 391, 357-62
- Glover JC, Renaud JS, Rijli FM. (2006) Retinoic acid and hindbrain patterning. *J Neurobiol*, 66, 705-25
- Godsave SF, Koster CH, Getahun A, Mathu M, Hooiveld M, van der Wees J, Hendriks J, Durston AJ. (1998) Graded retinoid responses in the developing hindbrain. *Dev Dyn*, 213, 39-49

- Goodman DS, Huang HS. (1965) Biosynthesis of vitamin a with rat intestinal enzymes. *Science*, 149, 879-80
- Goodman DS. (1984) Overview of current knowledge of metabolism of vitamin A and carotenoids. *J Natl Cancer Inst.*, 73, 1375-9
- Gough WH, VanOoteghem S, Sint T, Kedishvili NY. (1998) cDNA cloning and characterization of a new human microsomal NAD⁺-dependent dehydrogenase that oxidizes all-trans-retinol and 3 α -hydroxysteroids. *J Biol Chem*, 273, 19778-85
- Gould SE, Grainger RM. (1997) Neural induction and antero-posterior patterning in the amphibian embryo: past, present and future. *Cell Mol Life Sci*, 53, 319-38
- Grandel H, Lun K, Rauch GJ, Rhinn M, Piotrowski T, Houart C, Sordino P, Kuchler AM, Schulte-Merker S, Geisler R, Holder N, Wilson SW, Brand M. (2002) Retinoic acid signalling in the zebrafish embryo is necessary during pre-segmentation stages to pattern the anterior-posterior axis of the CNS and to induce a pectoral fin bud. *Development*, 129, 2851-65
- Grondona JM, Kastner P, Gansmuller A, Décimo D, Chambon P, Mark M. (1996) Retinal dysplasia and degeneration in RARbeta2/RARgamma2 compound mutant mice.
- Gu X, Xu F, Wang X, Gao X, Zhao Q. (2005) Molecular cloning and expression of a novel CYP26 gene (*cyp26d1*) during zebrafish early development. *Gene Expr Pattns*, 5, 733-9
- Gu X, Xu F, Song W, Wang X, Hu P, Yang Y, Gao X, Zhao Q. (2006) A novel cytochrome P450, zebrafish *Cyp26D1*, is involved in metabolism of all-trans retinoic acid. *Mol Endocrinol*, 20, 1661-72
- Guger KA, Gumbiner BM. (1995) beta-Catenin has Wnt-like activity and mimics the Nieuwkoop signaling center in *Xenopus* dorsal-ventral patterning. *Dev Biol*, 172, 115-25
- Haeseleer F, Huang J, Lebioda L, Saari JC, Palczewski K. (1998) Molecular characterization of a novel short-chain dehydrogenase/reductase that reduces all-trans-retinal. *J Biol Chem*, 273, 21790-9
- Hale F. (1933) Pigs born without eyeballs. *J Hered*, 24, 105-6
- Hammerschmidt M, Pelegri F, Mullins MC, Kane DA, van Eeden FJ, Granato M, Brand M, Furutani-Seiki M, Haffter P, Heisenberg CP, Jiang YJ, Kelsh RN, Odenthal J, Warga RM, Nüsslein-Volhard C. (1996) *Dino* and *mercedes*, two genes regulating dorsal development in the zebrafish embryo. *Development*, 123, 95-102

Han CL, Liao CS, Wu CW, Hwong CL, Lee AR, Yin SJ. (1998) Contribution to first-pass metabolism of ethanol and inhibition by ethanol for retinol oxidation in human alcohol dehydrogenase family--implications for etiology of fetal alcohol syndrome and alcohol-related diseases. *Eur J Biochem*, 254, 25-31

Hansen CS, Marion CD, Steele K, George S, Smith WC. (1997) Direct neural induction and selective inhibition of mesoderm and epidermis inducers by Xnr3. *Development*, 124, 483-92

Haramoto Y, Tanegashima K, Onuma Y, Takahashi S, Sekizaki H, Asashima M. (2004) *Xenopus tropicalis* nodal-related gene 3 regulates BMP signaling: an essential role for the pro-region. *Dev Biol*, 265, 155-68

Hardcastle Z, Chalmers AD, Papalopulu N. (2000) FGF-8 stimulates neuronal differentiation through FGFR-4a and interferes with mesoderm induction in *Xenopus* embryos. *Curr Biol*, 10, 1511-4

Harland R, Gerhart J. (1997) Formation and function of Spemann's organizer. *Annu Rev Cell Biol Dev*, 13, 611-67

Harrison EH, Napoli JL. (1990) Bile salt-independent retinyl ester hydrolase activities associated with membranes of rat tissues. *Methods Enzymol*, 189, 459-69

Harrison EH, Gad MZ. (1989) Hydrolysis of retinyl palmitate by enzymes of rat pancreas and liver. Differentiation of bile salt-dependent and bile salt-independent, neutral retinyl ester hydrolases in rat liver. *J Biol Chem*, 264, 17142-7

Haselbeck RJ, Hoffmann I, Duester G. (1999) Distinct functions for Aldh1 and Raldh2 in the control of ligand production for embryonic retinoid signaling pathways. *Dev Genet*, 25, 353-64

Heasman J, Crawford A, Goldstone K, Garner-Hamrick P, Gumbiner B, McCrea P, Kintner C, Noro CY, Wylie C. (1994) Overexpression of cadherins and underexpression of beta-catenin inhibit dorsal mesoderm induction in early *Xenopus* embryos. *Cell*, 79, 791-803

Hemmati-Brivanlou A, de la Torre JR, Holt C, Harland RM. (1991) Cephalic expression and molecular characterization of *Xenopus* En-2. *Development*, 111, 715-24

Hernandez RE, Rikhof HA, Bachmann R, Moens CB. (2004) *vhnf1* integrates global RA patterning and local FGF signals to direct posterior hindbrain development in zebrafish. *Development*, 131, 4511-20

- Hernandez RE, Putzke AP, Myers JP, Margaretha L, Moens CB. (2007) Cyp26 enzymes generate the retinoic acid response pattern necessary for hindbrain development. *Development*, 134, 177-87
- Herr FM, Ong DE (1992). Differential interaction of lecithin-retinol acyltransferase with cellular retinol binding proteins. *Biochemistry*, 31, 6748-55
- Hill J, Clarke JD, Vargesson N, Jowett T, Holder N. (1995) Exogenous retinoic acid causes specific alterations in the development of the midbrain and hindbrain of the zebrafish embryo including positional respecification of the Mauthner neuron. *Mech Dev*, 50, 3-16
- Hoffmann I, Ang HL, Duester G. (1989) Alcohol dehydrogenases in *Xenopus* development: conserved expression of ADH1 and ADH4 in epithelial retinoid target tissues. *Dev Dyn*, 213, 261-70
- Holder N, Hill J. (1991) Retinoic acid modifies development of the midbrain-hindbrain border and affects cranial ganglion formation in zebrafish embryos. *Development*, 113, 1159-70
- Holleman T, Chen Y, Grunz H, Pieler T. (1998) Regionalized metabolic activity establishes boundaries of retinoic acid signalling. *EMBO*, 17, 7361-72
- Holowacz T, Sokol S. (1999) FGF is required for posterior neural patterning but not for neural induction. *Dev Biol*, 205, 296-308
- Horton C, Maden M. (1995) Endogenous distribution of retinoids during normal development and teratogenesis in the mouse embryo. *Dev Dyn*, 202, 312-23
- Hou S, Maccarana M, Min TH, Strate I, Pera EM. (2007) The secreted serine protease xHtrA1 stimulates long-range FGF signaling in the early *Xenopus* embryo. *Dev Cell*, 13, 226-41
- Houliston E, Elinson RP. (1991) Patterns of microtubule polymerization relating to cortical rotation in *Xenopus laevis* eggs. *Development*, 112, 107-17
- Imaoka S, Wan J, Chow T, Hiroi T, Eyanagi R, Shigematsu H, Funae Y. (1998) Cloning and characterization of the CYP2D1-binding protein, retinol dehydrogenase. *Arch Biochem Biophys*, 353, 331-6
- Iozzo RV. (1998) Matrix proteoglycans: from molecular design to cellular function. *Annu Rev Biochem*, 67, 609-52
- Isaacs HV. (1997) New perspectives on the role of the fibroblast growth factor family in amphibian development. *Cell Mol Life Sci*, 53, 350-61

Jones-Villeneuve EM, McBurney MW, Rogers KA, Kalnins VI. (1982) Retinoic acid induces embryonal carcinoma cells to differentiate into neurons and glial cells. *J Cell Biol*, 1982, 253-62

Kallberg Y, Oppermann U, Jörnvall H, Persson B. (2002) Short-chain dehydrogenases/reductases (SDRs). *Eur J Biochem*, 269, 4409-17

Kawaguchi R, Yu J, Honda J, Hu J, Whitelegge J, Ping P, Wiita P, Bok D, Sun H. (2007) A membrane receptor for retinol binding protein mediates cellular uptake of vitamin A. *Science*, 315, 820-5

Kawakami Y, Raya A, Raya RM, Rodríguez-Esteban C, Belmonte JC. (2005) Retinoic acid signalling links left-right asymmetric patterning and bilaterally symmetric somitogenesis in the zebrafish embryo. *Nature*, 435, 165-71

Kawano Y, Kypta R. (2003) Secreted antagonists of the Wnt signalling pathway. *J Cell Sci*, 116, 2627-34

Kazanskaya O, Glinka A, Niehrs C. (2000) The role of *Xenopus dickkopf1* in prechordal plate specification and neural patterning. *Development*, 127, 4981-92

Kedishvili NY, Gough WH, Davis WI, Parsons S, Li TK, Bosron WF. (1998) Effect of cellular retinol-binding protein on retinol oxidation by human class IV retinol/alcohol dehydrogenase and inhibition by ethanol. *Biochem Biophys Res Commun.*, 249, 191-6

Kedishvili NY, Belyaeva OV, Gough WH. (2001) Cloning of the human RoDH-related short chain dehydrogenase gene and analysis of its structure. *Chem Biol Interact*, 130-132, 457-67

Kessel M, Schulze F, Fibi M, Gruss P. (1987) Primary structure and nuclear localization of a murine homeodomain protein. *Proc Natl Acad Sci U S A.* 84, 5306-10

Kessel M, Gruss P. (1990) Murine developmental control genes. *Science*, 249, 374-9

Kessel M, Gruss P. (1991) Homeotic transformations of murine vertebrae and concomitant alteration of Hox codes induced by retinoic acid. *Cell*, 67, 89-104

Kessel M. (1992) Respecification of vertebral identities by retinoic acid. *Development*, 115, 487-501

Kessel M. (1993) Reversal of axonal pathways from rhombomere 3 correlates with extra Hox expression domains. *Neuron*, 10, 379-93

Kessler DS, Melton DA. (1994) Vertebrate embryonic induction: mesodermal and neural patterning. *Science*, 266, 596-604

Kikkawa M, Takano K, Shinagawa A. (1996) Location and behavior of dorsal determinants during first cell cycle in *Xenopus* eggs. *Development*, 122, 3687-96

Kolm PJ, Sive HL. (1997) Retinoids and posterior neural induction: a reevaluation of Nieuwkoop's two-step hypothesis. *Cold Spring Harb Symp Quant Biol.* 62, 511-21

Kraft JC, Bechter R, Lee QP, Juchau MR. (1992) Microinjections of cultured rat conceptuses: studies with 4-oxo-all-trans-retinoic acid, 4-oxo-13-cis-retinoic acid and all-trans-retinoyl-beta-glucuronide. *Teratology*, 45, 259-70

Kraft JC, Kimelman D, Juchau MR. (1994) *Xenopus laevis*: a model system for the study of embryonic retinoid metabolism. I. Embryonic metabolism of 9-cis- and all-trans-retinals and retinols to their corresponding acid forms. *Drug Metab Dispos*, 23, 72-82

Kramer KL, Yost HJ. (2003) Heparan sulfate core proteins in cell-cell signaling. *Annu Rev Genet*, 37, 461-84

Kudoh T, Wilson SW, Dawid IB. (2002) Distinct roles for Fgf, Wnt and retinoic acid in posteriorizing the neural ectoderm. *Development*, 129, 4335-46

Kuroda H, Wessely O, De Robertis EM. (2004) Neural induction in *Xenopus*: requirement for ectodermal and endomesodermal signals via Chordin, Noggin, beta-Catenin, and Cerberus. *PLoS*, 2, E92

Lamb TM, Harland RM. (1995) Fibroblast growth factor is a direct neural inducer, which combined with noggin generates anterior-posterior neural pattern. *Development*, 121, 3627-36

Lampert JM, Holzschuh J, Hessel S, Driever W, Vogt K, von Lintig J. (2003) Provitamin A conversion to retinal via the beta,beta-carotene-15,15'-oxygenase (bcox) is essential for pattern formation and differentiation during zebrafish embryogenesis. *Development*, 130, 2173-86

Langman J, Welch GW. (1967) Excess vitamin A and development of the cerebral cortex. *J Comp Neurol*, 131, 15-26

Larraín J, Oelgeschläger M, Ketpura NI, Reversade B, Zakin L, De Robertis EM. (2001) Proteolytic cleavage of Chordin as a switch for the dual activities of Twisted gastrulation in BMP signaling. *Development*, 128, 4439-47

Laurent MN, Blitz IL, Hashimoto C, Rothbacher U, Cho KW. (1997) The *Xenopus* homeobox gene *twi* mediates Wnt induction of goosecoid in establishment of Spemann's organizer. *Development*, 124, 4905-16

- Lee YM, Osumi-Yamashita N, Ninomiya Y, Moon CK, Eriksson U, Eto K. (1995) Retinoic acid stage-dependently alters the migration pattern and identity of hindbrain neural crest cells. *Development*, 121, 825-37
- Leonard L, Horton C, Maden M, Pizzey JA. (1995) Anteriorization of CRABP-I expression by retinoic acid in the developing mouse central nervous system and its relationship to teratogenesis. *Dev Biol*, 168, 514-28
- Leroy P, Nakshatri H, Chambon P. (1991) Mouse retinoic acid receptor alpha 2 isoform is transcribed from a promoter that contains a retinoic acid response element. *Proc Natl Acad Sci U S A.*, 88, 10138-42
- Leyns L, Bouwmeester T, Kim SH, Piccolo S, De Robertis EM. (1997) Frzb-1 is a secreted antagonist of Wnt signaling expressed in the Spemann organizer. *Cell*, 88, 747-56
- Li L, Yuan H, Weaver CD, Mao J, Farr GH 3rd, Sussman DJ, Jonkers J, Kimelman D, Wu D. (1999) Axin and Frat1 interact with dvl and GSK, bridging Dvl to GSK in Wnt-mediated regulation of LEF-1. *EMBO*, 18, 4233-40
- Li H, Wagner E, McCaffery P, Smith D, Andreadis A, Dräger UC. (2000) A retinoic acid synthesizing enzyme in ventral retina and telencephalon of the embryonic mouse. *Mech Dev*, 95, 283-9
- Lidén M, Eriksson U. (2006) Understanding retinol metabolism: structure and function of retinol dehydrogenases. *J Biol Chem.*, 281, 13001-4
- Lindahl R. (1992) Aldehyde dehydrogenases and their role in carcinogenesis. *Crit Rev Biochem Mol Biol.*, 27, 283-335
- Liu JP, Laufer E and Jessell TM. (2001). Assigning the positional identity of spinal motor neurons: rostrocaudal patterning of Hox-c expression by FGFs, Gdf11, and retinoids. *Neuron*, 32, 997-1012
- López SL, Dono R, Zeller R, Carrasco AE. (1995) Differential effects of retinoic acid and a retinoid antagonist on the spatial distribution of the homeoprotein Hoxb-7 in vertebrate embryos. *Dev Dyn*, 204, 457-71
- MacLean G, Abu-Abed S, Dollé P, Tahayato A, Chambon P, Petkovich M. (2001) Cloning of a novel retinoic-acid metabolizing cytochrome P450, Cyp26B1, and comparative expression analysis with Cyp26A1 during early murine development. *Mech Dev*, 107, 195-201
- Maden M. (1983) The effect of vitamin A on the regenerating axolotl limb. *J Embryol, Exp Morphol*, 77, 273-95
- Maden M, Gale E, Kostetskii I, Zile M. (1996) Vitamin A-deficient quail embryos have half a hindbrain and other neural defects. *Curr Bio*, 6 417-26

- Maden M. (1999) Heads or tails? Retinoic acid will decide. *BioEssays* 21, 809-812.
- Maden M. (2001) Role and distribution of retinoic acid during CNS development. *Int Rev Cytol*, 209, 1-77
- Maden M. (2002) Retinoid signalling in the development of the central nervous system. *Nat Rev Neurosci*, 3, 843-53
- Maden M. (2006) Retinoids and spinal cord development., *J Neurobiol*, 66, 726-38
- Maden M. (2007) Retinoic acid in the development, regeneration and maintenance of the nervous system. *Nat Rev Neurosci*, 8, 755-65
- Malpel S, Mendelsohn C, Cardoso WV. (2000) Regulation of retinoic acid signaling during lung morphogenesis. *Development*, 127, 3057-67
- Manns M, Fritsch B. (1992) Retinoic acid affects the organization of reticulospinal neurons in developing *Xenopus*. *Neurosci Lett*, 139, 253-6
- Mao J, Wang J, Liu B, Pan W, Farr GH 3rd, Flynn C, Yuan H, Takada S, Kimelman D, Li L, Wu D. (2001) Low-density lipoprotein receptor-related protein-5 binds to Axin and regulates the canonical Wnt signaling pathway. *Mol Cell*, 7, 801-9
- Mao B, Wu W, Davidson G, Marhold J, Li M, Mechler BM, Delius H, Hoppe D, Stannek P, Walter C, Glinka A, Niehrs C. (2002) Kremen proteins are Dickkopf receptors that regulate Wnt/beta-catenin signalling. *Nature*, 417, 664-7
- Mark M, Ghyselinck NB, Chambon P. (2006) Function of retinoid nuclear receptors: lessons from genetic and pharmacological dissections of the retinoic acid signaling pathway during mouse embryogenesis. *Annu Rev Pharmacol Toxicol*, 46, 451-80
- Marshall H, Nonchev S, Sham MH, Muchamore I, Lumsden A, Krumlauf R. (1992) Retinoic acid alters hindbrain Hox code and induces transformation of rhombomeres 2/3 into a 4/5 identity. *Nature*, 360, 737-41
- Marshall H, Studer M, Pöpperl H, Aparicio S, Kuroiwa A, Brenner S, Krumlauf R. (1994) A conserved retinoic acid response element required for early expression of the homeobox gene *Hoxb-1*. *Nature*, 370, 567-71
- Mathers PH, Grinberg A, Mahon KA, Jamrich M. (1997) The *Rx* homeobox gene is essential for vertebrate eye development. *Nature*, 387, 603-7
- Martín M, Gallego-Llamas J, Ribes V, Kedinger M, Niederreither K, Chambon P, Dollé P, Gradwohl G. (2005) Dorsal pancreas agenesis in retinoic acid-deficient *Raldh2* mutant mice. *Dev Biol*, 284, 399-411

- Matsuura T and Ross AC. (1993) Regulation of hepatic lecithin: retinol acyltransferase activity by retinoic acid. *Arch Biochem Biophys.*, 301, 221-7
- Maves L, Kimmel CB. (2005) Dynamic and sequential patterning of the zebrafish posterior hindbrain by retinoic acid. *Dev Biol*, 285, 593-605
- Mavilio F, Simeone A, Boncinelli E, Andrews PW. (1988) Activation of four homeobox gene clusters in human embryonal carcinoma cells induced to differentiate by retinoic acid. *Differentiation*, 37, 73-9
- McBurney MW, Jones-Villeneuve EM, Edwards MK, Anderson PJ. (1982) Control of muscle and neuronal differentiation in a cultured embryonal carcinoma cell line. *Nature*, 299, 165-7
- McCaffery P, Dräger UC. (1994) Hot spots of retinoic acid synthesis in the developing spinal cord. *Proc Natl Acad Sci U S A*, 91, 7194-7
- McGinnis W, Hart CP, Gehring WJ, Ruddle FH. (1984) Molecular cloning and chromosome mapping of a mouse DNA sequence homologous to homeotic genes of *Drosophila*. *Cell*, 38, 675-80
- McGinnis W, Krumlauf R. (1992) Homeobox genes and axial patterning. *Cell*, 68, 283-302
- McGrew LL, Lai CJ, Moon RT. (1995) Specification of the anteroposterior neural axis through synergistic interaction of the Wnt signaling cascade with noggin and follistatin. *Dev Bio*, 172, 337-42
- McLean KJ, Girvan HM, Munro AW. (2007) Cytochrome P450/redox partner fusion enzymes: biotechnological and toxicological prospects. *Expert Opin Drug Metab Toxicol*, 3, 847-63
- Means AL, Gudas LJ. (1995) The roles of retinoids in vertebrate development. *Annu Rev Biochem*, 64, 201-33
- Mendelsohn C, Ruberte E, LeMeur M, Morriss-Kay G, Chambon P. (1991) Developmental analysis of the retinoic acid-inducible RAR-beta 2 promoter in transgenic animals. *Development*, 113, 723-34
- Mic FA, Molotkov A, Fan X, Cuenca AE, Duester G. (2000) RALDH3, a retinaldehyde dehydrogenase that generates retinoic acid, is expressed in the ventral retina, otic vesicle and olfactory pit during mouse development. *Mech Dev*, 97, 227-30
- Mic FA, Sirbu IO, Duester G. (2004) Retinoic acid synthesis controlled by Raldh2 is required early for limb bud initiation and then later as a proximodistal signal during apical ectodermal ridge formation. *J Biol Chem*, 279, 26698-706

Miller JR, Rowing BA, Larabell CA, Yang-Snyder JA, Bates RL, Moon RT. (1999) Establishment of the dorsal-ventral axis in *Xenopus* embryos coincides with the dorsal enrichment of Dishevelled that is dependent on cortical rotation. *J Cell Biol*, 146, 427-37

Miller-Bertoglio V, Carmany-Rampey A, Fürthauer M, Gonzalez EM, Thisse C, Thisse B, Halpern ME, Solnica-Krezel L. (1999) Maternal and zygotic activity of the zebrafish *ogon* locus antagonizes BMP signaling. *Dev Biol*, 214, 72-86

Mizuguchi R, Sugimori M, Takebayashi H, Kosako H, Nagao M, Yoshida S, Nabeshima Y, Shimamura K, Nakafuku M. (2001) Combinatorial roles of *olig2* and *neurogenin2* in the coordinated induction of pan-neuronal and subtype-specific properties of motoneurons. *Neuron*, 31, 757-71

Molenaar M, van de Wetering M, Oosterwegel M, Peterson-Maduro J, Godsave S, Korinek V, Roose J, Destree O, Clevers H. (1996) XTcf-3 transcription factor mediates beta-catenin-induced axis formation in *Xenopus* embryos. *Cell*, 86, 391-9

Molotkov A, Molotkova N, Duester G. (2005) Retinoic acid generated by *Raldh2* in mesoderm is required for mouse dorsal endodermal pancreas development. *Dev Dyn*, 232, 950-7

Molotkova N, Molotkov A, Sirbu IO, Duester G. (2005) Requirement of mesodermal retinoic acid generated by *Raldh2* for posterior neural transformation. *Mech Dev*, 122, 145-55

Moos M Jr, Wang S, Krinks M. (1995) Anti-dorsalizing morphogenetic protein is a novel TGF-beta homolog expressed in the Spemann organizer. *Development*, 121, 4293-301

Morriss-Kay GM, Murphy P, Hill RE, Davidson DR. (1991) Effects of retinoic acid excess on expression of *Hox-2.9* and *Krox-20* and on morphological segmentation in the hindbrain of mouse embryos. *EMBO*, 10, 2985-95

Moser M, Binder O, Wu Y, Aitsebaomo J, Ren R, Bode C, Bautch VL, Conlon FL, Patterson C. (2003) BMPER, a novel endothelial cell precursor-derived protein, antagonizes bone morphogenetic protein signaling and endothelial cell differentiation. *Mol Cell Biol*, 23, 5664-79

Moss JB, Xavier-Neto J, Shapiro MD, Nayeem SM, McCaffery P, Dräger UC, Rosenthal N. (1998) Dynamic patterns of retinoic acid synthesis and response in the developing mammalian heart. *Dev Biol*, 199, 55-71

Muhr J, Graziano E, Wilson S, Jessell TM and Edlund T. (1999). Convergent inductive signals specify midbrain, hindbrain, and spinal cord identity in gastrula stage chick embryos. *Neuron*, 23, 689-702.

Mukhopadhyay M, Shtrom S, Rodriguez-Esteban C, Chen L, Tsukui T, Gomer L, Dorward DW, Glinka A, Grinberg A, Huang SP, Niehrs C, Belmonte JC, Westphal H. (2001) *Dickkopf1* is required for embryonic head induction and limb morphogenesis in the mouse. *Dev Cell*, 1, 423-34

Nakamura O and Takasaki H. (1971) Prospective fates of blastomeres at the 32-cell stage of *Xenopus laevis* embryos. *Proc Japan Acad*, 47, 407-12

Napoli JL, Pacia EB, Salerno GJ. (1989) Cholate effects on all-trans-retinyl palmitate hydrolysis in tissue homogenates: solubilization of multiple kidney membrane hydrolases. *Arch Biochem Biophys*, 274, 192-9

Napoli JL. (1999) Retinoic acid: its biosynthesis and metabolism. *Prog Nucleic Acid Res Mol Biol.*, 63, 139-88

Niederreither K, McCaffery P, Dräger UC, Chambon P, Dollé P. (1997) Restricted expression and retinoic acid-induced downregulation of the retinaldehyde dehydrogenase type 2 (RALDH-2) gene during mouse development. *Mech Dev*, 62, 67-78

Niederreither K, Subbarayan V, Dollé P, Chambon P. (1999) Embryonic retinoic acid synthesis is essential for early mouse post-implantation development. *Nat Genet*, 21, 444-8

Niederreither K, Vermot J, Schuhbauer B, Chambon P, Dollé P. (2000) Retinoic acid synthesis and hindbrain patterning in the mouse embryo. *Development*, 127, 75-85

Niederreither K, Vermot J, Messaddeq N, Schuhbauer B, Chambon P, Dollé P. (2001) Embryonic retinoic acid synthesis is essential for heart morphogenesis in the mouse. *Development*, 128, 1019-31

Niederreither K, Vermot J, Schuhbauer B, Chambon P, Dollé P. (2002) Embryonic retinoic acid synthesis is required for forelimb growth and anteroposterior patterning in the mouse. *Development*, 129, 3563-74

Niehrs C, Kazanskaya O, Wu W, Glinka A. (2001) *Dickkopf1* and the Spemann-Mangold head organizer. *Int J Dev Biol*, 45, 237-40

Nieto MA, Bradley LC, Wilkinson DG. (1991) Conserved segmental expression of *Krox-20* in the vertebrate hindbrain and its relationship to lineage restriction. *Development*, 2, 59-62

Nieuwkoop PD. (1985) Inductive interactions in early amphibian development and their general nature. *J Embryol, Exp, Morphol*, 89, 333-47

Nieuwkoop PD and Faber J. (1994) Normal Table of *Xenopus laevis* (Daudin) A systematical and chronological survey of the development from the fertilized egg till the end of metamorphosis.

Novitsch BG, Chen AI, Jessell TM. (2001) Coordinate regulation of motor neuron subtype identity and pan-neuronal properties by the bHLH repressor Olig2. *Neuron*, 31, 773-89

Novitsch BG, Wichterle H, Jessell TM, Sockanathan S. (2003) A requirement for retinoic acid-mediated transcriptional activation in ventral neural patterning and motor neuron specification. *Neuron*, 40, 81-95

O'Byrne SM, Wongsiriroj N, Libien J, Vogel S, Goldberg IJ, Baehr W, Palczewski K, Blaner WS. (2005) Retinoid absorption and storage is impaired in mice lacking lecithin:retinol acyltransferase (LRAT). *J Biol Chem* 280, 35647-57

Oelgeschläger M, Larrain J, Geissert D, De Robertis EM. (2000) The evolutionarily conserved BMP-binding protein Twisted gastrulation promotes BMP signalling. *Nature*, 405, 757-63

Oelgeschläger M, Kuroda H, Reversade B, De Robertis EM. (2003) Chordin is required for the Spemann organizer transplantation phenomenon in *Xenopus* embryos. *Dev Cell*, 4, 219-30

Oelgeschläger M, Reversade B, Larrain J, Little S, Mullins MC, De Robertis EM. (2003b) The pro-BMP activity of Twisted gastrulation is independent of BMP binding. *Development*, 130, 4047-56

Olivera-Martinez I, Storey KG. (2007) Wnt signals provide a timing mechanism for the FGF-retinoid differentiation switch during vertebrate body axis extension. *Development*, 134, 2125-35

Olson JA, Hayaishi O. (1965) The enzymatic cleavage of beta-carotene into vitamin A by soluble enzymes of rat liver and intestine. *Proc Natl Acad Sci U S A*, 54, 1364-70

Onichtchouk D, Chen YG, Dosch R, Gawantka V, Delius H, Massagué J, Niehrs C. (1999) Silencing of TGF-beta signalling by the pseudoreceptor BAMBI. *Nature*, 401, 480-5

Oppenheimer J M (1936) Transplantation experiments on developing teleosts. *J Exp Zool*, 72, 409-437

Pan FC, Chen Y, Bayha E, Pieler T. (2007) Retinoic acid-mediated patterning of the pre-pancreatic endoderm in *Xenopus* operates via direct and indirect mechanisms. *Mech Dev*, 124, 518-31

- Papalopulu N, Clarke JD, Bradley L, Wilkinson D, Krumlauf R, Holder N. (1991) Retinoic acid causes abnormal development and segmental patterning of the anterior hindbrain in *Xenopus* embryos. *Development*, 113, 1145-58
- Papalopulu N, Kintner C. (1996) A posteriorising factor, retinoic acid, reveals that anteroposterior patterning controls the timing of neuronal differentiation in *Xenopus* neuroectoderm. *Development*, 122, 3409-18
- Penzes P, Wang X, Napoli JL. (1997) Enzymatic characteristics of retinal dehydrogenase type I expressed in *Escherichia coli*. *Biochim Biophys Acta*, 1342, 175-81
- Pera EM, De Robertis EM. (2000) A direct screen for secreted proteins in *Xenopus* embryos identifies distinct activities for the Wnt antagonists Crescent and Frzb-1. *Mech Dev*, 96, 183-95
- Pera EM, Wessely O, Li SY, De Robertis EM. (2001) Neural and head induction by insulin-like growth factor signals. *Dev Cell*, 1, 655-65
- Pera EM, Ikeda A, Eivers E, De Robertis EM. (2003) Integration of IGF, FGF, and anti-BMP signals via Smad1 phosphorylation in neural induction. *Genes Dev*, 17, 3023-8
- Pera EM, Hou S, Strate I, Wessely O, De Robertis EM. (2005) Exploration of the extracellular space by a large-scale secretion screen in the early *Xenopus* embryo. *Int J Dev Biol*, 49, 781-96
- Peralba JM, Cederlund E, Crosas B, Moreno A, Julià P, Martínez SE, Persson B, Farr S J, Parés X, Jörnvall H. (1999) Structural and enzymatic properties of a gastric NADP(H)- dependent and retinal-active alcohol dehydrogenase. *J Biol Chem*, 274, 26021-6
- Perea-Gomez A, Vella FD, Shawlot W, Oulad-Abdelghani M, Chazaud C, Meno C, Pfister V, Chen L, Robertson E, Hamada H, Behringer RR, Ang SL. (2002) Nodal antagonists in the anterior visceral endoderm prevent the formation of multiple primitive streaks. *Dev Cell*, 3, 745-56
- Perozich J, Nicholas H, Lindahl R, Hempel J. (1999) The big book of aldehyde dehydrogenase sequences. An overview of the extended family. *Adv Exp Med Biol*, 463, 1-7
- Persson B, Zigler JS Jr, Jörnvall H. (1994) A super-family of medium-chain dehydrogenases/reductases (MDR). Sub-lines including zeta-crystallin, alcohol and polyol dehydrogenases, quinone oxidoreductase enoyl reductases, VAT-1 and other proteins.
- Piccolo S, Sasai Y, Lu B, De Robertis EM. (1996) Dorsoventral patterning in *Xenopus*: inhibition of ventral signals by direct binding of chordin to BMP-4. *Cell*, 86, 589-98

Piccolo S, Agius E, Leyns L, Bhattacharyya S, Grunz H, Bouwmeester T, De Robertis EM. (1999) The head inducer Cerberus is a multifunctional antagonist of Nodal, BMP and Wnt signals. *Nature*, 397, 707-10

Pierani A, Brenner-Morton S, Chiang C, Jessell TM. (1999) A sonic hedgehog-independent, retinoid-activated pathway of neurogenesis in the ventral spinal cord. *Cell*, 97, 903-15

Pijnappel WW, Hendriks HF, Folkers GE, van den Brink CE, Dekker EJ, Edelenbosch C, van der Saag PT, Durston AJ. (1993) The retinoid ligand 4-oxo-retinoic acid is a highly active modulator of positional specification. *Nature*, 366, 340-4

Polakis P. (2002) Casein kinase 1: a Wnt'er of disconnect. *Curr Biol*, 12, 499-501

Qian A, Cai Y, Magee TR, Wan YJ. (2000) Identification of retinoic acid-responsive elements on the HNF1alpha and HNF4alpha genes. *Biochem Biophys Res Commun.*, 276, 837-42

Quadro L, Blaner WS, Salchow DJ, Vogel S, Piantedosi R, Gouras P, Freeman S, Cosma MP, Colantuoni V, Gottesman ME. (1999) Impaired retinal function and vitamin A availability in mice lacking retinol-binding protein. *EMBO*, 18, 4633-44

Reijntjes S, Gale E, Maden M. (2003) Expression of the retinoic acid catabolising enzyme CYP26B1 in the chick embryo and its regulation by retinoic acid. *Gene Expr Patterns*, 3, 62-7

Reijntjes S, Gale E, Maden M. (2004) Generating gradients of retinoic acid in the chick embryo: Cyp26C1 expression and a comparative analysis of the Cyp26 enzymes. *Dev Dyn*, 230, 509-17

Reijntjes S, Blentic A, Gale E, Maden M. (2005) The control of morphogen signalling: regulation of the synthesis and catabolism of retinoic acid in the developing embryo. *Dev Biol*, 285, 224-37

Reversade B, De Robertis EM. (2005) Regulation of ADMP and BMP2/4/7 at opposite embryonic poles generates a self-regulating morphogenetic field. *Cell*, 123, 1147-60

Reynolds K, Mezey E, Zimmer A. (1991) Activity of the beta-retinoic acid receptor promoter in transgenic mice. *Mech Dev*, 36, 15-29

Richard-Parpaillon L, Héligon C, Chesnel F, Boujard D, Philpott A. (2002) The IGF pathway regulates head formation by inhibiting Wnt signaling in *Xenopus*. *Dev Biol*, 244, 407-17

- Riddle RD, Johnson RL, Laufer E, Tabin C. (1993) Sonic hedgehog mediates the polarizing activity of the ZPA. *Cell*, 75, 1401-16
- Rodríguez-Gallardo L, Climent V, García-Martínez V, Schoenwolf GC, Alvarez IS. (1997) Targeted over-expression of FGF in chick embryos induces formation of ectopic neural cells. *Int J Dev Biol*, 41, 715-23
- Romand R, Kondo T, Cammas L, Hashino E, Dollé P. (2008) Dynamic expression of the retinoic acid-synthesizing enzyme retinol dehydrogenase 10 (rdh10) in the developing mouse brain and sensory organs. *J Comp Neurol*, 508, 879-92
- Ross SA, McCaffery PJ, Drager UC, De Luca LM. (2000) Retinoids in embryonal development. *Physiol Rev*, 80, 1021-54
- Ross JJ, Shimmi O, Vilmos P, Petryk A, Kim H, Gaudenz K, Hermanson S, Ekker SC, O'Connor MB, Marsh JL. (2001) Twisted gastrulation is a conserved extracellular BMP antagonist. *Nature*, 410, 479-83
- Rossant J, Zirngibl R, Cado D, Shago M, Giguère V. (1991) Expression of a retinoic acid response element-hsplacZ transgene defines specific domains of transcriptional activity during mouse embryogenesis. *Genes Dev*, 5, 1333-44
- Rowitch DH, Lu QR, Kessar N, Richardson WD. (2002) An 'oligarchy' rules neural development. *Trends Neurosci*, 25, 417-22
- Ryckebusch L, Wang Z, Bertrand N, Lin SC, Chi X, Schwartz R, Zaffran S, Niederreither K. (2008) Retinoic acid deficiency alters second heart field formation. *Proc Natl Acad Sci U S A*, 105, 2913-8
- Saari JC, Bredberg DL. (1989) Lecithin:retinol acyltransferase in retinal pigment epithelial microsomes. *J Biol Chem*, 264, 8636-40
- Sakai M. (1996) The vegetal determinants required for the Spemann organizer move equatorially during the first cell cycle. *Development*, 122, 2207-14
- Sakai Y, Meno C, Fujii H, Nishino J, Shiratori H, Saijoh Y, Rossant J, Hamada H. (2001) The retinoic acid-inactivating enzyme CYP26 is essential for establishing an uneven distribution of retinoic acid along the antero-posterior axis within the mouse embryo. *Genes Dev*, 15, 213-25
- Salic AN, Kroll KL, Evans LM, Kirschner MW. (1997) Sizzled: a secreted Xwnt8 antagonist expressed in the ventral marginal zone of *Xenopus* embryos. *Development*, 124, 4739-48
- Salic A, Lee E, Mayer L, Kirschner MW. (2000) Control of beta-catenin stability: reconstitution of the cytoplasmic steps of the wnt pathway in *Xenopus* egg extracts. *Mol Cell*, 5, 523-32

Sandell LL, Sanderson BW, Moiseyev G, Johnson T, Mushegian A, Young K, Rey JP, Ma JX, Staehling-Hampton K, Trainor PA. (2007) RDH10 is essential for synthesis of embryonic retinoic acid and is required for limb, craniofacial, and organ development. *Genes Dev*, 2, 1113-24

Sasai Y, Lu B, Steinbeisser H, Geissert D, Gont LK, De Robertis EM. (1994) *Xenopus* chordin: a novel dorsalizing factor activated by organizer-specific homeobox genes. *Cell*, 79, 779-90

Sasai Y, De Robertis EM. (1997) Ectodermal patterning in vertebrate embryos. *Dev Biol*, 182, 5-20

Scadding SR, Maden M. (1994) Retinoic acid gradients during limb regeneration. *Dev Biol*, 162, 608-17

Scardigli R, Schuurmans C, Gradwohl G, Guillemot F. (2001) Crossregulation between Neurogenin2 and pathways specifying neuronal identity in the spinal cord. *Neuron*, 31, 203-17

Scharf SR, Gerhart JC. (1983) Axis determination in eggs of *Xenopus laevis*: a critical period before first cleavage, identified by the common effects of cold, pressure and ultraviolet irradiation. *Dev Biol*, 99, 75-87

Schneider RA, Hu D, Rubenstein JL, Maden M, Helms JA. (2001) Local retinoid signaling coordinates forebrain and facial morphogenesis by maintaining FGF8 and SHH. *Development*, 128, 2755-67

Schuh TJ, Hall BL, Kraft JC, Privalsky ML, Kimelman D. (1993) v-erbA and citral reduce the teratogenic effects of all-trans retinoic acid and retinol, respectively, in *Xenopus* embryogenesis. *Development*, 119, 785-98

Scott MP, Tamkun JW, Hartzell GW 3rd. (1989) The structure and function of the homeodomain. *Biochim Biophys Acta*, 989, 25-48

Scott WJ, Collins MD, Ernst AN, Supp DM, Potter SS. (1994) Enhanced expression of limb malformations and axial skeleton alterations in legless mutants by transplacental exposure to retinoic acid. *Dev Biol*, 164, 277-89

Scott WJ Jr, Walter R, Tzimas G, Sass JO, Nau H, Collins MD. (1994b) Endogenous status of retinoids and their cytosolic binding proteins in limb buds of chick vs mouse embryos. *DEV BIOL*, 165, 397-409

Scott IC, Blitz IL, Pappano WN, Maas SA, Cho KW, Greenspan DS. (2001) Homologues of Twisted gastrulation are extracellular cofactors in antagonism of BMP signalling. *Nature*, 410, 475-8

Sharpe CR, Gurdon JB. (1990) The induction of anterior and posterior neural genes in *Xenopus laevis*. *Development*, 109, 765-74

- Sharpe CR, Goldstone K. (1997) Retinoid receptors promote primary neurogenesis in *Xenopus*. *Development*, 124, 515-23
- Sharpe C, Goldstone K. (2000) The control of *Xenopus* embryonic primary neurogenesis is mediated by retinoid signalling in the neurectoderm. *Mech Dev*, 91, 69-80
- Shen S, van den Brink CE, Kruijer W, van der Saag PT. (1992) Embryonic stem cells stably transfected with mRAR beta 2-lacZ exhibit specific expression in chimeric embryos. *Int J Dev Biol*, 36, 465-76
- Shiga T, Gaur VP, Yamaguchi K, Oppenheim RW. (1995) The development of interneurons in the chick embryo spinal cord following in vivo treatment with retinoic acid. *J Comp Neurol*, 360, 463-74
- Shiotsugu J, Katsuyama Y, Arima K, Baxter A, Koide T, Song J, Chandraratna RA, Blumberg B. (2004) Multiple points of interaction between retinoic acid and FGF signaling during embryonic axis formation. *Development*, 131, 2653-67
- Simon A, Hellman U, Wernstedt C, Eriksson U. (1995) The retinal pigment epithelial-specific 11-cis retinol dehydrogenase belongs to the family of short chain alcohol dehydrogenases. *J Biol Chem*, 270, 1107-12
- Simon A, Romert A, Gustafson AL, McCaffery JM, Eriksson U. (1999) Intracellular localization and membrane topology of 11-cis retinol dehydrogenase in the retinal pigment epithelium suggest a compartmentalized synthesis of 11-cis retinaldehyde. *J Cell Sci*, 112, 549-58
- Simeone A, Avantaggiato V, Moroni MC, Mavilio F, Arra C, Cotelli F, Nigro V, Acampora D. (1995) Retinoic acid induces stage-specific antero-posterior transformation of rostral central nervous system. *Mech Dev*, 51, 83-98
- Sirbu IO, Gresh L, Barra J, Duester G. (2005) Shifting boundaries of retinoic acid activity control hindbrain segmental gene expression. *Development*, 132, 2611-22
- Sirbu IO, Duester G. (2006) Retinoic-acid signalling in node ectoderm and posterior neural plate directs left-right patterning of somitic mesoderm. *Nat Cell Biol*, 8, 271-7
- Sirbu IO, Zhao X, Duester G. (2008) Retinoic acid controls heart anteroposterior patterning by down-regulating *Isl1* through the *Fgf8* pathway. *Dev Dyn*, 237, 1627-35
- Sive HL, Hattori K, Weintraub H. (1989) Progressive determination during formation of the anteroposterior axis in *Xenopus laevis*. *Cell*, 58, 171-80

- Sive HL, Draper BW, Harland RM and Weintraub H.(1990) Identification of a retinoic acid-sensitive period during primary axis formation in *Xenopus laevis*. *Genes Dev*, 4, 932-942
- Smith WC, Nakshatri H, Leroy P, Rees J, Chambon P. (1991) A retinoic acid response element is present in the mouse cellular retinol binding protein I (mCRBPI) promoter. *EMBO*, 10, 2223-30
- Smith WC, Knecht AK, Wu M, Harland RM. (1993) Secreted noggin protein mimics the Spemann organizer in dorsalizing *Xenopus* mesoderm. *Nature*, 361, 547-9
- Smith JC, Cunliffe V, Green JB, New HV. (1993b) Intercellular signalling in mesoderm formation during amphibian development. , 340, 287-96
- Sockanathan S, Jessell TM. (1998) Motor neuron-derived retinoid signaling specifies the subtype identity of spinal motor neurons. *Cell*, 94, 503-14
- Sockanathan S, Perlmann T, Jessell TM. (2003) Retinoid receptor signaling in postmitotic motor neurons regulates rostrocaudal positional identity and axonal projection pattern. *Neuron*, 40, 97-111
- Sokol SY, Klingensmith J, Perrimon N, Itoh K. (1995) Dorsalizing and neuralizing properties of *Xdsh*, a maternally expressed *Xenopus* homolog of *dishevelled*. *Development*, 121, 3487
- Spemann H, Mangold H. (1924) Über Induktion von Embryonalanlagen durch Implantation artfremder Organisatoren. *Roux's Arch Entw Mech Org*, 100, 599-638
Reprinted and translated. *Int J Dev Biol*, 45, 13-18
- Stafford D, Prince VE. (2002) Retinoic acid signaling is required for a critical early step in zebrafish pancreatic development. *Curr Biol*, 12, 1215-20
- Strate I. (2005) Charakterisierung der Retinol-Dehydrogenase RDH10 in der Frühentwicklung von *Xenopus laevis*. Diplomarbeit
- Studer M, Pöpperl H, Marshall H, Kuroiwa A, Krumlauf R. (1994) Role of a conserved retinoic acid response element in rhombomere restriction of *Hoxb-1*. *Science*, 265, 1728-32
- Su J, Chai X, Kahn B, Napoli JL. (1998) cDNA cloning, tissue distribution, and substrate characteristics of a cis-Retinol/3alpha-hydroxysterol short-chain dehydrogenase isozyme. *J Biol Chem*, 273, 17910-6
- Sun BI, Bush SM, Collins-Racie LA, LaVallie ER, DiBlasio-Smith EA, Wolfman NM, McCoy JM, Sive HL. (1999) *Derrière*: a TGF-beta family member required for posterior development in *Xenopus*. *Development*, 126, 1467-82

Sundin O, Eichele G. (1992) An early marker of axial pattern in the chick embryo and its respecification by retinoic acid. *Development*, 114, 841-52

Swindell EC, Thaller C, Sockanathan S, Petkovich M, Jessell TM, Eichele G. (1999) Complementary domains of retinoic acid production and degradation in the early chick embryo. *Dev Biol*, 216, 282-96

Tahayato A, Dollé P, Petkovich M. (2003) Cyp26C1 encodes a novel retinoic acid-metabolizing enzyme expressed in the hindbrain, inner ear, first branchial arch and tooth buds during murine development. *Gene Expr Patterns*, 3, 449-54

Taira M, Jamrich M, Good PJ, Dawid IB. (1992) The LIM domain-containing homeo box gene *Xlim-1* is expressed specifically in the organizer region of *Xenopus* gastrula embryos. *Genes Dev*, 6, 356-66

Taira M, Otani H, Jamrich M, Dawid IB. (1994) Expression of the LIM class homeobox gene *Xlim-1* in pronephros and CNS cell lineages of *Xenopus* embryos is affected by retinoic acid and exogastrulation. *Development*, 120, 1525-36

Takada S, Stark KL, Shea MJ, Vassileva G, McMahon JA, McMahon AP. (1994) *Wnt-3a* regulates somite and tailbud formation in the mouse embryo. *Genes Dev*, 8, 174-89

Takahashi S, Yokota C, Takano K, Tanegashima K, Onuma Y, Goto J, Asashima M. (2000) Two novel nodal-related genes initiate early inductive events in *Xenopus* Nieuwkoop center. *Development*, 127, 5319-29

Tamai K, Zeng X, Liu C, Zhang X, Harada Y, Chang Z, He X. (2004) A mechanism for Wnt coreceptor activation. *Mol Cell*, 13, 149-56

Tashiro K, Yamada R, Asano M, Hashimoto M, Muramatsu M, Shiokawa K. (1991) Expression of mRNA for activin-binding protein (follistatin) during early embryonic development of *Xenopus laevis*. *Biochem Biophys Res Commun*. 174, 1022-7

Thaller C, Eichele G. (1987) Identification and spatial distribution of retinoids in the developing chick limb bud. *Nature*, 327, 625-8

Thaller C, Eichele G. (1990) Isolation of 3,4-didehydroretinoic acid, a novel morphogenetic signal in the chick wing bud. *Nature*, 345, 815-9

Thaller C, Hofmann C, Eichele G. (1993) 9-cis-retinoic acid, a potent inducer of digit pattern duplications in the chick wing bud. *Development*, 118, 957-65

Thomas P, Beddington R. (1996) Anterior primitive endoderm may be responsible for patterning the anterior neural plate in the mouse embryo. *Curr Biol*, 6, 1487-96

- Tickle C, Alberts B, Wolpert L, Lee J. (1982) Local application of retinoic acid to the limb bud mimics the action of the polarizing region. *Nature*, 296, 564-6
- Tryggvason K, Romert A, Eriksson U. (2001) Biosynthesis of 9-cis-retinoic acid in vivo. The roles of different retinol dehydrogenases and a structure-activity analysis of microsomal retinol dehydrogenases. *J Biol Chem*, 276, 19253-8
- Uehara M, Yashiro K, Mamiya S, Nishino J, Chambon P, Dolle P, Sakai Y. (2007) CYP26A1 and CYP26C1 cooperatively regulate anterior-posterior patterning of the developing brain and the production of migratory cranial neural crest cells in the mouse. *Dev Biol*, 302, 399-411
- Ulven SM, Gundersen TE, Weedon MS, Landaas VO, Sakhi AK, Fromm SH, Geronimo BA, Moskaug JO, Blomhoff R. (2000) Identification of endogenous retinoids, enzymes, binding proteins, and receptors during early postimplantation development in mouse: important role of retinal dehydrogenase type 2 in synthesis of all-trans-retinoic acid. *Dev Biol*, 220, 379-91
- van der Wees J, Schilthuis JG, Koster CH, Diesveld-Schipper H, Folkers GE, van der Saag PT, Dawson MI, Shudo K, van der Burg B, Durston AJ. (1998) Inhibition of retinoic acid receptor-mediated signalling alters positional identity in the developing hindbrain. *Development*, 125, 545-56
- Vermot J, Pourquié O. (2005) Retinoic acid coordinates somitogenesis and left-right patterning in vertebrate embryos. *Nature*, 435, 215-20
- Vermot J, Gallego Llamas J, Fraulob V, Niederreither K, Chambon P, Dollé P. (2005) Retinoic acid controls the bilateral symmetry of somite formation in the mouse embryo. *Science*, 308, 563-6
- Vincent JP, Oster GF, Gerhart JC. (1986) Kinematics of gray crescent formation in *Xenopus* eggs: the displacement of subcortical cytoplasm relative to the egg surface. *Dev Biol*, 113, 484-500
- Vincent JP, Gerhart JC. (1987) Subcortical rotation in *Xenopus* eggs: an early step in embryonic axis specification. *Dev Biol*, 123, 526-39
- Viviano CM, Brockes JP. (1996) Is retinoic acid an endogenous ligand during urodele limb regeneration? *Int J Dev Biol*, 40, 817-22
- Vogel S, Gamble M, Blaner W. (1999) *Handb. Exp. Pharmacol*, 139, 31-96
- von Bubnoff A, Schmidt JE, Kimelman D. (1996) The *Xenopus laevis* homeobox gene *Xgbx-2* is an early marker of anteroposterior patterning in the ectoderm. *Mech Dev*, 54, 149-60

- von Lintig J, Vogt K. (2000) Filling the gap in vitamin A research. Molecular identification of an enzyme cleaving beta-carotene to retinal. *J Biol Chem*, 275, 11915-20
- von Lintig J, Wyss A. (2001) Molecular analysis of vitamin A formation: cloning and characterization of beta-carotene 15,15'-dioxygenases. *Arch Biochem Biophys*, 385, 47-52
- Wagner DS, Mullins MC. (2002) Modulation of BMP activity in dorsal-ventral pattern formation by the chordin and ogon antagonists. *Dev Biol*, 245, 109-23
- Wang X, Penzes P, Napoli JL. (1996) Cloning of a cDNA encoding an aldehyde dehydrogenase and its expression in *Escherichia coli*. Recognition of retinal as substrate. *J Biol Chem*, 271, 16288-93
- Wang Z, Dollé P, Cardoso WV, Niederreither K. (2006) Retinoic acid regulates morphogenesis and patterning of posterior foregut derivatives. *Dev Biol*, 297, 433-45
- Weaver C, Farr GH 3rd, Pan W, Rowning BA, Wang J, Mao J, Wu D, Li L, Larabell CA, Kimelman D. (2003) GBP binds kinesin light chain and translocates during cortical rotation in *Xenopus* eggs. *Development*, 130, 5425-36
- Weaver C, Kimelman D. (2004) Move it or lose it: axis specification in *Xenopus*. *Development*, 131, 3491-9
- Wendling O, Ghyselinck NB, Chambon P, Mark M. (2001) Roles of retinoic acid receptors in early embryonic morphogenesis and hindbrain patterning. *Development*, 128, 2031-8
- Wessely O, Agius E, Oelgeschläger M, Pera EM, De Robertis EM. (2001) Neural induction in the absence of mesoderm: beta-catenin-dependent expression of secreted BMP antagonists at the blastula stage in *Xenopus*. *Dev Biol*, 234, 161-73
- Wessely O, Kim JI, Geissert D, Tran U, De Robertis EM. (2004) Analysis of Spemann organizer formation in *Xenopus* embryos by cDNA macroarrays. *Dev Biol*, 269, 552-66
- White JA, Guo YD, Baetz K, Beckett-Jones B, Bonasoro J, Hsu KE, Dilworth FJ, Jones G, Petkovich M. (1996) Identification of the retinoic acid-inducible all-trans-retinoic acid 4-hydroxylase. *J Biol Chem*, 271, 29922-7
- White JC, Shankar VN, Highland M, Epstein ML, DeLuca HF, Clagett-Dame M. (1998) Defects in embryonic hindbrain development and fetal resorption resulting from vitamin A deficiency in the rat are prevented by feeding pharmacological levels of all-trans-retinoic acid. *Proc Natl Acad Sci U S A*, 95, 13459-64

White JC, Highland M, Kaiser M, Clagett-Dame M. (2000) Vitamin A deficiency results in the dose-dependent acquisition of anterior character and shortening of the caudal hindbrain of the rat embryo. *Dev Biol*, 220, 263-84

White JA, Ramshaw H, Taimi M, Stangle W, Zhang A, Everingham S, Creighton S, Tam SP, Jones G, Petkovich M. (2000b) Identification of the human cytochrome P450, P450RAI-2, which is predominantly expressed in the adult cerebellum and is responsible for all-trans-retinoic acid metabolism. *Proc Natl Acad Sci U S A*, 97, 6403-8

White RJ, Nie Q, Lander AD, Schilling TF. (2007) Complex regulation of *cyp26a1* creates a robust retinoic acid gradient in the zebrafish embryo. *PLoS Biol*, 5, e304

Wiellette EL, Sive H. (2003) *vhnf1* and *Fgf* signals synergize to specify rhombomere identity in the zebrafish hindbrain. *Development*, 130, 3821-9

William CM, Tanabe Y, Jessell TM. (2003) Regulation of motor neuron subtype identity by repressor activity of *Mnx* class homeodomain proteins. *Development*, 130, 1523-36

Wilson JG, Warkany J. (1948) Malformations in the genito-urinary tract induced by maternal vitamin A deficiency in the rat. *Am J Anat*, 83, 357-407

Wilson JG, Warkany J. (1949) Aortic-arch and cardiac anomalies in the offspring of vitamin A deficient rats. *Am J Ant*, 85, 113-55

Wilson L, Gale E, Chambers D, Maden M. (2004) Retinoic acid and the control of dorsoventral patterning in the avian spinal cord. *Dev Biol*, 269, 433-46

Wodarz A, Nusse R. (1998) Mechanisms of Wnt signaling in development. *Annu Rev Cell Dev Biol*, 14, 59-88

Wood H, Pall G, Morriss-Kay G. (1994) Exposure to retinoic acid before or after the onset of somitogenesis reveals separate effects on rhombomeric segmentation and 3' *HoxB* gene expression domains. *Development*, 120, 2279-85

Wu BX, Chen Y, Chen Y, Fan J, Rohrer B, Crouch RK, Ma JX. (2002) Cloning and characterization of a novel all-trans retinol short-chain dehydrogenase/reductase from the RPE. *Invest Ophthalmol Vis Sci*, 43, 3365-72

Wu BX, Moiseyev G, Chen Y, Rohrer B, Crouch RK, Ma JX. (2004) Identification of RDH10, an All-trans Retinol Dehydrogenase, in Retinal Muller Cells. *Invest Ophthalmol Vis Sci.*, 45, 3857-62

Yamada T. (1994) Caudalization by the amphibian organizer: brachyury, convergent extension and retinoic acid. *Development*, 120, 3051-62

- Yamaguchi TP, Bradley A, McMahon AP, Jones S. (1999) A Wnt5a pathway underlies outgrowth of multiple structures in the vertebrate embryo. *Development*, 126, 1211-23
- Yamamoto H, Simon A, Eriksson U, Harris E, Berson EL, Dryja TP. (1999) Mutations in the gene encoding 11-cis retinol dehydrogenase cause delayed dark adaptation and fundus albipunctatus. *Nat Genet*, 22, 188-91
- Yamamoto M, Saijoh Y, Perea-Gomez A, Shawlot W, Behringer RR, Ang SL, Hamada H, Meno C. (2004) Nodal antagonists regulate formation of the anteroposterior axis of the mouse embryo. *Nature*, 428, 387-92
- Yang ZN, Davis GJ, Hurley TD, Stone CL, Li TK, Bosron WF. (1994) Catalytic efficiency of human alcohol dehydrogenases for retinol oxidation and retinal reduction. *Alcohol Clin Exp Res*, 18, 587-91
- Yang ZN, Davis GJ, Hurley TD, Stone CL, Li TK, Bosron WF. (1994) Catalytic efficiency of human alcohol dehydrogenases for retinol oxidation and retinal reduction. *Alcohol Clin Exp Res.*, 18, 487-91
- Yashiro K, Zhao X, Uehara M, Yamashita K, Nishijima M, Nishino J, Saijoh Y, Sakai Y, Hamada H. (2004) Regulation of retinoic acid distribution is required for proximodistal patterning and outgrowth of the developing mouse limb. *Dev Cell*, 6, 411-22
- Yelin R, Schyr RB, Kot H, Zins S, Frumkin A, Pillemer G, Fainsod A. (2005) Ethanol exposure affects gene expression in the embryonic organizer and reduces retinoic acid levels. *Dev Biol*, 279, 193-204
- Yost RW, Harrison EH, Ross AC. (1988) Esterification by rat liver microsomes of retinol bound to cellular retinol-binding protein. *J Biol Chem*, 263, 18693-701
- Yost C, Farr GH 3rd, Pierce SB, Ferkey DM, Chen MM, Kimelman D. (1998) GBP, an inhibitor of GSK-3, is implicated in *Xenopus* development and oncogenesis. *Cell*, 93, 1031-41
- Yuge M, Kobayakawa Y, Fujisue M, Yamana K. (1990) A cytoplasmic determinant for dorsal axis formation in an early embryo of *Xenopus laevis*. *Development*, 110, 1051-6
- Zakin L, Reversade B, Kuroda H, Lyons KM, De Robertis EM. (2005) Sirenomelia in *Bmp7* and *Tsg* compound mutant mice: requirement for Bmp signaling in the development of ventral posterior mesoderm. *Development*, 132, 2489-99
- Zhang Z, Balmer JE, Lovlie A, Fromm SH, Blomhoff R. (1996) Specific teratogenic effects of different retinoic acid isomers and analogs in the developing anterior central nervous system of zebrafish. *Dev Dyn*, 206, 73-86

Zhao D, McCaffery P, Ivins KJ, Neve RL, Hogan P, Chin WW, Dräger UC. (1996) Molecular identification of a major retinoic-acid-synthesizing enzyme, a retinaldehyde-specific dehydrogenase. *Eur J Biochem*, 240, 15-22

Zhao Q, Dobbs-McAuliffe B, Linney E. (2005) Expression of *cyp26b1* during zebrafish early development. *Gene Expr Patterns*, 5, 363-9

Zhuang R, Lin M, Napoli JL. (2002) *cis*-Retinol/androgen dehydrogenase, isozyme 3 (CRAD3): a short-chain dehydrogenase active in a reconstituted path of 9-*cis*-retinoic acid biosynthesis in intact cells. *Biochemistry*, 41, 3477-83

Zimmerman LB, De Jesús-Escobar JM, Harland RM. (1996) The Spemann organizer signal noggin binds and inactivates bone morphogenetic protein 4. *Cell*, 86, 599-606

Publications

Strate I, Min TH, Iliev D, Pera EM (2009). The Retinol Dehydrogenase-10 is a feedback regulator of retinoic acid signalling during axis formation and patterning of the central nervous system.

Development, 136, 461-72

Meszaros R, **Strate I**, Pera EM, Durbeej M (2008). Expression of the novel gene Ened during mouse and Xenopus embryonic development.

Int. J. Dev. Biol., 52, 1119-22

Hou S, Maccarana M, Min TH, **Strate I**, Pera EM (2007). The secreted serine protease xHtrA1 stimulates long-range FGF signaling in the early Xenopus embryo.

Developmental Cell, 13, 166-7

Pera EM, Hou S, **Strate I**, Wessely O, De Robertis EM (2005). Exploration of the extracellular space by a large-scale secretion screen in the early Xenopus embryo.

Int. J. Dev. Biol., 49, 781-96

Acknowledgments

I would like to thank my supervisor Dr. Edgar Pera for giving me the possibility to work with him in Sweden and for being always enthusiastic about my project. I appreciate his critical comments on my work and his permanent encouragement in times of big frustration. I am grateful for his continuous support during my studies. His passion for science is truly motivating.

I want to thank Prof. Ernst Wimmer for accepting the correference, but also for awakening my interest in developmental biology.

I express my gratitude to Prof. Tomas Pieler for introducing me to the exciting field of *Xenopus* research.

I would like to thank my past and present colleagues Ingela Liljequist-Soltic, Dobromir Iliev and Mohsen Sagha for creating a relaxed working atmosphere and for helping me out, especially during the revision time of my RDH10-manuscript. I want to express my deep gratitude to Shareen Tan for being a wonderful colleague and flatmate. We have been through good and bad times together. I also thank Shirui Hou for supporting me in all aspects when I started working with *Xenopus* and for being such a good friend through all the years.

I wish to thank the Fly-Boys, Prof. Stefan Baumgartner, Sol Da Rocha Baez, Dr. Udo Häcker, Shai Mulinari and Darren Cleare for putting some fun into the daily routine. Thank you for listening to all my problems and for cheering me up!

I would like to thank all people working on B13 in the past and present, especially Maithe Perez, Wilma Martinez, Khalid Fahmy, Pietro Farinelli and Kirsten Wunderlich for creating a joyful working atmosphere.

I thank Ulla Nilsson for giving me such a nice and warm home in Sweden.

Ich danke meinen Eltern für ihre volle Unterstützung während der letzten Jahre, ihre Fürsorge und ihr Verständnis für “unnormale” Arbeitszeiten.

Danke auch an meine Schwester Katja, Michael und die kleine Jana für jegliche Aufheiterung, wenn es bitter nötig war.

Curriculum Vitae

Ina Strate

Date of birth: April 18th, 1981
Place of birth: Detmold, Germany
Nationality: German

Degrees:

2005: “Diplom” in Biology,
Georg August University, Göttingen, Germany

2002: “Vordiplom” in Biology,
Georg August University, Göttingen, Germany

Research experience:

since 01/10/2005: Ph.D. thesis in the Vertebrate Developmental Biology
Laboratory, Lund Stem Cell Center , Sweden

Title: “Establishment of retinoic acid gradients in the
early development of *Xenopus laevis*”
Supervisor: Assoc. Prof. Edgar Pera

01/03/2005-29/09/2005 : Diploma thesis at the “Göttingen Center of Molecular
Biology (GZMB)”, Göttingen, Germany
Department of Developmental Biochemistry
(Head: Prof. T. Pieler)

Title: “Characterization of the Retinol Dehydrogenase
RDH10 in the early development of *Xenopus laevis*”
Supervisor: Dr. Edgar Pera
Grading: 1.0 (“very good”)

Nov. 2004-Febr. 2005: Lab-rotation student in the Department of Developmental Biochemistry, GZMB

Project: “Expression analysis of genes isolated in a screen for secreted proteins in the *Xenopus* embryo”
Supervisor: Dr. Edgar Pera

Education:

Sept. 2000-Nov. 2004 Studies in Biology at the Georg August University, Göttingen, Germany

Final oral examination (“Diplom”) on 11/11/2004 in Developmental Biology, Zoology and Chemistry
Grading: 2.1 (“good”)

Oral examination (“Vordiplom”) on 16/10/2002 in Zoology, Microbiology, Chemistry, Physics
Grading: 2.1 (“good”)

16/06/2000 Final high school examination (“Abitur”) at the Christian-Dietrich-Grabbe-Gymnasium, Detmold, Germany

Awards:

- "Xenopus Conference 2008 Travel Grant"
- “NIH (National Institute of Health, USA)-funded Travel Grant”

